Stony Brook University

Identification and characterization of β-actin mRNA localization factors in the nervous system

John Richard Sinnamon
Doctoral Dissertation
Program in Neuroscience
Department of Neurobiology and Behavior
December 2013

Stony Brook University
The Graduate School

John Richard Sinnamon

We, the dissertation committee for the above candidate for the
Doctor of Philosophy degree, hereby recommend
acceptance of this dissertation.

Dr. Kevin Czaplinski (advisor)
Department of Biochemistry and Cell Biology

Dr. David Talmage (committee chair)
Professor
Department of Pharmacological Sciences

Dr. Simon Halegoua
Professor
Department of Neurobiology and Behavior

Dr. Jeffery Twiss
Professor, Neurobiology
Department of Biological Sciences, University of South Carolina

This dissertation is accepted by the Graduate School

_____
Charles Taber
Dean of the Graduate School

Abstract

The local translation of trafficked mRNAs temporally and spatially regulates protein expression. In neurons, mRNAs are trafficked to both axons and dendrites and the local translation of these mRNAs is important for axon guidance as well as synaptic plasticity. The active trafficking of mRNAs involves the interaction between *cis*-acting localization elements, known as 'zipcodes,' and *trans*-acting factors, including RNA-binding proteins. However, the exact molecular mechanism of mRNA localization in the mammalian nervous system remains unknown. To better understand this process, the zipcode element of β-actin (Actb) mRNA was used to identify putative β-actin zipcode binding proteins from the rodent brain (bZBPs).

Hnrnpab was confirmed as a bZBP and was found to have an unexpected isoform dependent specificity. The larger isoform, Hnrnpab1, is specific for Actb mRNA and the zipcode localization element. The alternatively spliced isoform, Hnrnpab2, interacts with the zipcode element and the 5' UTR of Actb mRNA as well as γ-actin (Actg) mRNA. Analysis using a novel fluorescent *in situ* hybridization method demonstrated a decrease in Actb mRNA in the periphery of cells in the absence of Hnrnpab. This effect can be rescued only with the Hnrnpab1 isoform, suggesting a distinct function in Actb mRNA localization. Mice lacking Hnrnpab show a number of changes in protein expression which suggest a role in nervous system development and glutamate signaling. Hnrnpab$^{-/-}$ neural stem and progenitor cells undergo altered differentiation patterns in culture, and mature Hnrnpab$^{-/-}$ neurons demonstrate increased sensitivity to glutamate-induced excitotoxicity. These studies represent an important step in understanding the underlying molecular mechanism of mRNA trafficking by identifying several putative localization factors using the localization element of Actb mRNA and establishing Hnrnpab1 as

a zipcode binding protein, which mediates Actb mRNA localization. They also explore the role of Hnrnpab in the nervous system and provide evidence for isoform dependent functions.

Dedication

This thesis is dedicated to my family, who have always supported and encouraged me and to the memory of Richard F. Anton, Evelyn M. Anton and William J. Sinnamon.

Table of Contents

Chapter 1: Introduction……1

Chapter 2: Identification of Hnrnpab1 as a brain zipcode binding protein……24

Chapter 3: Hnrnpab1 is required for the normal distribution of Actb mRNA……44

Chapter 4: Hnrnpab regulates neural development and neuron cell survival in mice…….61

Chapter 5: Discussion……..91

Materials and Methods…….95

References……118

List of Figures and Tables:

Table I – Proteins identified from RNP purifications…….19

Figure 1: mRNA trafficking to localized translation domains……20

Figure 2- Actb zipcodes are evolutionarily conserved……...….21

Figure 3 –The 3' untranslated region of human Actb and Actg mRNA are not homologus…..23

Figure 4: Identification of bZBPs using GRNA chromatography……..38

Figure 5- Hnrnpab1 and 2 amino acid sequence alignment……..……..39

Figure 6: Hnrnpab1 is a Actb specific bZBP……..…….40

Figure 7: Full length Hnrnpab is required for the interaction with β-actin mRNA…….41

Figure 8: Multiple portions of Hnrnpab are capable of direct RNA interaction…….....42

Figure 9: Creation of N2A cells expressing bZBPs…….....43

Figure 10– FISH-STICs probe diagram……...54

Figure 11– Detection of Actb mRNA with a single FISH-STIC probe……..…....55

Figure 12-Actb and Actg have spatially distinct distribution in the same cells……...56

Figure 13 – FISH-STICs detection of Nrg1-III and Actg mRNA in primary neurons……...57

Figure 14 – FISH-STICs probe specificity……..58

Figure 15- Hnrnpab is required for proper Actb mRNA localization…….....59

Figure 16- Hnrnpab1 rescues Actb mRNA localization...……...60

Figure 17 – AV0462 ES cell gene trap disrupts Hnrpab expression……..74

Figure 18- The workflow diagram for quantitative shotgun proteomics of Hnrnpab-/- newborn hippocampus…….75

Table II: Upregulated proteins from Hnrnpab-/- newborn hippocampus……...76

Table III: Downregulated proteins from Hnrnpab-/- newborn hippocampus…….....79

Table IV: Inginuity Pathway Analysis of proteomics…….80

Figure 19 – Hnrnpab disruption affects the differentiation of neural lineage cells in neurosphere cultures…….....83

Figure 20 – Hnrnpab disruption increases sensitivity of cells to glutamate-stimulated excitotoxicity……..……..84

Figure 21 – Hnrnpab disruption leads to increased neurite length……..…….85

Figure 22- Immunofluorescence of Hnrnpab in the brain of adult mice……..86

Figure 23–Hnrnpab localizes to the nucleus in early primary neuron…….87

Figure 24 – Hnrnpab isoforms are predominantly nuclear in developing neurons……..…88

Figure 25 – Hnrnpab isoforms appear in the cytoplasm of mature neurons……89

Figure 26 –Quantification of the nuclear and cytoplasmic localization of Hnrnpab1 and Hnrnpab2 isoforms...…….....90

Chapter 1: Introduction

Localization of mRNAs to specific subcellular compartments in the cytoplasm is a mechanism by which protein expression can be restricted both spatially and temporally. The localization of mRNAs encoding for proteins with specialized functions can establish asymmetry in a cell and has been shown to be important for both embryonic axis formation and asymmetric cell division. Specific extra-cellular stimuli can lead to the local translation of mRNAs resulting in faster responses to protein demands than transmission of the stimulus to the nucleus to induce transcription, export, translation and subsequent protein targeting. This advantage is exemplified by the process of axon path-finding and axon regeneration. In addition, a given mRNA can produce multiple copies of a given protein which is more efficient than transporting proteins translated elsewhere. However, before an mRNA can be locally translated it must first be trafficked to the site of translation.

Localization elements

mRNAs are trafficked through the recognition of *cis*-acting sequences, contained within the mRNA itself, by *trans*-acting factors – typically RNA binding proteins (RBPs). The sequences which mediate the process of localization are referred to as localization elements (LEs) and often nicknamed 'zipcodes.' Typically LEs are located within the 3' un-translated region (UTR) of an mRNA, although several have been found in the 5' UTR and even in the coding region[1]. RNAs can contain several LEs, which function in different aspects of localization. For example, the myelin basic protein (MBP) mRNA contains an 11 nucleotide (nt) LE also called the A2 response element (A2RE) because it is the binding site for the RBP heterogenous ribonucleoprotein A2 (hnRNP A2). The A2RE of MBP mRNA is both necessary

and sufficient for trafficking RNA to the processes of oligodendrocytes. However, this sequence is only responsible for trafficking the mRNA out of the cell body and into the processes, a second sequence called the RNA localization region (RLR) also contained within the 3' UTR, is required for the movement of the mRNA into the myelinating compartment[2].

RNA has the capacity to fold into secondary structures which can play a role in the ability of an mRNA to localize. A 625 nt section of the bicoid 3' UTR was first found to be necessary and sufficient for the localization of the mRNA into *Drosophila* oocytes. This sequence was determined to contain several localization elements required for the successive localization of the mRNA from the nurse cells to the oocyte then to the anterior pole of the oocyte where it is anchored for translation. Each of these elements was found to form a stem loop structure and mutations which changed the primary sequence but not the secondary structure still allowed for localization[3, 4].

The identification of LEs is not always clear, as demonstrated by the work to identify the LE of the dendritcally localized alpha subunit of $Ca^{2+/}$calmodulin kinase II (CaMKIIα). Initial studies revealed a 94 nt element in the 3' UTR of CaMKIIα, which was sufficient to localize a GFP reporter to dendrites. To test the function of this element *in vivo*, a mutation was made deleting the majority of the 3'UTR of CaMKIIα but retaining the 94nt element in mice[5]. *In situ* hybridization revealed that there was no localization of CaMKIIα mRNA in the mutant mice, demonstrating this element alone is not sufficient for localization *in vivo,* but confirming the requirement for sequences within the 3' UTR[6]. Other groups have isolated additional elements in the 3' UTR using similar reporter assays, including a 1200 nt element, a cytoplasmic polyadenylation element (CPE) and a G-quartet structure as required for localization of CaMKIIα mRNA[7-9].

These studies highlight both the importance and difficulty of establishing localization elements, which has led to many groups simply using the 3'UTR rather than specific LEs for experimentation. One drawback to using the 3'UTR for trafficking studies is that there are other sequences contained within the 3' UTR of mRNAs. For example, downstream of the 340 nt Vg1LE is another 250nt element responsible for translational repression[10]. There are other sequences contained within the 3' UTR such as A-U rich elements (AREs), which regulate the stability of the mRNA[11]. Several LEs have been identified but there is no consensus for what defines a localization element within an mRNA or what the destination is of a trafficked mRNA. Binding motifs for individual RNA binding proteins such as the A2RE for hnRNP A2 have been defined and are present in several mRNAs, however these mRNAs go to different subcellular compartments and it is not clear what function these motifs play in the regulation of each mRNA.

Ribonucleoprotein complex formation

ASH1 mRNA model

The complex of mRNAs and RBPs is referred to as a ribonucleoprotein complex (RNP) or L-RNP, if the complex is involved in localization. The best described example for the formation of an L-RNP and the trafficking of the complex comes from work in *Saccharomyces cerevisae*. The ASH1 mRNA is localized to the bud-tip of yeast, where it locally translated to repress mating type switching in the daughter cell. ASH1 mRNA contains four LEs (E1, E2A, E2B E3), located both in the coding region and over-lapping with the 3' UTR. The function of the LEs is synergistic and requires the formation of step-loop structures, which are recognized by the RBP She2[12]. She2 is co-transcriptionally recruited to the ASH1 mRNA by the RNA

polymerase II elongation factor DSIF, where it interacts with each of the four LEs as a dimer. She2 recruits the translational repressors Loc1 and pumillo homology domain family member6 (Puf6) in the nucleus[13, 14]. After the complex is exported to the cytoplasm, She2 recruits the adapter protein She3. She3 is referred to as an adapter protein because it binds to both She2 and the type 5 myosin motor Myo4[15, 16]. Through this interaction the entire ASH1 L-RNP is trafficked down actin filaments to the bud tip where it is anchored and locally translated[17]. The ASH1 L-RNP example of mRNA-RBP-adapter-motor has become the basic model for trafficked mRNAs, even if the final motors are not myosins as in yeast. Evidence from several model systems support aspects of this model, although it has not been directly demonstrated for any other mRNA and there are no homologs of the She proteins.

Nuclear L-RNP initiation

The concept of nuclear initiation for L-RNP formation is supported by the role of the exon junction complex (EJC) in localization. The exon junction complex (EJC) contains four proteins (eIF4AIII, MLN51, Magoh and Y14) and binds approximately 20 nts downstream from the exons of a spliced mRNA. The EJC accompanies the mRNA into the cytoplasm where it is removed during the first round of translation. All four components of the complex and splicing of the first intron are required for proper localization of oskar mRNA to the posterior pole of the *Drosophila* oocyte [18-20]. All four components of the EJC can also be found in the dendrites of neurons and depletion of eIF4AIII increases synaptic strength and the number of GluR1 subunits of AMPA receptors at synapses[21]. Similar to the EJC, nuclear cap-binding complex (CBC), consisting of a CBP20/80 heterodimer, have also been found to be present in dendrites and associated with complexes containing dendritically localized mRNAs. CBC associates with the

cap of newly transcribed mRNA and are later displaced by the binding of the cytoplasmic cap binding protein eIF4E. The presence of CBC and or the EJC suggests the mRNAs being localized are translationally repressed[22, 23]. However, it remains unclear if the binding of either cap-binding proteins or the EJC is a general requirement for mRNA trafficking.

Molecular Motors and adapter proteins

There is evidence that in metazoans mRNA trafficking occurs along microtubules. For example, inhibiting the minus end microtubule motor protein dynein in *Drosophila* affects the localization of the pair-rule mRNAs [24]. Two proteins, bicaudal-D (BicD) and egalitarian (EGL) are also required for this process and have been implicated as possible adapter proteins. Using affinity chromatography, BicD, EGL and the dynein heavy chain were all found to bind to the localization element of several pair-rule mRNAs, including hairy, K10 and gurken. While both gurken and bicoid mRNAs require BicD and EGL for trafficking, they have different localizations which are both inhibited by antibodies against dynein, suggesting there are multiple mechanisms involved[25, 26].

Kinesin motors have also been implicated in the trafficking of MBP mRNA in oligodendrocytes and Vg-1 mRNA in *Xenopus* oocytes. Using fluorescent RNAs it was determined that MBP mRNA containing complexes move anterograde towards the cell periphery in a kinesin dependent manner since anti-sense oligonucleotides against the kinesin heavy chain inhibit this localization[27]. In Messitt et al., the authors identified a small population of microtubules with the minus ends towards the vegetal pole of *Xenopus* oocytes (the over-whelming majority have the opposite orientation). The authors went on to show by RNA interference that kinesins 1 and 2 are involved in the localization of Vg1 mRNA. However, Vg1

mRNA can still localize halfway towards the vegetal pole without either kinesin suggesting there is more to the mechanism and while no direct adapter protein has been demonstrated, the dsRNA binding protein Staufen has been proposed to play a role in this process [28].

Several approaches to purify neuronal trafficking RNPs have been applied to determine the components required for transport in the nervous system. Kanai et al. used the cargo domain of the kinesin Kif5, to create a GST fusion protein to isolate putative RNP complexes from the mouse brain. They isolated a large (~1000S) detergent resistant, RNase sensitive complex, which included forty-two proteins and the mRNAs for Arc and CaMKIIα. RBPs including those required for CaMKIIα mRNA localization as well as translational components were included in this complex. However, none of the identified proteins were able to interact with the cargo domain in the presence of RNase, confounding the identification of an "adapter" protein [29]. Using sub-cellular fractionation from E18 rat brain, another group isolated a complex containing Actb mRNA. Proteomic analysis of this fraction included many of the RBPs known to be involved in the regulation of Actb mRNA and similar components as the Kanai et al. study [30]. A third group took a more targeted approach to identify components of the Retinoic acid receptor alpha (RARα) protein complex from hippocampal neurons. RARα is cytoplasmic in mature neurons, and co-purifies several RNA binding proteins. Many of the proteins identified in the other two purification strategies also co-purifed with RARα, which also associates with CaMKIIα mRNA and was found to inhibit its translation[31]. It is unclear if these biochemical approaches purified one or many RNA complexes. The relative consistency and co-localization of the identified factors suggest there may be a common set of trafficking factors although more work needs to be done to identify the required components of each complex for trafficking.

Trafficking of single or multiple mRNAs

The size of these putative RNP complexes is quite large, however, the mRNA composition of individual endogenous L-RNPs remains relatively unknown. It has been suggested that multiple mRNAs containing the same regulatory elements are co-transported in large L-RNPs. Labeling of RNAs and RBPs in yeast with distinct tags followed by live cell imaging have suggested the ASH1 mRNA localization complex may mediate the localization of as many as 20 mRNAs[32]. Gao et al. 2008 demonstrated the mRNAs for Arc, CaMKIIα and neurogranin all contain sequences similar to the A2RE found in MBP mRNA. Using pair-wise comparisons of exogenous fluorescent RNAs they found >70% of dendritic puncta contained two different types of these RNAs. Similar analysis of endogenous mRNA revealed a >50% over-lap of any two of these mRNAs, suggesting they can be contained within the same complex. However, they found little over-lap between CaMKIIα and Actb mRNA, which does not contain an A2RE, corroborating the idea that not all mRNAs are transported together[33].

Other evidence suggests mRNAs are localized individually and in low copy numbers. The Kiebler group examined the co-transport of dendritic RNAs by performing two color FISH for MAP2, CaMKIIα, Actb and the non-localized β-globin mRNA. The co-localization of any two dendritic mRNAs did not differ from the co-localization with β-globin mRNA, indicating these mRNAs do not frequently traffic together [34]. They went on to perform *in situ* hybridization using probes directed against the same sequence on each RNA, predicting if there were many RNA molecules then both probes would co-localize frequently. Conversely, if there were one or a few RNA molecules then only one probe would bind per molecule. When comparing these over-lapping sequences, they found less than 20% co-localization of CaMKIIα probes, less than 15% co-localization of Actb probes and less than a 30% over-lap for

MAP2 probes, suggesting low copy numbers of individual RNAs. Using the same approach with competitor sequences they were able to determine on average each complex contained between 1 and 5 individual RNAs [34]. These two models are not mutually exclusive since the Kiebler group did not examine mRNAs regulated by the same proteins and both highlight the need to identify individual trafficking pathways.

Modification of L- RNPs

Once the L-RNP has reached its destination it is remodeled to allow for the local translation of the trafficked mRNA. In several cases the post-translational modification of bound RBPs is involved in the remodeling process. For example, hnRNP A2 is involved in both the trafficking and the translational repression of MBP mRNA in oligodendrocytes. hnRNP A2 mediates MBP translation repression by interacting with another RBP, hnRNP E1[35]. In erythroid cells hnRNP E1 and hnRNP K prevent the translation of 15-lipoxygenase mRNA by preventing association of the 60s ribosomal subunit with the 48S pre-initiation complex and this is one possibility for how MBP may be translationally repressed[36]. hnRNP A2 is also a target of Fyn, a Src family tyrosine kinase. Activation of Fyn stimulates translation of an A2RE-containing translation reporter construct and leads to phosphorylation of hnRNP A2 on an unidentified site. This increase in translation is co-incident with a shift of hnRNP A2 from RNA-containing to RNA-free cellular fractions [37]. These results indicate phosphorylation of hnRNP A2 by Fyn releases MBP mRNA from its translationally silenced state, perhaps by concomitant release of hnRNP A2 and potentially other A2-interacting factors from MBP L-RNP granules.

Modification of cytoplasmic polyadenylation element binding protein 1(CPEB1) and cytoplasmic polyadenylation is another method by which RNPs are modified for translation.

CaMKIIα mRNA contains two cytoplasmic polyadenylation elements (CPEs) and is cytoplasmically polyadenylated in response to visual experience and NMDA stimulation[38, 39]. NMDA receptor stimulation has been linked to the phosphorylation of CPEB1 by activation of the Aurora A kinase that can phosphorylate CPEB1 at a conserved site (Ser 174 in *Xenopus* and Thr171 in mouse) [40]. The result of this modification is the CPEB-mediated recruitment of the cytoplasmic polyadenylation machinery to CPE-containing mRNAs in neurons. Elongation of the polyA tail on CaMKII α mRNA will then translationally activate this and other mRNAs that contain CPE elements[40]. Interestingly, CamKII itself can also phosphorylate this conserved site within CPEB1, and the phosphorylation state is sensitive to activity levels of protein phosphatase 1 (PP1). This dynamic control of CPEB1 phosphorylation by the activity of glutamate receptors could therefore serve as an important cue for localizing synaptic activity-dependent translation at synapses [41-43]. Several studies link these biochemical changes in CPEB1 to synaptic plasticity in brain function, suggesting this mechanism helps interpret synaptic activity to determine, which synapses require local protein synthesis for plasticity during learning and memory[44].

mRNA trafficking and local translation in the nervous system

There has been evidence for local translation in both the axonal and dendritic compartments of neurons for decades and recently it has become clear mRNA localization and local translation are integral to the function of the nervous system. Axon guidance cues and neuronal activity stimulate mRNA trafficking to these compartments and can signal for the subsequent L-RNP remodeling and local translation of trafficked mRNAs. Figure 1 is a model for how we believe mRNA trafficking and local translation of neuronal transcripts occurs.

Evidence for mRNA localization and translation in axons began with the initial observation of axonal ribosomes by electron microscopy and the identification of ribosomal RNAs and mRNAs in the axonal compartment[45, 46]. Metabolic labeling studies have provided key evidence for axonal translation by establishing that axons isolated in culture are capable of translating existing mRNAs [47-53]. Recent evidence has also shown that the proteins synthesized in the axon are capable of being inserted into the plasma membrane despite the absence of a traditional rough endoplasmic reticulum and Golgi apparatus[53]. The best described functions for axonal mRNA localization and local translation are in regulating axon path-finding and regeneration.

Axon-pathfinding

Growing axons receive input from their environment in order to establish proper synaptic connections. The tip of the growing axon, known as the growth cone, interprets chemotropic signals and responds by either turning towards or away from the received signal. This process is not dependent on signals from the soma as axons separated from the cell body are capable of path-finding and responding to guidance cues. The growth cone will turn towards attractive cues while it will turn away from repulsive cues and this process depends on differential local translation[54, 55]. In *Xenopus* retinal ganglion neurons, Actb mRNA is asymmetrically translated in the direction of a gradient of the attractive guidance cue netrin-1 and blocking this translation inhibits growth cone turning. In contrast, the repulsive cue sema3a, stimulates the translation of proteins such as cofilin, which are involved in the disassembly of the cytoskeleton and lead to growth cone collapse [56, 57]. Both cues increase the phosphorylation of eukaryotic translation initiation factor 4E (eIF4E) and stimulate protein synthesis in soma-less growth

cones, however only netrin-1 dependent translation is inhibited by blocking phospho-iniositide 3-kinase (PI3K), indicating the two cues may regulate translation differently [56, 57].

Several studies suggest that between 6% and 10% of the total number of mRNAs are present in vertebrate sensory axons [58-60]. A recent study using laser capture micro-dissection has also identified a subset of mRNAs enriched in the growth cone of developing axons relative to the rest of the axonal compartment, demonstrating the localization of mRNAs can be specific for and within the axon. The number and diversity of growth cone enriched mRNAs increased once they had reached their target relative to those which were path-finding[61]. This suggests the cell is capable of trafficking different mRNAs to regulate the developmental transition of a growth cone to a presynaptic terminal.

In comparing the full length axons of embryonic and adult dorsal root ganglia (DRG) neurons there are similar numbers of unique mRNAs indicating the over-all capacity of axonal localization does not change in development. Pathway analysis of mRNAs enriched in embryonic axons correspond primarily to the processes of cellular assembly and growth, post-transcriptional modification, cell morphology and molecular transport[58]. In contrast, adult axons contain mRNAs encoding for proteins involved in the immune response, cell-cell signaling and interaction. Both embryonic and adult axons contain mRNAs for translational and mitochondrial function. However, the level of these transcripts is reduced in the adult axons, corresponding with their decreased regenerative capacity[58].

Axonal Regeneration and survival

Axonal regeneration has important implications in recovery following injury to the brain, spinal cord and peripheral nervous system. Analysis of mRNA and protein found in the axons of

injury conditioned DRG neurons identified over 300 locally translated proteins[62]. Using cortical neurons in microfluidic chambers it was demonstrated that central nervous system axons also contain mRNAs and that following axotomy over 866 transcripts are changed by more than 20% in these regenerating axons. Analysis of function revealed increases in cell-cell signaling, differentiation and secretion while mitochondrial function and intracellular transport were decreased[63]. Regenerating axons are responsive to extra-cellular cues similar to pathfinding axons. Using 50 mRNAs detected in regenerating axons it has been established that individual stimuli can either increase or decrease the levels of individual mRNAs in this compartment. Growth promoting factors (nerve growth factor (NGF), brain-derived neurotrophic factor (BDNF) and neurotrophin-3) as well as growth inhibiting factors (sema3a and myelin-associated glycoprotein (MAG)) increase or decrease the level of individual mRNAs in the axon, respectively. Levels of certain mRNAs were dependent not only on whether a cue was growth promoting or growth inhibiting but on the specific factor. This suggests extra-cellular signaling is capable of regulating the trafficking of individual mRNAs[59]. The local translation of transcription factors in the axon regulates cell survival both during development and regeneration. In cultured sensory neurons, survival signaling via NGF requires the axonal synthesis of cyclic AMP responsive element binding protein (CREB), which is retrogradely transported back to the cell body[64]. Other transcription factors such as STAT3 have been shown to be translated in response to injury and in *Caenorhabditis elegans* the axonal translation of the CAAT enhancer binding protein (cebp-1) is required for axonal regeneration[65, 66].

Local protein synthesis in dendrites

mRNA trafficking and local translation also occur in the dendrites of neurons. The dendritic arbor of neurons can be extremely complex with as many as 10,000 dendritic spines and many more synaptic inputs. The pathfinding nature and length of the axon makes it easier to biochemically isolate the axon to identify the population of axonal mRNAs. Dendritically localized mRNAs have been traditionally been identified individually by *in situ* hybridization. These mRNAs include microtubule associated protein-2 (MAP2), the alpha subunit of Ca^{2+}/Calmodulin dependent kinase II(CaMKIIα) and activity-regulated cytoskeleton-associated protein (Arc) [67-69].

In an effort to better identify dendritic mRNAs, microarrays have been used with tissue enriched for dendrites and the Allen Brain Project performed high-throughput *in situ* hybridization on the synaptic neuropil [70, 71]. However, there is little over-lap between these studies. Recently the most complete analysis of dendritic mRNAs came by analyzing the CA1 hippocampal neuropil by deep sequencing and filtering based on previous expression profiles. This unbiased approach yielded approximately 3,000 putative dendritic mRNAs, 74 of which were confirmed using high resolution *in situ* hybridization[72]. However, the population of mRNAs in dendrites is dynamically regulated. Many mRNAs which traffic to dendrites in developing neurons are not present in the dendrites of mature neurons[73]. Arc, Actb and CaMKIIα have all been shown to be localized dendritically and be translated in response to synaptic activity [74-76]. Dendrites also respond to extra-cellular cues and the localization and translation of specific mRNAs can be regulated by these cues. For example, the addition of NMDA to cultured hippocampal neurons decreases the amount of AMPA receptor mRNA while activation of group I mGluRs increases the amount of AMPA receptor mRNA[77].

Asymmetrical cell division

The localization of mRNAs is an important part of the asymmetrical division of stem cells. Neuroblasts in *Drosophila* divide unequally to generate both a neuroblast and a ganglion mother cell (GMC), which divides further into two neurons. The mRNA for the transcription factor prospero is localized to the basal pole of neuroblasts during mitosis and then specifically to the GMC, in a process mediated by the RNA-binding protein Staufen [78]. This process is conserved in the developing mammalian cortex where Staufen2 is asymmetrically distributed in radial glial progenitors along with the mRNA for mammalian prospero, where it is thought to inhibit differentiation [79, 80].

Actb mRNA as a model for mRNA trafficking

Actb mRNA is one of the most universally trafficked mRNAs. Actb mRNA was first demonstrated to localize to the leading edge of migrating chicken embryonic fibroblasts (CEFs) based on a localization element in the 3' UTR. Using expression of LacZ/Actb chimeric mRNAs a 54-nt segment and less active 43-nt segment were capable of localizing the reporter to the leading edge. These segments were referred to as the zipcode A and B sequence respectively. Blocking these sequences with oligonucleotides inhibited the localization of the endogenous mRNA in both CEFs and chick forebrain neurons [81, 82]. These sequences are highly conserved in evolution and are contained within the first 233 nts of the human Actb mRNA (Figure 2). In the literature the zipcode A sequence has often been referred to as the Actb mRNA zipcode while the zipcode B sequence has since been uncharacterized. Actb mRNA localizes to the growth cone of neurons, and increases following the addition of neurotrophins or KCl [75, 83]. In addition, Actb mRNA also localizes to dendritic spines in hippocampal neurons where it

has a role in dendritic spine morphology and arborization [84]. Disruption of the cytoskeleton by treatment with cytochalasin D delocalizes the mRNA from the leading edge of migrating fibroblasts, suggesting a role for actin in this process.

The *in vivo* local translation of Actb mRNA has recently been demonstrated. Transgenic mice expressing the 3'UTR of Actb mRNA or the 3' UTR of Actg fused to a myristolated and destabilized GFP reporter were created by the Twiss group. Actg is an important control because it has an almost identical coding region to Actb, but has a different 3' UTR and is a non-trafficking mRNA (Figure 3). Using these mouse lines they demonstrated that the 3'UTR of Actb but not Actg is sufficient for local translation in axons in culture and in the sciatic nerve. Interestingly, the expression of the reporter decreased the localization of endogenous Actb mRNA as well as other mRNAs including GAP-43 mRNA, suggesting a limited amount of localization machinery is available. The presence of the Actb (but not Actg) reporter decreased the ability of axons to regenerate, presumably because of the decrease of Actb, and possibly other mRNAs [85, 86]. Interestingly, reporters containing the 3'UTR of GAP-43 mRNA also deplete endogenous Actb mRNA, providing further evidence for common trafficking machinery being involved with these two mRNAs. [87]. These studies are the first *in vivo* demonstrations that the 3' UTR of Actb is sufficient for axonal translation and required for axonal regeneration.

To visualize the active trafficking of Actb mRNA, the Singer group recently created a knock in mouse line containing the MS2 binding site (MBS) contained within the 3' UTR of Actb but downstream of the zipcode. The MS2 sequence, derived from the MS2 bacteriophage, forms into hairpin structures recognized by the bacteriophage capsid protein also known as the MS2 capsid protein (MCP). Co-expression of the MBS and MCP-fluorescent protein fusions allow for the *in vivo* imaging of endogenous mRNA immediately following transcription. This

study demonstrated the active trafficking of endogenous Actb mRNA in primary hippocampal neurons [88].

Several RBPs have been identified as being involved in the localization of Actb mRNA. Using the 54 nt zipcode sequence, a 68 kDa protein was isolated from chick fibroblasts and shown to interact directly with the Actb zipcode, and was named zipcode binding protein 1 (ZBP1)[89]. Most of the work on the regulation of Actb mRNA has since centered on the interaction of ZBP1 with Actb mRNA. ZBP1 is a highly conserved RBP containing two RNA recognition motifs (RRMs) and four hnRNP K homology (KH) domains. A crystal structure of two of the four KH domains with a small 28 nt motif in the zipcode A sequence has been solved and determined to be the ZBP1 binding site. It is believed that the other domains somehow mediate the localization of the ZPB1 containing L-RNP[90].

The localization of Actb mRNA to the growth cone of chick neurons in response to neurotrophins was demonstrated to be dependent on the interaction of ZBP1 with the 3' UTR of Actb. The interaction of ZBP1 with Actb mRNA may occur in the nucleus but requires stabilization by another protein, zipcode binding protein 2 (ZBP2)[91]. Phosphorylation by Src tyrosine kinase at Y396 in response to BDNF treatment disrupts ZBP1 binding to mRNA leading to an increase in Actb translation in neuroblastoma cells[92]. ZBP1 inhibits translation of Actb mRNA in cell-free translation assays by preventing 60S subunits from joining the 48S pre-initiation complex. ZBP1 gene-trap mice exhibit dwarfism and perinatal lethality; however there is no difference in either Actb mRNA or protein levels seen in tissue from these mice[93]. Neurons derived from $ZBP1^{-}$ embryos have a decrease in response to Netrin-1 and growth cone turning. $ZBP1^{+/-}$ mice express approximately 40% of WT ZBP1 and exhibit no overt phenotype. Adult $ZBP1^{+/-}$ DRGs in culture exhibit less axonal Actb and GAP-43 mRNA and have reduced

regeneration[85]. Despite the almost exclusive focus on ZBP1, it is expressed primarily during development and only 50% of Actb mRNA containing puncta co-localize with ZBP1, suggesting the involvement of other RBPs.

Several other factors have been demonstrated to be involved in the regulation of Actb mRNA in the cytoplasm, although none have been shown to interact directly with the zipcode. Spinal muscular atrophy (SMA) is a common recessive motoneuron disease caused by mutations in the survival motoneuron1 (SMN1) gene. Motoneurons from a mouse model of SMA have reduced axon growth, correlating with a reduction in both Actb mRNA and protein. Smn associates with Actb mRNA in human neuroblastoma cells and over-expression leads to an increase in neurite outgrowth in PC-12 cells. Over-expression of the Smn interacting protein hnRNP R also increases neurite outgrowth in PC-12 cells and hnRNP R co-immunoprecipitates Actb mRNA[94, 95]. Gel shifts using recombinant hnRNP R and the 3'UTR of Actb, suggest the interaction may be direct. hnRNP Q is closely related to hnRNP R , associates with Smn and shows a weak association with Actb mRNA[96]. These studies suggest these proteins may function in a complex involved in the regulation of Actb mRNA. However, hnRNP R immunoprecipitated the entire 3'UTR of Actb better than the zipcode element, suggesting these proteins may not be involved in the actual trafficking of Actb mRNA[94, 95]. 68-kDa RBP Src associated in mitosis (Sam68) has been shown to bind to Actb mRNA *in vivo* and *in vitro*. The binding site for Sam68 has been determined to be a poly(U) sequence found upstream of the zipcode element and binding depends on the KH-domain of Sam68[97, 98]. In cultures, knock-down of Sam68 reduces dendritic spine density and dendritic Actb mRNA. Sam68 knockout mice have a similar decrease in the number of synpases and lower levels of synaptic Actb

protein, suggesting that Sam68 may also play a role in the localization of Actb mRNA in dendrites[99].

Polypyrimidine tract binding protein (PTB)/ hnRNP I knockdown inhibits neurite outgrowth in PC-12 cells, and PTB mediated mRNA localization appears to also be involved in neurite outgrowth through regulating Actb mRNA localization[100]. PTB associates with Actb mRNA in cytoplasmic extract, and a PTB binds to the chicken Actb mRNA zipcode in gel shifts [100]. The localization of PTB at neurite terminals appears to be dependent on phosphorylation of PTB at ser16 mediated by cyclic AMP dependent protein Kinase (PKA)[101]. This site is within the nuclear localization sequence and not within its RNA binding domains and should not therefore affect RNA binding directly[101]. Interestingly, expression of PTB in the nervous system appears to be limited to neural progenitor cells, glia and other non-neuronal cells, while a paralog called neural/brain PTB (nPTB, brPTB) is expressed in neurons[102]. It has not been determined if nPTB binds to the Actb mRNA zipcode and determine or if nPTB is involved in the process of Actb mRNA trafficking in the nervous system. Despite the variety of factors, which have been identified as interacting with the Actb mRNA, it remains unclear where they bind and how they function in the post-transcriptional regulation of the mRNA.

	Kanai et al 2004	Chen et al. 2008	Elvira et al 2006
mRNAs	CamKIIα	CamKIIα	β-actin
	Arc		
Protein synthesis	EF-1α	eIF3α	
	eIF2α	eIF3β	eIF4α
	eIF2β	PABP1	PABP
	eIF2γ	RPs (S3,4,5,6,12,13,16,17,19,25)	
	ribosomal protein L3	RPs: L23, p40, 60s RP	
	Hsp70	Hsp70	
RNA helicases	DDX1	DDX1	DDX1
	DDX3	DDX3	DDX3
	DDX5	DDX5	DDX5
			DDX6
			DDX9
Hnrnps	***hnRNPAB***	***hnRNPAB***	***hnRNPAB***
	hnrnpD	***HnRNPD***	***hnRNPD***
	hnRNPU	hnRNPU	hnRNPU
	hnRNPQ	hnRNPQ	hnRNPQ
	hnRNPA0		***hnRNPA0***
	hnRNPA1		hnRNPA1
			hnRNPA2/B1
			hnRNPK
			hnRNPC
			hnRNPL
			hnRNPE2
			hnRNPA3
			hnRNPH
			hnRNPM
			hnRNPR1
RBPs	FMR1	Tho complex 4	
	FXR1	FXR	
	FXR2		
	Purα	Purα	
	Purβ	Purβ	ZBP1
	Staufen		Staufen2
	ALY	FUS	Matrin-3
	EWS	EWS	Elavl-like(2-4)
	NonO	***NonO***	ZBP2
	PSPC1	GP137	PTB
	PSF	***PSF***	RNA granule protein 105
	TLS	G3BP	G3BP1
	Nucleolin	ssDNA binding protein1	Nucleolin
	cold inducible RBP	cold inducible RBP	***Nucleophosmin***
	RNA binding motif protein 3	RNA binding motif protein 3	Activator of dsRNA kinase
			CYFIP2
			Y box binding protein 1

Table I – Proteins identified from RNP purifications. Each column represents a separate study and separate purification strategy. Proteins from each publication and re-formatted into the above table and categorized by function. Proteins highlighted in yellow are common to all three purifications, proteins in bold/italic were identified from the GRNA chromatography experiment.

Figure 1

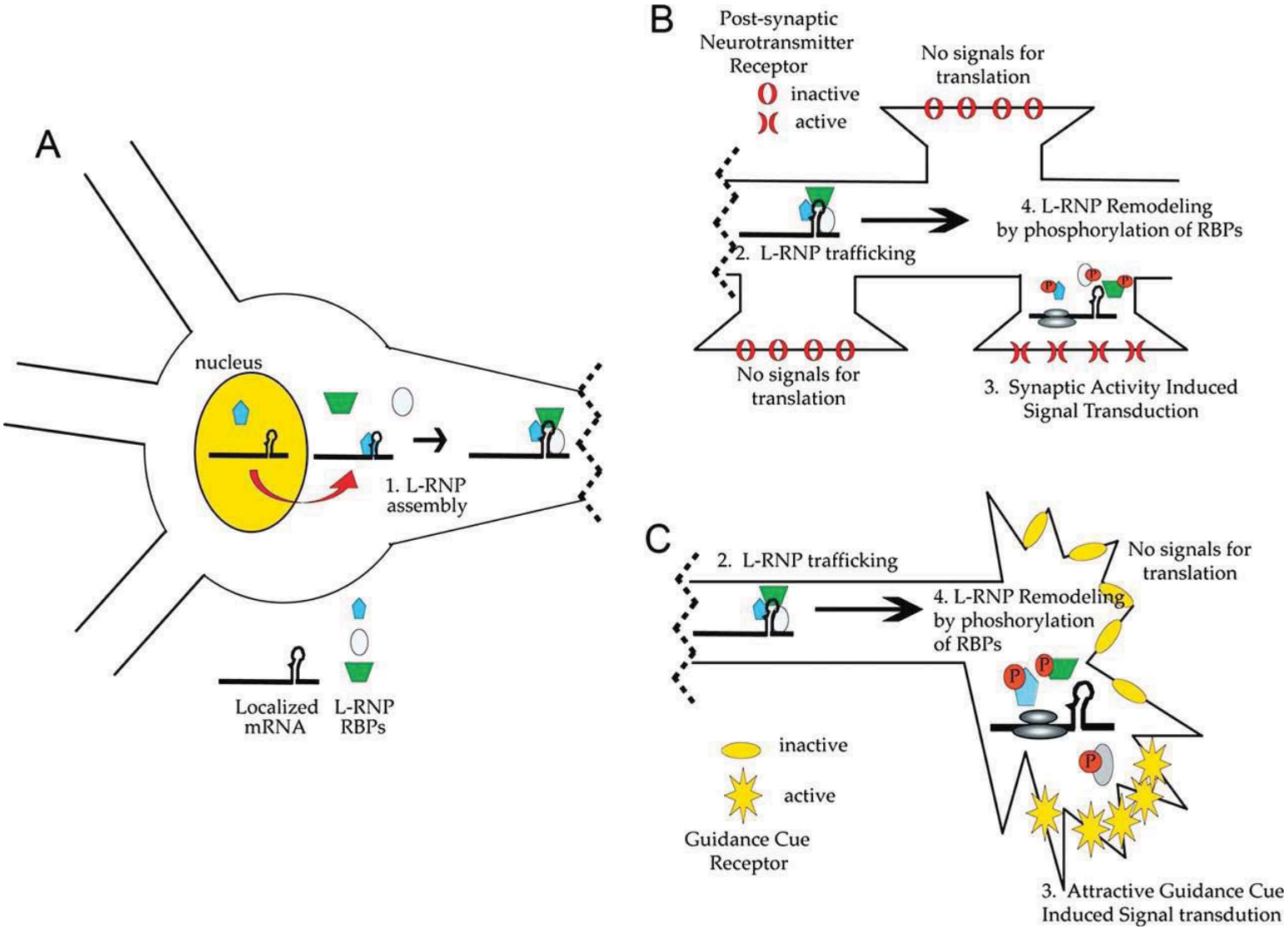

Figure 1: mRNA trafficking to localized translation domains (A) L-RNP formation occurs in the cell soma, where nuclear RBPs (blue pentagon) bind mRNAs to be localized and export with them to the cytoplasm. After export, cytoplasmic RBPs or other L-RNP factors join the mRNA to form a translationally repressed L-RNP (step 1). The L-RNP interacts with the cytoskeleton (not pictured) to traffic the L-RNP (step 2) to either dendrites (B) or axons (C). The factors and connections to the cytoskeleton remain poorly understood, although microtubule motor dependent cargo trafficking plays a role in this process. Trafficking L-RNPs are formed so that they initiate translation on encountering a translation inducing signaling environment (step 3). (B) In dendrites L-RNPs remodel when they encounter the cytoplasm near activated synapses (step 4). The kinases activated by synaptic activity modify factors on the L-RNP (P groups attached to RBPs) to induce remodeling of the L-RNP so that the RNA is now available for translation. The lack of signaling in inactive synapses can explain why only active synapses activate translation. (C) In axon growth cones L-RNPs remodel when guidance cues asymmetrically signal to growth cones, activating the kinases that phosphorylate RBPs in the L-RNP. The text describes examples of RBPs contained within L-RNPs that are modified by signal transduction kinases.

Figure 2

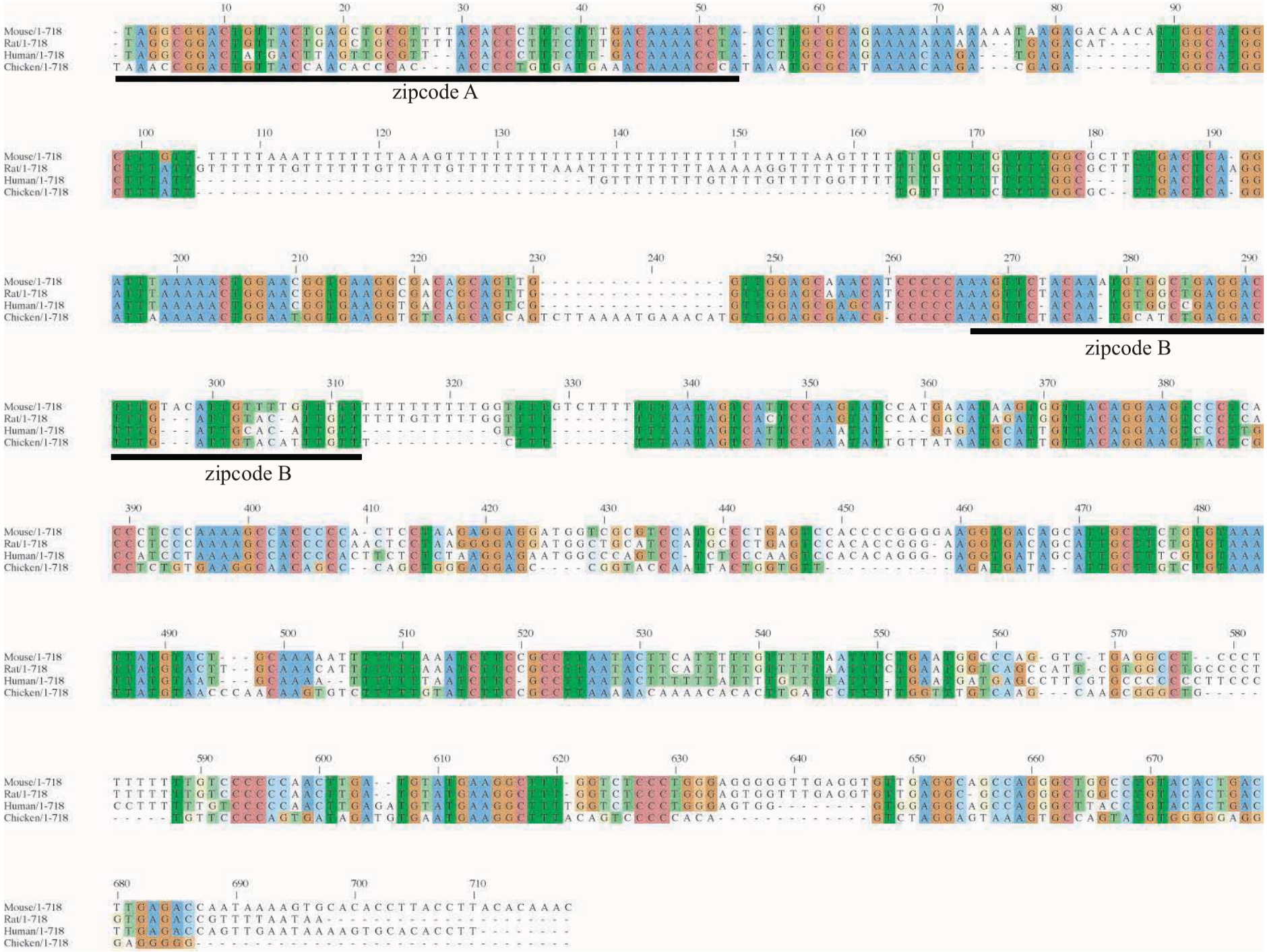

Figure 2- Actb zipcodes are evolutionarily conserved. Actb 3' UTR for indicated species are aligned with the zipcode A and B sequence from chicken indicated by the black bars.

Figure 3


[Actb 15 AGTTGCGTTACACCCTTTCTTGACAAAACCTAACTTGCGCAGAAAACAAG 64
[Actg 12 AGATGCGTAGCA----------- 23
[Actb 65 ATGAGATTGGCATGGCTTTATTTGTTTTTTTTGTTTTGTTTTGGTTTTTT 114
[Actg 24 ----------- 23
[Actb 115 TTTTTTTTTTGGCTTGACTCAGGATTTAAA---------- 144
[Actg 24 TTTGCTGCATGGGTTAATTGAGAATAGAAATTTGCCCCTGGCAAATGCAC 73
[Actb 145 ----------AACTGGAA---------- 152
[Actg 74 ACACCTCATGCTAGCCTCACGAAACTGGAATAAGCCTTCGAAAAGAAATT 123
[Actb 153 --CGGTGAAGGTGA----------CAGCAGTCGGTTGGAGCGAGCATCCC 190
[Actg 124 GTCCTTGAAGCTTGTATCTGATATCAGCACTGGATTGTAG---------- 163
[Actb 191 CCAAAGTTCACAATGTGGCCGAGGACTTTGA---------- 221
[Actg 164 ----------AACTTGTTGCTGATTTTGACCTTGTATTGAAGTTAACT 201
[Actb 222 TTGCACATTGTTGTTTTTTTAATAGTCATTCCAAATATGAGA-------- 263
[Actg 202 GTTCCCCTTGGTATTTGTTTAATACCCTGTACATATCTTTGAGTTCAACC 251
[Actb 264 ----------- 263
[Actg 252 TTTAGTACGTGTGGCTTGGTCACTTCGTGGCTAAGGTAAGAACGTGCTTG 301
[Actb 264 ----------- 263
[Actg 302 TGGAAGACAAGTCTGTGGCTTGGTGAGTCTGTGTGGCCAGCAGCCTCTGA 351
[Actb 264 ----------- 263
[Actg 352 TCTGTGCAGGGTATTAACGTGTCAGGGCTGAGTGTTCTGGGATTTCTCTA 401
[Actb 264 ----------- 263
[Actg 402 GAGGCTGGCAAGAACCAGTTGTTTTGTCTTGCGGGTCTGTCAGGGTTGGA 451
[Actb 264 ----------TGCGTTGTTACAGGAAGTCCCTTGCC 289
[Actg 452 AAGTCCAAGCCGTAGGACCCAGTTTCCTTTCTTAGCTGATGTCTTTGGCC 501
[Actb 290 ATCCTAAAAGCCACCCCACTTCTCTCTAAGGAGAATGGCCCAGTCCTCTC 339
[Actg 502 A----------- 502

```
[Actb            340 CCAAGTCCACACAGGGGAGGTGATAGCATTGCTTT---------------   374
                     |..|||...|||..|.|..|.||.|||..||
[Actg            503 ----GAACACCGTGGGCTGTTACTTGCTTTGAGTTGGAAGCGGTTTGCAT   548

[Actb            375 -----CGTGTAAATTATGTAATGCAAAATTTTTTTAATCTTCGCCTTAAT   419
                      |.|||||||....|.||.|..|||||.|.|||..||
[Actg            549 TTACGCCTGTAAATGTATTCATTCTTAATTTATGTAAGGTT---------   589

[Actb            420 ACTTTTTTATTTTGTTTTATTTTGAATGATGAGCCTTCGTGCCCCCCCTT   469

[Actg            590 --------------------------------------------------   589

[Actb            470 CCCCCTTTTTTGTCCCCCAACTTGAGATGTATGAAGGC-----------T   508
                      ||||||||.|.|.|...|....|.|.||||||..           |
[Actg            590 -----TTTTTTGTACGCAATTCTCGATTCTTTGAAGAGATGACAACAAAT   634

[Actb            509 TTTGGTCTCCCTGGGAGTGGGTGGAGGCAGCCAGGGCTTACCTGTACACT   558
                     ||||||.|                                  |.|||..|
[Actg            635 TTTGGTTT-----------------------------------TCTACTGT   650

[Actb            559 GACTTGAGACCAGTTG------------------------------AATA   578
                     .|..|||||.||.|.|                               ||||
[Actg            651 TATGTGAGAACATTAGGCCCCAGCAACACGTCATTGTGTAAGGAAAAATA   700

[Actb            579 AAAGTGCACACCTTAAAAATGAAAAAAAAAAAAAAAAAAAA    619
                     |||||||...|.|    ||..||||||||||||||||||
[Actg            701 AAAGTGCTGCCGT----AACCAAAAAAAAAAAAAAAAAAA    737
```

Figure 3 –The 3' untranslated region of human Actb and Actg mRNA are not homologus. The indicated sequences were obtained from the NCBI database and aligned using the EMBL pair-wise sequence alignment tool which looks for the highest level of homology using the Smith-Waterman algorithm. The displayed sequence has less than 25% identity with a gap allowance of 20 and contains over 65% gaps. If the gap allowance is raised only the poly(A) tail remains homologous.

Chapter 2: Identification of Hnrnpab1 as a brain zipcode binding protein

**This chapter is part of a manuscript in the process of being submitted for publication*

Abstract: No direct biochemical isolation of Actb zipcode binding proteins from a mammalian system has been reported and it is unlikely the known ZBPs are sufficient to explain the trafficking of Actb mRNA on their own. I used RNA affinity chromatography using the Actb mRNA zipcode and identified twelve putative brain zipcode binding proteins (bZBPs) from the rodent brain. Of the putative bZBPs only Hnrnpab1is a true Actb mRNA binding protein and full length Hnrnpab1 is required for the interaction.

Results:

Identification of putative Actb brain zipcode binding proteins (bZBP)

As a first step in understanding the mechanism of Actb mRNA trafficking in the nervous system, I wanted to identify what factors interacted with the Actb mRNA localization element (LE) in the mammalian nervous system. The LE for Actb mRNA has not been mapped in mammals, however, the chicken zipcode A and B sequences are highly conserved. I chose to define the LE based on the first 233 nucleotides (nts) of the 3' UTR of Actb mRNA since this sequence contains both the zipcode A and B sequences. I will refer to this element as the zipcode or zipcode 233 in the remainder of this document. I used this sequence to perform GRNA chromatography, an RNA affinity purification strategy used to identify novel mRNA localization factors [103]. GRNA chromatography uses glutathione S-transferase (GST) fused to the 21 amino acid peptide of the lambda phage N anti-terminator protein, which interacts specifically with the BoxB sequence of the N utilization site of lambda phage RNA that is fused to a target RNA to create an RNA affinity column using glutathione sepharose [103].

Cytoplasmic extract from embryonic rodent brain was incubated with GRNA columns containing a no RNA control, the Actb zipcode and the Actb 5' UTR, which is not required for

localization. Unbound proteins were washed away and proteins retained on the RNA columns were eluted and run on a gradient SDS-PAGE gel. Silver staining revealed multiple proteins unique to the RNA containing lanes as well as both the zipcode and 5' UTR of Actb (Figure 4, compare lanes 1, 2 and 3). Bands enriched in the zipcode containing lane were cut out of the gel and sent for mass spectrometric identification. The location of the bands and the identity of the proteins contained in each band are indicated by arrows in Figure 4.

Hnrnpab1 and Hnrnpab2 bind to different sequences in the Actb mRNA

In looking at the list of putative bZBPs and researching their functions, heterogenous ribonucleoprotein type A/B (Hnrnpab) seemed likely to be involved in mediating Actb mRNA localization. Rodent Hnrnpab recognizes the trafficking sequence of Myelin Basic Protein (MBP) mRNA and co-localizes with MBP mRNA in cultured oligodendrocytes [104] Hnrnpab orthologs co-purify with the Actb trafficking sequence from chicken brain [91] and bind specifically to a vegetal pole trafficking element from Vg1 mRNA and is required for its trafficking in *Xenopus* oocytes [103]. The Hnrnpab like protein Squid (Sqd), binds to gurken mRNA localization sequences in *Drosophila* and has also been shown to traffic oskar mRNA in *Drosophila* [105-107]. Hnrnpab has also been identified in unbiased screens for proteins involved in localization of mRNAs in the nervous system, including Actb mRNA but was never studied directly for a role in Actb trafficking [29-31].

To examine the interaction between Hnrnpab and the zipcode, I repeated the GRNA chromatography and probed the eluted proteins with an antibody raised an Hnrnpab N-terminal peptide. The mammalian HNRNPAB gene produces two isoforms as a result of alternative splicing of the 7th exon (Figure 5). The full length protein is referred to as Hnrnpab1 and the

smaller spliced isoform as Hnrnpab2. Both isoforms were present in the extract and were eluted from the zipcode, but Hnrnpab2 was also eluted from the 5'UTR (Figure 6A). This result was unexpected because both isoforms of Hnrnpab contain identical RNA recognition motifs (RRMs) and would be predicted to have the same nucleic acid specificity. The differences in where the two proteins bind suggest they have different roles in the regulation of Actb mRNA.

To confirm a difference in the specificity between the two isoforms, I expressed each isoform with an N-terminal Flag-epitope tag in immortalized neural cells (INCs) generated from Hnrnpab knockout mice [108]. These cells provide an Hnrnpab null background to study the two isoforms independent of one another. Using RNP immunoprecipitation (RIP), I isolated Hnrnpab1 and 2 immune complexes and looked by RT-PCR (RIP-RT-PCR) to see if either isoform interacted with Actb mRNA and not Actg mRNA, which is not trafficked as Actb mRNA is [109-111]. Actb mRNA co-purified with both isoforms of Hnrnapb but not a GFP control, confirming both isoforms interact with Actb mRNA independent of the presence of the other isoform. Importantly, Actg mRNA co-purified only with Hnrnpab2, corroborating the difference in specificity observed in the GRNA chromatography and indicating it is unlikely to be involved in the trafficking of Actb mRNA (Figure 6B).

Full length Hnrpab1 is required for interaction with Actb mRNA

The difference between the two isoforms of Hnrnpab is the presence of exon7 in Hnrnpab1. Since Hnrnpab1 bound the zipcode but not the 5' UTR, I hypothesized the specificity must somehow be mediated by exon 7. To determine if exon 7 or any single domain of Hnrnpab was sufficient for interaction with Actb mRNA, I examined the ability of several Hnrnpab truncations to co-purify Actb mRNA. The truncations, diagramed in Figure 7A, were stably expressed in Hnrnpab$^{-/-}$ INCS as Flag-tagged proteins. The N and C terminal fragments of

Hnrnpab1 were not detectable when expressed on their own, and so they were fused to cyan fluorescent protein (CFP), which facilitated accumulation of the two truncations. RIP- revealed that all of the truncations were expressed and successfully immunoprecipitated (Figure 7B). However, RT-PCR of bound mRNA revealed only full length Hnrnpab was capable of interacting with Actb mRNA (Figure 7C).

To confirm that the RRM containing Hnrnpab constructs were capable of interacting directly with RNA, I used cross-linking immunoprecipitation (CLIP). UV-light can form a covalent cross-link between proteins and closely associated nucleic acids. To ensure the binding of the Hnrnpab constructs was to RNA and not DNA, a high concentration of DNase was added to the extract prior to immunoprecipitation. The CLIP experiment demonstrated that all of the RRM containing constructs were capable of cross-linking to RNA (Figure 8). Together these results suggest that Hnrnpab1 interacts directly with RNA but that the specific interaction with Actb is dependent on the presence of exon 7 but only in the context of the full length protein.

Only Hnrnpab1 and Elavl1 (HuR) bind to Actb but not Actg mRNA

I went on to corroborate the binding of the other putative bZBPs by expressing Flag-epitope tagged versions in neuro2A (N2A) cells, a mouse neuroblastoma line. I confirmed expression of each putative bZBP in both whole cell lysate and in the cytoplasmic lysates used for RIP (Figure 9). SFPQ and NONO, are detectable in whole cell lysates but are not seen in high concentrations in cytoplasmic lysates and therefore were not examined by RIP. I was unable to clone the PKR ORF and therefore, PKR was not tested in this assay.

The bZBPs that were extractable in cytoplasmic lystates were immunoprecipitated with the anti-Flag M2 monoclonal antibody and evaluated for their ability to co-purify Actb mRNA as compared to a GFP expressing N2A cell control. Preliminary studies suggest nucleophosmin,

hnRNP D, PSPC1 and HuR all co-purify Actb mRNA. However, only Elavl1 (HuR) does not also co-purify Actg mRNA. HuR binds a U-rich region within nt 155-190 of the zipcode used for GRNA chromatography, and HuR binding within this region is strongly associated with Actb mRNA stability since siRNA knockdown of HuR leads to a decrease in Actb mRNA stability [112]. Because HuR binds outside of the zipcode A or B regions and is involved in mediating Actb mRNA stability it is unlikely that HuR is involved in active trafficking of Actb mRNA. Of the putative bZBPs I identified, only Hnrnpab1 bound to the zipcode of Actb mRNA and did not bind to Actg mRNA, strongly indicating a role in Actb mRNA trafficking.

Discussion

GRNA purification of putative bZBPs

The purification of a putative trafficking complex containing Actb mRNA by Elvira et al. identified many of the same proteins identified as enriched for the Actb zipcode by GRNA chromatography. Nucleophosmin (Npm1), hnRNP A0, Hnrnpab and hnRNP D were all detectible in this complex, which also included the Actb mRNA binding proteins ZBP1, ZBP2, PTB, hnRNP U, hnRNP R and several Elavl proteins (although interesting not Elavl1), see table I and [30]. Other proteins identified by the GRNA chromatography have been identified in other purifications of putative trafficking complexes. hnRNPA0, NONO/p54NRB, PSPC1 and SFPQ/PSF were found in a complex containing Arc and CaMKIIα mRNA and both NONO and SFPQ were also found along with PKR in a separate study with CaMKIIα mRNA, see table I and [29, 31]. However, when examining these studies what stuck out the most to me is there are only seven proteins present in all of three purifications, Deadbox helicases DDX1, 3 and 5, hnRNP U, hnRNP D and Hnrnpab. And of these seven proteins only Hnrnpab has an established

role in mRNA trafficking, providing further support for its importance in mRNA localization in the nervous system.

Hnrnpab1 and Hnrpab2 both bind the zipcode but Hnrpab2 binds other regions of the Actb mRNA

Examining the biochemical interaction between Hnrnpab and the zipcode revealed the two isoforms of Hnrnpab have different binding targets within Actb mRNA and suggest they may function in different aspects of its regulation. The presence of exon 7 in Hnrnpab1 must be involved in mediating binding to the zipcode as this is the only difference between the two proteins (Figure 5). We hypothesize that exon 7 may interact with the RNA recognition motifs of Hnrnpab1 and stabilize the interaction with the zipcode. Unpublished work by others in the lab demonstrates by electric mobility shift assay (EMSA) that the purified RRMs of Hnrnpab bind to the human 54 nt zipcode A sequence with a nanomolar affinity. Importantly, there is no detectable interaction of the RRMs with the 115 nt sequence in between the two zipcode elements. It will be interesting to test if the presence of exon 7 affects the affinity of the RRMs and if they are capable of interacting with the 43 nt zipcode B sequence. I hypothesize the presence of exon 7 will allow for a stable dimer of Hnrnpab1 on the zipcode A sequence, while Hnrnpab2 may form a more unstable heterodimer with Hnrnpab1 or homodimer with another Hnrnpab2 molecule.

Functions of t he ot her proteins i dentified by G RNA and t heir pos sible r ole i n A ctb m RNA regulation

Based on the role each protein identified by GRNA chromatography plays in other contexts a plausible function for each protein in Actb mRNA regulation can by hypothesized. ***However, it is important to remember that of all of the proteins identified; only Hnrnpab1 is a true bZBP***. hnRNP A0, is a member of the hnRNP A family of proteins, although it shares limited homology to the rest of the family[113]. It is produced from a processed pseudogene and is less abundant and less understood than other family members. hnRNP A0 was originally identified as binding to a $G_4(AU_3)_4A$ sequence from HeLa cells and was later identified as part of a group of proteins which bound to a tumor necrosis factor alpha (TNF-α) AU rich element (ARE) probe from RAW 264.7 extract[113, 114]. The ARE of TNF-α located in the 3' UTR of the mRNA regulates its translation. However, other mRNAs including those for cyclo-oxygenase 2 (COX2) and FBJ murine osteosarcoma transcription factor (c-FOS) contain AREs, which regulate the stability of the mRNA[114]. TNF-α and COX2 mRNA can be found in hnRNP A0 immune complexes and macrophage inflammatory protein 2 (MIP2) can be found only if the cells are treated with lipopolysaccharide (LPS) treated cells. hnRNP A0 is phosphorylated by MAPKAP-2, which results in a reduction in the ability of hnRNP A0 to immunoprecipitate the above mRNAs[114]. It remains unclear what role hnRNP A0 plays in the regulation of these mRNAs. However, hnRNP A0 has been shown to bind to and stabilize Gadd45a mRNA following phosphorylation by p38[115]. The other members of the hnRNP A family are involved in splicing and hnRNP A0 has been found in complexes involved in splicing, suggesting it may play multiple roles in RNA regulation.

Embryonic lethal-abdnormal vision-like protein 1 (Elavl1) is a member of the Elav-like family of proteins which are orthogues of the Elav gene in *Drosophila*[116, 117]. They are more commonly known as the Hu family of proteins, named because they were identified as reacting to antigens in paraneoplasmic neurological disorder from serum of the patient denoted as Hu[118]. There are four members of the family Elavl 1-4 also known as HuR (also called HuA), B, C and D, which are very similar but differ in the hinge region between the second and third RNA recognition motif (RRM). HuR is expressed in all tissues, while HuB through D are expressed only in neurons (also called the nElavls or nHu proteins). All four proteins bind AU rich elements within mRNAs, although other binding sequences have been described[119].

HuR function in multiple aspects of mRNA regulation including stabilization and translation. The stabilization effects of HuR is believed to be due to their ability to compete for binding with destabilizing proteins, which stimulate the deadenylase poly(A) ribonuclease (PARN) or other RNA degradation mechanisms[89]. However, recent evidence suggests that HuR may bind both competitively and cooperatively with the destabilizing protein HnrnpD (AUF1) on p21 and cyclin D1 mRNAs. In addition, HuR has been shown to regulate the translation of target mRNAs by binding to either the 3' or 5' UTR. For example, HuR increases the translation of cytochome C and p53 through interactions with the 3' UTR, while it binds to the 5' UTR and enhances the association of hypoxia inducible factor 1α mRNA with translating ribosomes[119]. HuR can also repress translation of given mRNA. Interestingly, HuR both stabilizes and suppresses the translation of Cox2 and TNF mRNA[120].

There is emerging evidence that the Hu proteins may also play a role in mRNA localization, although that role may be in stabilizing the localized transcript or regulating translation. The Twiss group has recently shown that HuD binds to an AU rich element which is

necessary and sufficient for trafficking GAP43 mRNA[121]. HuD has also been implicated with other trafficked mRNAs including tau and cpg15. Multiple members of the Hu family have also been identified in a putative trafficking complex containing Actb mRNA[30]. HuR is an established Actb mRNA binding protein, however it binds to a U rich sequence downstream of the zipcode A sequence and increases the stability of the transcript[112]. Due to the inclusion of the HuR binding site within the zipcode 233, the presence of HuR was expected and provided evidence that the purification strategy was a success.

hnRNP D (AUF1), is the founding member of the hnRNP D family, which contains both Hnrnpab and hnRNP DL (hnRNP D-like, also known as JKTBP). hnRNP D contains four isoforms as a result of alternative splicing of exons 2 and 7. The isoforms are named for their molecular weights, p45 is the full length protein, p42 contains exon 7 but not exon 2, p40 contains exon 2 but not exon 7 and p37 lacks both alternatively spliced exons[122, 123]. All four isoforms contain the identical RRMs which are required but not sufficient for high affinity nucleic acid interaction and the exon 2 sequence appears to inhibit ARE binding by up to 5 fold [124, 125]. The different isoforms have different sub-cellular localizations, P45 and P42 are primarily nuclear while P37 and P40 are both nuclear and cytoplasmic[122]. The isoforms can all form dimers and can bind sequentially, although the p42 and p45 oligomers are more stable, suggesting a stabilizing effect of the exon 7 sequence[125]. Initially identified as increasing the decay of c-myc mRNA, there are now a large number of mRNA targets, although like c-myc most of them are AU rich and destabilized by hnRNP D [126]. There is some evidence the different isoforms of hnRNP D have different target mRNAs and possibly different functions in regulating stability, although the isoforms have traditionally been studied individually[126, 127]. Actb mRNA, while containing an U rich region, has not been described as an hnRNP D binding

target and although as previously mentioned hnRNP D is present in all putative trafficking granules, it has not been studied in the context of mRNA trafficking.

Nucleophosmin (Npm1) also known as B23, NO38 or numatrin, is a member of the Nucleoplasmin family of proteins and functions in multiple aspects of cell proliferation. Npm1 has two splice variants, full length Npm1.1 and Npm1.2, which does not contain the C-terminal domain required for both RNA interaction and nucleolar targeting[128]. The Npm1 gene is a common target for chromosome translocation and frame-shift mutations in the C-terminus are found in many myeloid leukaemias. Npm1 is a protein and histone chaperone and is involved in a wide variety of cellular processes including ribosome biogenesis and transport and transcription[128]. Npm1 is also recently been associated with many poly(A) mRNAs and with CPSF poly-adenylation factor. Knockdown of Npm1in HeLa cells causes an increase in poly(A) tail length and retention of poly(A) mRNA, suggesting a role in poly(A) termination and mRNA export[129]. Interestingly, Npm1 was also found to bind to the minimal repressive element of the CCN2 mRNA in chicken chondrocytes and Npm1 level was correlated with CCN2 mRNA stability[130]. Due to the wide number of functions of Npm1, there are multiple possibilities for its association with the Actb mRNA zipcode including transcription, poly(A) tail regulation and stability. Comparing the zipcode and 5' UTR GRNA lanes would suggest Npm1 has a relatively high affinity for the zipcode and should be pursued further.

Three members of the *Drosophila* behavior/ human splicing (DBHS) family of RNA binding proteins were identified by the GRNA chromatography as enriched for the zipcode sequence: polypyramide tract binding protein (PTB) associated splicing factor (PSF), also known as splicing factor proline/glutamine rich (SFPQ), 54kDa nuclear RNA binding protein (p54 nrb), also known as non-POU containing, octamer binding protein (NONO), and paraspeckle

component 1 (PSPC1). SFPQ was initially identified and characterized as interacting with PTB, an important determinant of the 3' splice site. It has since been shown to be part of the human splicesome, the splicesome C complex and co-purified with the U4/U5-U6 snRNPs[131]. However, the majority of SFPQ is not associated with PTB but with the nuclear matrix. SFPQ associates with the homologous protein NONO, although its ability to regulate splicing was originally thought to be independent of this interaction. However, evidence suggests an association of NONO with the 5' splice site and both proteins bind to the U5 snRNA and co-sediment with the U4/U5-6 snRNPs[132, 133]. SFPQ and NONO have been shown to be in a transcriptional repression complex containing the repressor protein sin3A and histone deacetylases (HDACs) and to regulate the transcription of multiple genes[131]. Recent evidence also points to an involvement in DNA double strand break repair and in the recruitment of the exonuclease XRN2 to mediate pre-mRNA processing and transcriptional termination[134, 135].

Paraspeckles were identified initially following the proteomic analysis of human nucleoli [136]. One of the novel proteins identified in the proteomic screen was found to localize in sub nuclear foci in the interchromatin space which were not nuclear speckles. These foci were later named paraspeckles and the novel protein leading to their identification PSPC1[137]. PSPC1 is also a member of the DBHS family and shares significant homology to both SFPQ and NONO. It is localized to paraspeckles in transcriptionally active cells but when RNA polymerase II is inhibited it localizes to perinucleolar cap structures[137]. Paraspeckles are only found in mammalian nuclei (although they are absent from human embryonic stem cells) and require SFPQ and NONO for structural integrity in HeLa cells [137, 138]. Two RNA components of paraspeckles have also been identified. Ctn RNA is implicated in RNA nuclear retention while the nuclear RNA (ncRNA) NEAT1, is essential for the formation of paraspeckles[139].

It is hypothesized that one function of paraspeckles is the retention of A to I edited RNAs. This process is mediated by double stranded RNA-dependent adenosine deaminases, which convert random adenosines to inosines. Many edited RNAs are confined to the nucleus by a complex containing both NONO and SFPQ and the nuclear matrix protein matrin 3. NONO has been shown to bind to I-RNA both *in vitro* and *in vivo* retention of edited RNAs is correlated with paraspeckle formation[139]. I could find no evidence that Actb mRNA is A to I edited but recent evidence points to PSPC1 as a part of the SFPQ-NONO complex involved in the transcriptional repression of the androgen receptor. Knocking down SFPQ using siRNA suppressed the distribution of a reporter RNA containing the CAMKIIα 3' UTR, although this observation has not been followed up. All three members of the DHBS family have been identified in L-RNP purification strategies, although their potential role in trafficking has for the most part been ignored. [29]. I hypothesize they are part of the initial co-transcriptional formation of the Actb RNP although this remains to be tested.

The protein SET/I2PP2A/TAF-1β, identified as a translocated gene in acute undifferentiated leukemia and a potent inhibitor of the serine/threonine phosphatase PP2A, can be found in two isoforms (SETα and SETβ) and is an important multi-functional protein[140]. SET has been shown to regulate multiple aspects of cellular function including histone modification, G2/M transition, gene transcription, DNA replication, kinase/phosphatase activity and nucleosome assembly [141-144] Additional evidence points to a cytoplasmic role of SET in mediating apoptosis. SET has been shown to interact with the c-terminal fragment of amelyoid precursor protein (APP) and over-expression of SET leads to an increase in apoptosis in the context of expression of this fragment in PC-12 cells [145]. An increase in cytoplasmic SET was

also seen in human Alzheimer's brain tissue compared to healthy controls, further suggesting a role for SET in mediating neuronal apoptosis [146].

This is the first direct evidence of SET having a role in regulating Actb, however other studies have suggested a possible role in regulating the cytoskeleton and mRNA. SET has been shown to interact with the Rho GTPase Rac1 and reduction in SET expression inhibits Rac1-induced migration, which does involve cytoskeletal dynamics[147]. SETα, SETβ, pp32, and APRIL were all identified as interacting with the hinge region of the mRNA stability factor Elavl1 (HuR) in an RNA independent manor, although the function of this interaction has not been determined[148]. In addition, the RNA binding protein hnRNP A2 was found to interact with SET and cooperate in the inhibition of PP2A[149]. The interaction with other pos-transcriptional regulators indicates that SET may have a more complex function in the cells than previously thought and the role SET plays in transcription may indicate it is involved in the co-transcriptional assembly of the Actb L-RNP complex.

Proteins not found in the GRNA chromatography

In comparing the proteins identified by the GRNA chromatography to the RNA binding proteins known to be involved in post-transcriptional regulation of Actb mRNA, there is no overlap. However, this is not completely surprising since of the proteins described in the literature only ZBP1 has been shown to be specific for the zipcode of Actb mRNA. However, the absence of ZBP1 in the visible specific bands resulting from the GRNA is also not unexpected. The ZBP1 ortholog Vg1RBP/Vera has been shown to bind to the Vg1 LE during *Xenopus* oogenesis but was not identified in a similar unbiased screen for proteins binding specifically to the Vg1 LE and Vg1RBP also recognizes non-localizing RNAs [103]. There are striking

similarities between the process of trafficking Vg1 mRNA in *Xenopus* and Actb mRNA. Another Actb mRNA regulating protein PTB/ hnRNP I, is involved in the localization of Vg1 mRNA but was also not directly identified in RNA chromatography using the Vg1 LE[103, 150]. However, the Hnrnpab ortholog 40LoVe was specific for the LE of Vg1 and did not bind to non-localizing RNAs and is specific for the Actb zipcode. Vg1RBP, hnRNP I and 40LoVe all interact in the process of trafficking Vg1 mRNA and I would hypothesize this is true for Actb mRNA as well.

Experimental Contributions

Catherine Waddell: creation of immortalized neural cells, creation of Hnrnpab deletion vectors.

Antonius Koller: proteomic analysis of GRNA chromatography gel.

Figure 4

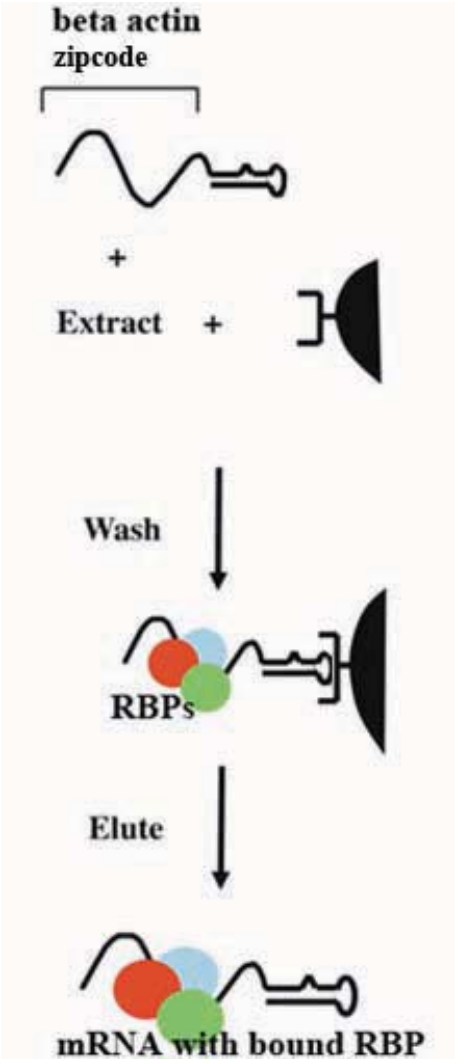

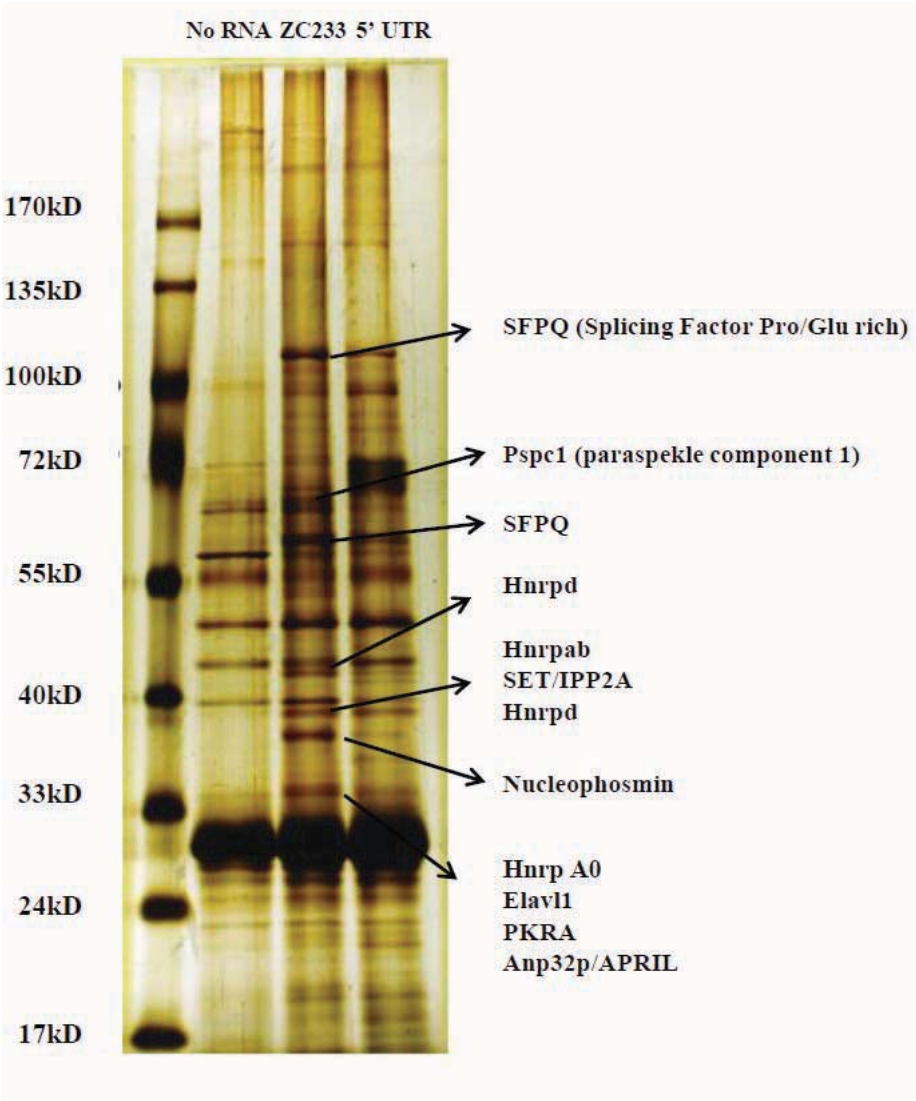

Figure 4: Identification of bZBPs using GRNA chromatography. Embryonic rodent brain extract was passed over columns containing a no RNA control (lane 1), the first 233 nucleotides of the human β-actin mRNA 3' UTR (lane 2) and the 5' UTR of human β-actin mRNA (lane 3). Elutes from columns were run on a gradient SDS-PAGE gel and silver stained. Bands enriched for both RNA containing lanes and the zipcode containing lane were sent for mass spectrometry analysis. The identified proteins from the isolated lanes are indicated by arrows.

Figure 5:

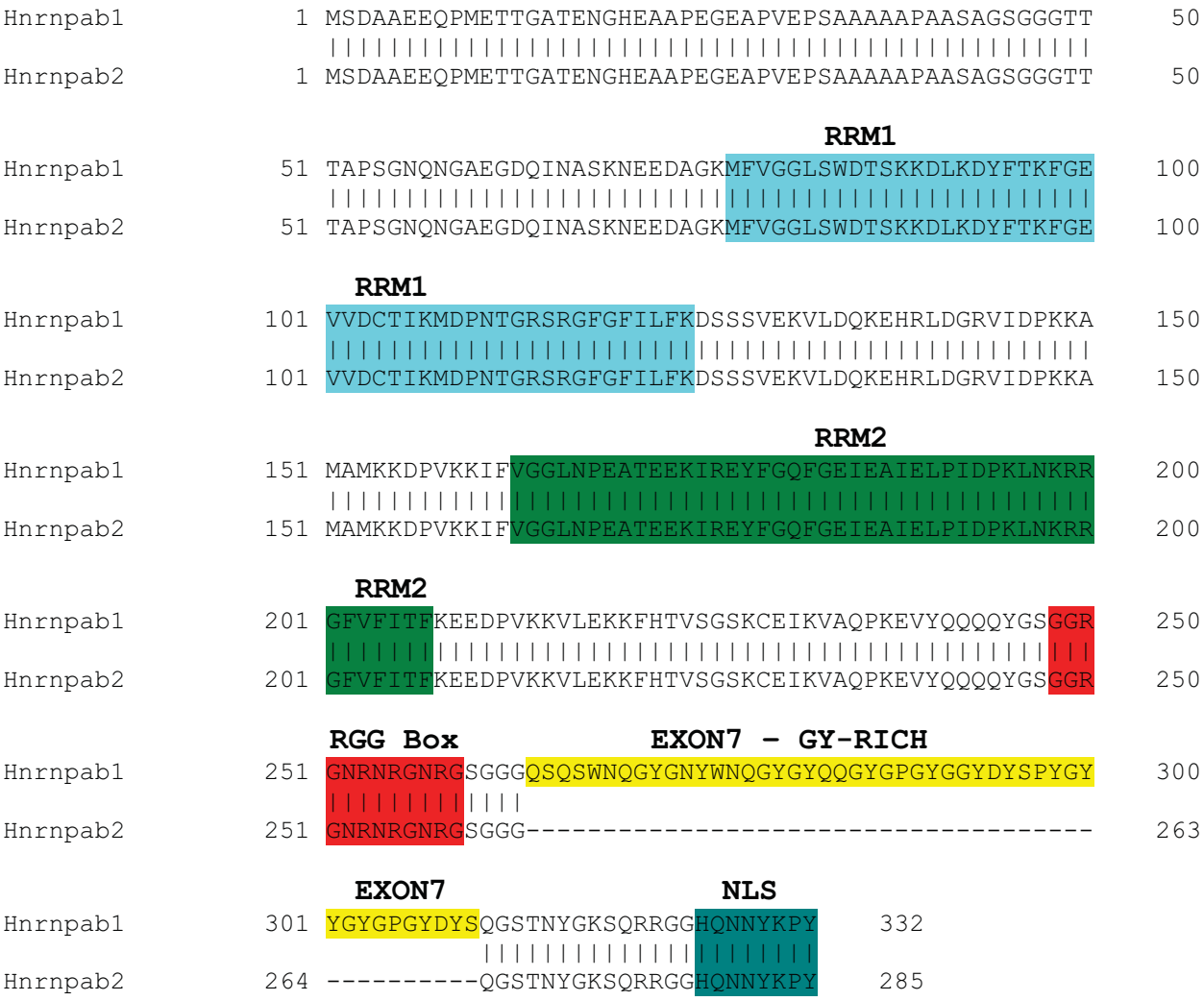

Figure 5- Hnrnpab1 and 2 amino acid sequence alignment. Mouse amino acid sequence obtained from the NCBI website was aligned using Clustal Omega software. The relevant domains were then highlighted. The nuclear localization sequence (NLS) is inferred based on results from hnRNP D and hnRNP DL and unpublished results from our lab.

Figure 6

A

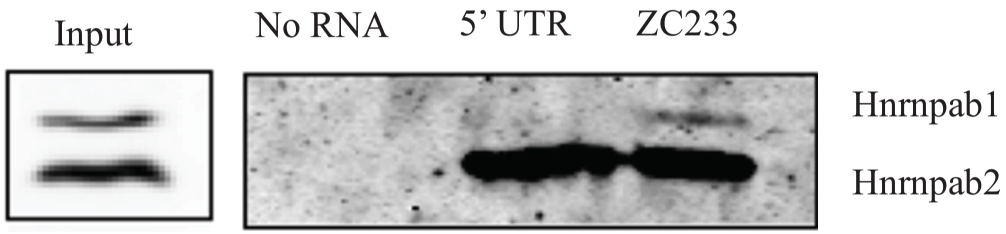

B

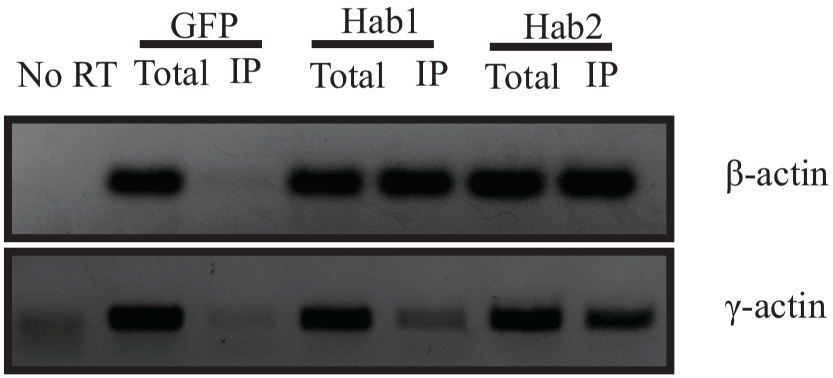

Figure 6: Hnrnpab1 is a Actb specific bZBP. A, GRNA chromatography elutes from the indicated columns were run on an SDS-PAGE gel and probed using an antibody against the N-terminus of Hnrnpab, which recognizes both isoforms. B, Cytoplasmic extract from cell lines expressing the indicated bZBPs was immunoprecipitated using M2 anti-Flag antibody. 200ng of total RNA and 100ng of immunoprecipitated RNA were reverse transcribed and amplified using Actb or Actg specific primers.

Figure 7

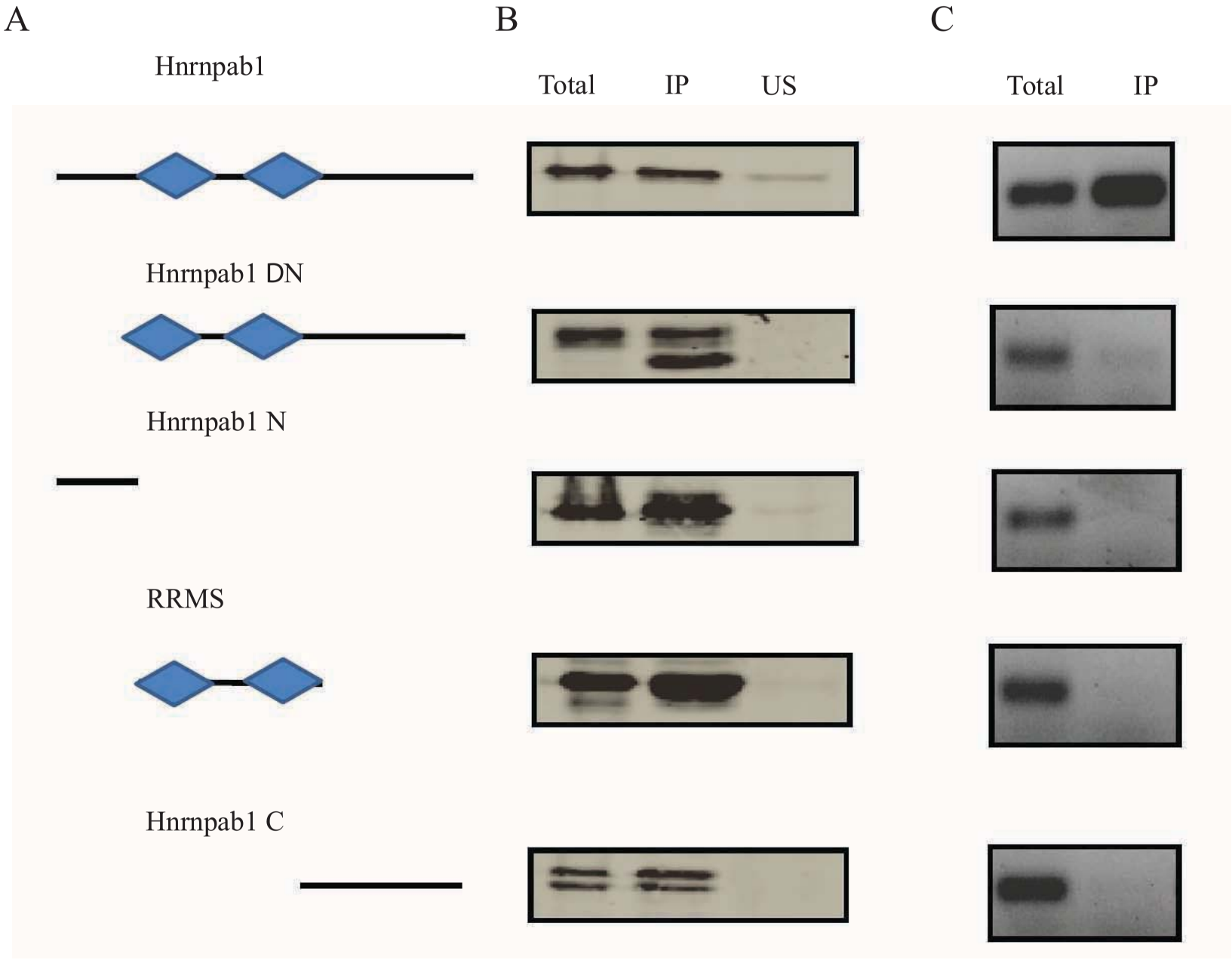

Figure 7: Full length Hnrnpab is required for the interaction with β-actin mRNA. A, diagram of deletion constructs expressed in INCs using lenti-viral particles. B, immunoblot of 50 ug of total extract, 1/5 of the immunoprecipitated protein and 50 ug of the unbound supernatant probed with M2 anti-Flag antibody. C, β-actin RT-PCR of 200 ng of total RNA and 100 ng of immunoprecipitated RNA.

Figure 8

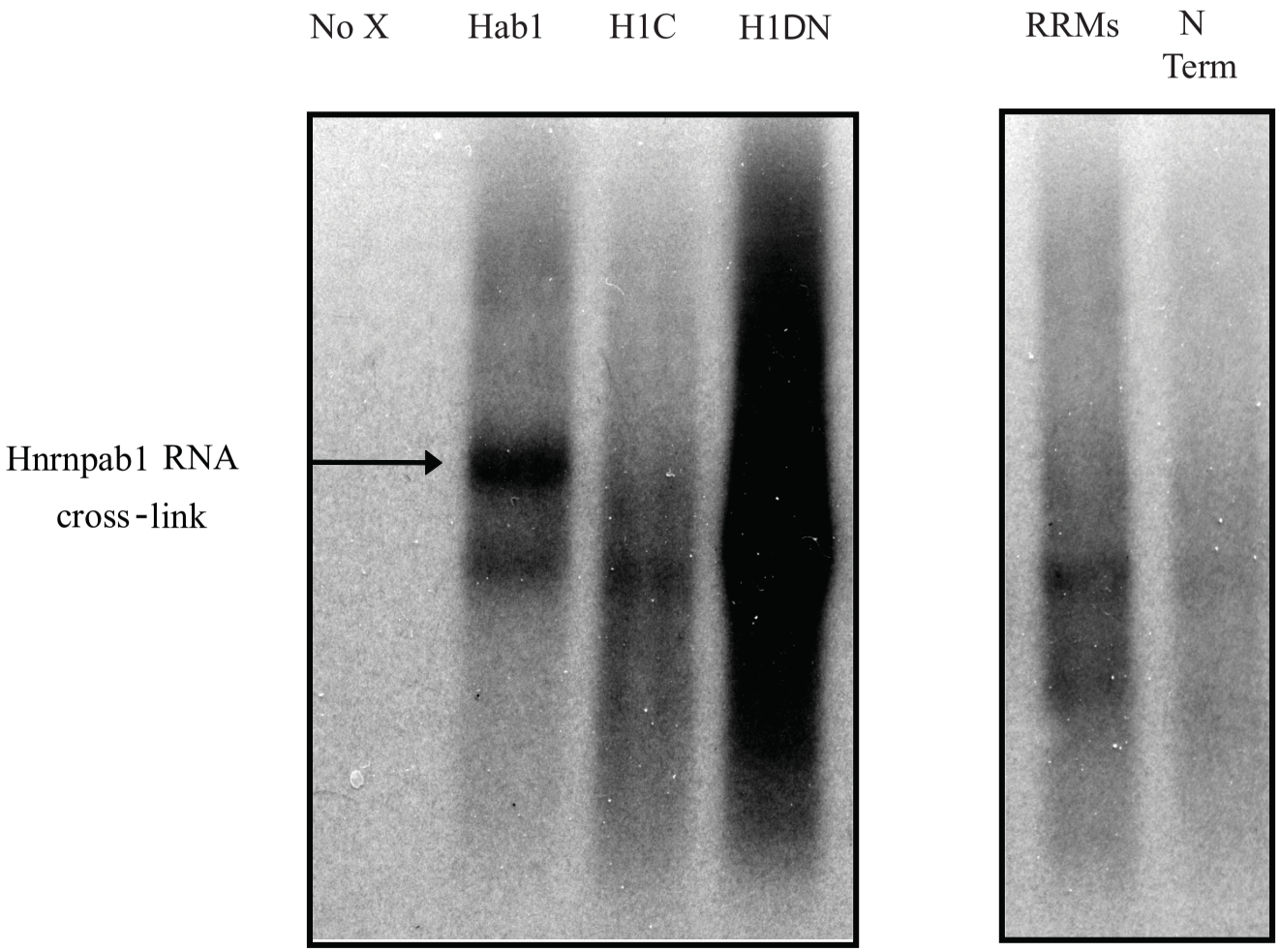

Figure 8: Multiple portions of Hnrnpab are capable of direct RNA interaction. Cells expressing the indicated Hnrnpab constructs were UV cross-linked, lysed in the presence of DNase and immunoprecipitated. Bound RNA was labeled with P^{32} and the RNA/Protein complexes were run on a bis-tris gel, transferred to nitrocellulose and exposed to film.

Figure 9

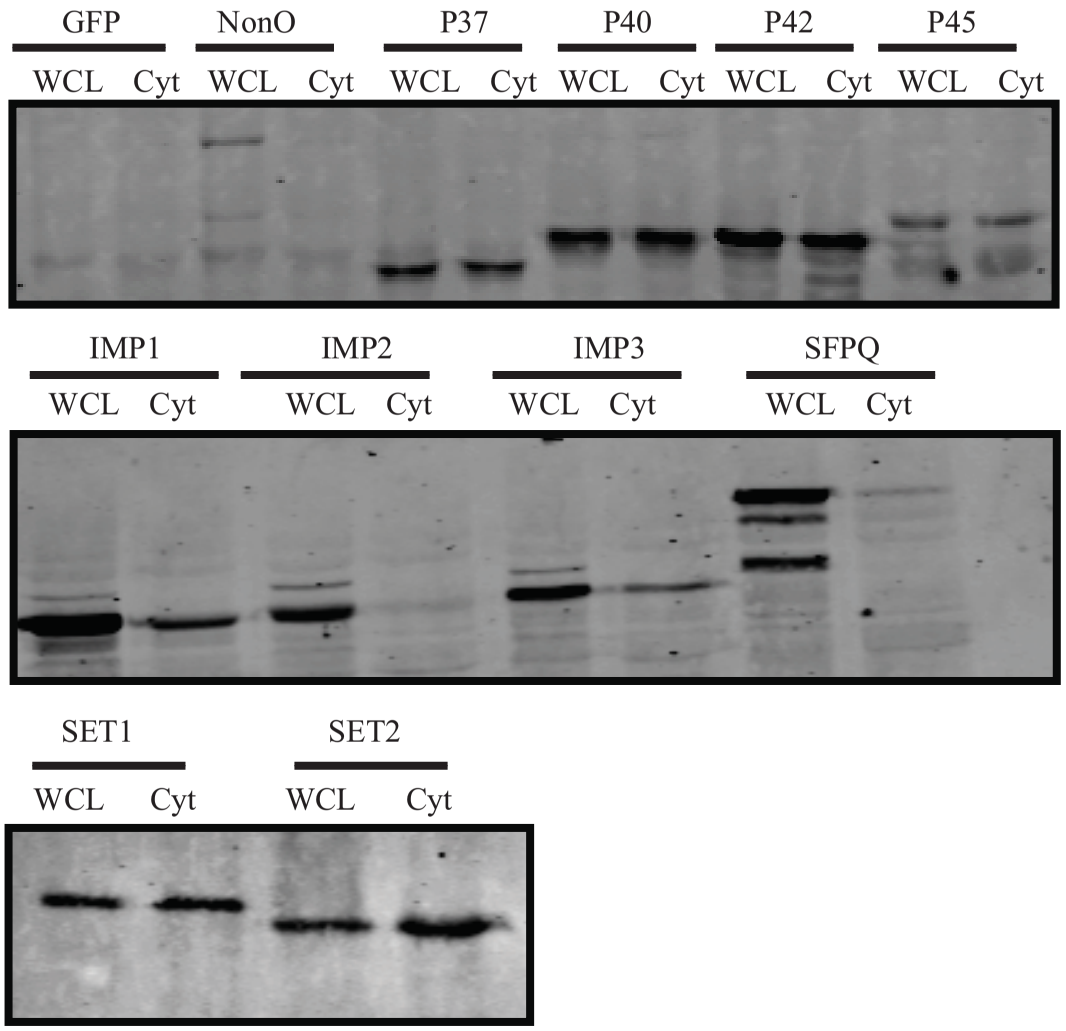

Figure 9: Creation of N2A cells expressing bZBPs. bZBP open reading frames were cloned into a lenti-viral expression vector and lenti-viral particles were used to infect neuro-2A cells. 50 ug of whole cell lysate and 100 ug of cytoplasmic lysate from N2A cells expressing the indicated bZBPs were run on an immunoblot and probed with the M2 anti-Flag antibody.

Chapter 3: Hnrnpab1 is required for the normal distribution of Actb mRNA

**this chapter is part of a manuscript which has been accepted for publication in RNA*

Abstract

To study an mRNA's localization requires the visualization of the distribution of a given mRNA within the cell. This requires detection of single mRNAs in single cells. The standard for detection of transcripts with single molecule resolution is fluorescent *in situ* hybridization (FISH) using multi-labeled anti-sense oligodeoxynucleotides (ODNs). However, these probes have many practical limitations. To determine the effect of Hnrnpab on Actb mRNA localization we developed a novel strategy for binding high concentration of commercially synthesized fluorescently labeled ODNs we call **F**luorescence **I**n **S**itu **H**ybridization with **S**equential **T**ethered and **I**ntertwined ODN **C**omplexes (FISH-STICs). In this chapter, I discuss the development of the FISH-STICs method and use it to demonstrate Hnrnpab1 is required for the normal distribution of Actb mRNA.

Introduction:

In v itro transcribed *in s itu* hybridization (ISH) probes have long been applied in histology, and whole mount gene expression pattern analysis, but they have found little application in single molecule RNA detection desirable in studies of mRNA localization [151, 152]. For that purpose multiply labeled fluorescent ODN probes can image single mRNAs (fluorescence in situ hybridization, FISH) [153, 154]. Synthesis of these FISH probes requires in house DNA synthesis to accommodate the multiple modified nucleotides for coupling, and post-synthesis dye coupling can be inefficient and difficult to control. Unlabeled probes compete with labeled probes in this case making well-labeled probes a must for the success of the technique. A desirable feature of these probes is that they can bind up to 5 dye molecules to stretches of mRNA 45-50 nucleotides (nt) in length making them amenable to detecting small patches of

RNA under the careful imaging conditions required to detect such probes. As a practical matter, the expense and difficulty involved makes these probes inaccessible to most labs. A cocktail of consecutive 20mer antisense ODN probes each coupled with a single dye molecule at the 5' end increases accessibility and mRNA detectability when larger stretches of an RNA are available to image [155]. In house coupling of dye to modified oligonucleotides is still difficult to control and large amounts of modified nucleotides and dyes for coupling still make the technique more expensive and involved than most labs would undertake on their own. Stellaris RNA FISH (Biosearch Technologies) offers such probes commercially for researchers who don't have the in house expertise or equipment to create these probes on their own. QuantiGene probes from Panomics (Affymetrix Inc.) detect single mRNA molecules with sequential ODN probes that use branched DNA to amplify signals [156, 157]. This probe synthesis approach is proprietary and cannot be re-created in house to reduce the cost. Other methods to make FISH more accessible to labs unable to rationalize the expense of the commercial offerings are desirable.

We devised a strategy for creating ODN *in s itu* hybridization probes we call **F**luorescence **I**n **S**itu **H**ybridization with **S**equential **T**ethered and **I**ntertwined ODN **C**omplexes (FISH-STICs). This method for FISH probe design offers labs an ability to detect mRNAs that does not require an in house DNA synthesizer for custom modifications that ODN supply companies do not offer, or offer only at great expense. This approach uses entirely commercially purchased synthetic ODN that can be used without any modification or processing. It increases the fluorescence output of small stretches of RNA that can be recognized by multiply labeled ODN, making such small stretches of nucleic acid more easily detectable.

Methods to quantify mRNA localization have, until recently, remained mostly subjective. One conventional method to quantify localization is to compare the number of cells, in which an

mRNA is localized or mislocalized. The comparison is based on the blind counting of cells based on predetermined criteria by observers who are blind to experimental conditions. This type of analysis, while limiting bias, still relies on individual qualitative interpretation and is limited to strong differences in distribution. More quantitative approaches of been used such as comparing the most and least dense cellular areas, setting a threshold of signal for localization or comparing the distance between an mRNA and specific cellular compartments[158-160]. All of these approaches are considered valid, but they can each lead to different conclusions.

Recently an objective quantitative method was developed to characterize the molecular distribution of mRNA in cultured cells based on two measures, the polarization and dispersion indexes [161]. The polarization index (PI) compares the centroid (the average location in all three dimensions) of the mRNA population to the centroid of the cell. An mRNA which is completely asymmetrically localized would have a PI of 1, with a decreasing PI as mRNA appears more symmetrical. The dispersion index (DI) calculates the distribution of mRNA within the cell and compares it to a theoretical uniform distribution. Therefore, a cell with a completely even distributed of mRNA would have a DI value of 1. The DI value decreases as an mRNA becomes more concentrated in the center of the cell and increases beyond 1 if the mRNA is concentrated in the periphery of the cell. These measures were validated in several model systems and the polarization of Actb mRNA was correlated with the direction of migration in fibroblasts [161].

Results:

The FISH STICs method works in principle like traditional immunofluorescence with successive binding leading to an amplification of signal. The design involves a series of three hybridizations facilitated by tag sequences on the primary and secondary oligonucleotides. These

tag sequences were blasted against the genome to ensure that there would be no off target effects. The primary ODN hybridizes to a 50 nucleotide sequence within an mRNA of interest. Contained within the primary ODN is a 35 nucleotide tag sequence, which is repeated three times, allowing for multiple secondary ODNs to hybridize. A third oligo containing a directly coupled fluorescent dye then hybridizes to the tag sequence of the secondary ODN, which contains five repeats of a 25 nucleotide tag sequence (Figure 10). Actb mRNA is well established localized mRNA in both cultured cells and primary neurons. Actg mRNA, however produces an almost identical protein but has a unique distribution from Actg mRNA. These two mRNAs, therefore, represented an ideal way to test FISH STICs probes. Using probes against single 50-mer sequences within mouse Actb mRNA on mouse embryonic fibroblasts (MEFs), small fluorescent primary ODN and secondary ODN dependent puncta were clearly visible (Figure 11). This result demonstrates that single primary probes are sufficient to detect mRNA in cultured cells. We noticed that FISH-STIC probes had the potential to form mRNA independent probe complexes, which were as bright as or brighter than the FISH signal (Figure 11– arrowheads). These complexes are not dependent on any individual component of the probe mixture or cover-slip coating, are present using either Cy3 or Cy5 dyes but, the different colors do not over-lap and are dependent on the presence of the primary and secondary oligonucleotide. The presence and intensity of these complexes is variable from experiment to experiment and can be limited by increased agitation and wash volume.

Single FISH-STIC probes are capable of detecting mRNA, but the method can easily be adapted for multiple probes to create a stronger fluorescent signal for quantitative image analysis. To this end, we created an additional Actb and Actg primary probe. These probes contain different 50mer sequences from the original primary ODNs but contain the same tag

sequences so the same secondary and tertiary oligos may be used. Actb and Actg puncta are distinct suggesting that these probes are hybridizing to distinct mRNAs (Figure 12C and D). I analyzed FISH-STICs images and quantified the distribution Actb and Actg mRNA signal within the same cell using the metric described by Park et al.[161]. Consistent with Actb mRNA being a localized transcript, Actb mRNA had a higher median polarization index than Actg (Actb = 0.359 Actg = 0.320) and a significantly lower median dispersion index (Actb = 0.434, Actg = 0.609) (Figure 12 panels G and H respectively). These results demonstrate the ability of FISH-STICs to detect distinct mRNAs in two colors and establish different distributions of Actb and Actg mRNA in the same cell.

One of the advantages of the FISH-STICs method is the same secondary and tertiary ODNs can be used to look at multiple mRNAs across different experiments. To demonstrate this versatility and to investigate the ability of the FISH-STICs method to detect cell-specific mRNAs in a different cell type, we designed three probes against the neuron-specific type III isoform of Neuregulin 1 (Nrg1) using the same tag sequences used in the Actb primary oligos. The Nrg1 gene produces numerous isoforms within different tissues due to alternative promoters and splice sites [162]. Nrg1-III is neuron specific in the central nervous system, so we designed three FISH-STIC primary probes against Nrg1-III specific exons. I hybridized Nrg1 and Actg probes to cortical neurons plated on poly-l-lysine coated glass cover-slips. Type III Nrg1 expression was robust in these neurons (Figure 13). To confirm FISH-STICs probe detection is RNA specific we designed three probes against the choline acetyl-transferase (ChAT) mRNA. I hybridized the ChAT probes along with probes for Actb in MEFs. As expected there was no ChAT specific signals detected but the Actb signal was robust (Figure 14 A-C).

To determine the effect of Hnrnpab disruption on Actb mRNA localization, I used the FISH-STICs method and calculated the polarization and dispersion indexes of Actb and Actg mRNA in Hnrnpab $^{+/-}$ and Hnrnpab $^{-/-}$ MEFs (Figure 16). The polarization of Actb mRNA did not vary based on genotype and was comparable to the Actb polarization index in WT MEFs (Figure 17A, Figure 13G). The dispersion of Actb mRNA was significantly lowered in the Hnrnpab$^{-/-}$ MEFs as indicated by a decrease in the dispersion index (Figure 16). This result indicates that in the absence of Hnrnpab, Actb mRNA is still asymmetrically distributed but there is less Actb mRNA localized to the periphery of the cell. Both the polarization and dispersion indexes for Actg mRNA were unchanged across genotype, indicating the observed effect is specific for Actb mRNA.

To confirm the observed effect is due to the loss of Hnrnpab expression, I expressed Hnrnpab1 and 2 and an Hnrnpab mini gene in Hnrnpab $^{-/-}$ MEFs to see if they could rescue the decrease in Actb distribution. Expression of Hnrnpab1 restored the dispersion index of Actb mRNA to similar levels as Hnrnpab $^{+/-}$ MEFs and had no effect on the dispersion of Actg mRNA (Figure 17). This result is consistent with the biochemistry shown in Chapter 2 that Hnrnpab1 bound to the trafficking sequence of Actb mRNA but did not associate with Actg mRNA. Expression of Hnrnpab2 increased the dispersion index of both Actb and Actg mRNA, which is consistent with the both Actb and Actg mRNA being found in Hnrnpab2 immune complexes (Figure 17 and Figure 6). The Hnrnpab mini-gene also had higher dispersion indexes for both Actb and Actg mRNA. This result indicates that only the Hnrnpab1 isoform is responsible for the trafficking of Actb mRNA and that Hnrpab2 is involved functions in a different capacity in the regulation of both Actb mRNA and Actg mRNA.

Discussion:

Development of FISH-STICs

Our FISH-STICs design is possible because commercial DNA synthesis technology has improved to be able to synthesize 150-mer ODN reliably. Limitations to synthesis of commercial probes commercially come from the increased probability of premature truncation with ODN size during the synthesis, which goes from 3' to 5'. By placing the antisense hybridizing sequences at the 5' end any truncated ODN will be unable to hybridize, and not interfere with successful full-length probes. We first chose three consecutive oligos because our experience with single molecule FISH using multiply labelled single 50-mer ODN indicated that if the technique worked, this would be clearly visible [163]. We selected 35nt and 25nt for the intermediate tag sequences since these were large enough changes to accommodate decreasing stringency during successive steps, but variations in these lengths can easily be envisioned. Our tag sequences were generated through a random sequence generating website, so any sequence lacking a high complementarity to existing RNA sequences in the cell can work.

Our design for FISH-STIC probes facilitates flexibility to increase fluorescence output of FISH target sites, an important parameter when considering copy number of target transcripts. Multiple primary ODN with a common secondary tag sequence to the same mRNA can all be co-hybridized in the same probe mix, and this boosts fluorescence signals for an individual RNA sequence without changing any other parameter of our protocol. The probes here used two (Actb and Actg) or three (Nrg1-III and ChAT) primary ODN with the same secondary tags but more primary probes are certainly possible if much stronger signal is desirable. Also, one secondary/dye ODN set can also be used for many different primary probe sets (here, Actb and Nrg1-III used the same Cy3 set and Actg and ChAT used the same Cy5 set), omitting the need to

order a secondary/dye ODN set for every gene to be analyzed. A practical advantage to FISH-STICs is that all of the oligos used in this method can be ordered from any commercial ODN vendors that synthesize 150bp ODN, and they can be used without the need to couple dyes to modified ODN in house which can be inefficient and adds additional time and cost to probe synthesis. The smallest scale available from our vendor at the time of writing this was 4nmol of oligo. 4nmol of oligo is sufficient to make 40ml of probe solution at the concentration we started these studies with (0.1μM). We use 50μl per coverslip; therefore this scale of 150mer is sufficient for 800 hybridization reactions, making this very inexpensive on a per-reaction basis. After protocol optimization, FISH-STICs works at 10-fold lower ODN concentration during hybridization, so in reality one can get many more hybridizations than this from one probe.

Importantly, the STIC concept should also be amenable to more than 3 consecutive probes to produce even stronger signals. Introducing another amplifying ODN between the primary and secondary or between the secondary and tertiary has the potential to make the individual 50-mer probes much brighter than we have demonstrated here. If we accommodated a second amplifying probe that incorporates 4 copies of a third unique repeated tag and modified the tertiary dye oligo to hybridize to this new third probe, then an individual primary mRNA binding site would be able to attract up to 60 individual fluorophores, an equivalent increase to three additional primary ODN in our current configuration. FISH-STICs' features make it possible to characterize different mRNA isoforms produced in the same cell at the single molecule level even when the isoforms differ by only as little as 50-nt or smaller, the size difference being limited by the ability of mismatches to the 50mer to impair hybridization. This situation applies to alternative splicing, alternative transcription initiation or alternative 3' end cleavage and polyadenylation.

Actb mRNA distribution is decreased in Hnrnpab $^{-/-}$ MEFs but can be rescued by Hnrnpab1 expression

FISH-STICs allowed me the practical ability to test the hypothesis that Hnrnpab is involved in mediating Actb mRNA localization and the development of the polarization and dispersion indexes allowed me to quantify actin mRNA distribution. In the absence of Hnrnpab there was no difference in the polarization of Actb mRNA, but there was a reduction in Actb mRNA in the periphery of the cell as measured by the dispersion index (Figure 17). This result was only rescued by the expression of the Hnrnpab1 isoform, confirming its role in mediating the trafficking of Actb mRNA (Figure 18). Hnrnpab2 alone or in the context of the Hnrnpab mini-gene did increase the dispersion index of Actb mRNA, however these constructs also increased the dispersion index of Actg mRNA. This suggests Hnrnpab2 may play a broader role in mediating actin mRNA other than mRNA trafficking (Figure 18).

Examining migrating MEFs derived from ZBP1$^{-/-}$ mice containing the Actb-MS2 binding site knock in, Katz et al. 2012 demonstrated a decrease in the polarization index of Actb-MBS mRNA. The decrease in polarization index correlates with a decrease in the asymmetrical localization of Actb mRNA in these cells and suggests a role for ZBP1 in this process[164]. Since the authors did not measure the dispersion index, it is unknown if ZBP1 also affects the amount of mRNA localized to the periphery. In Hnrnpab$^{-/-}$ MEFs, Actb mRNA is still asymmetrically localized but is not distributed to cell periphery. One possible mechanism which would explain these results is ZBP1 is involved in establishing the initial asymmetrical distribution of Actb mRNA but Hnrnpab1 is required for trafficking Actb mRNA to the cell periphery. This model is similar to MBP mRNA, which requires two different localization steps to properly localize MBP to the processes of oligodendrocytes.

The biochemical evidence in chapter 2 in combination with the FISH data presented in this chapter demonstrates Hnrnpab1 is an Actb mRNA trafficking factor. In addition, the data also suggest Hnrnpab2 is involved in both Actb and Actg mRNA regulation. While Actg mRNA is not trafficked like Actb mRNA it does have a distinct sub-cellular localization and may be post-transcriptionally regulated. The presence of Actg mRNA in the immune complexes of Npm1, PSPC1 and hnRNP D support this hypothesis. If Hnrnpab2 is involved in the stability of both Actb and Actg mRNA but is compensated for in Hnrnpab $^{-/-}$ cells, then when Hnrnpab2 is expressed in those cells the mRNAs would have an even longer half-life and over-time diffusion could increase the distribution of both mRNAs. This model can be tested by looking at the half-life of both Actb and Actg mRNA in Hnrnpab$^{-/-}$ cells and Hnrnpab$^{-/-}$ cells expressing Hnrnpab2.

Chapter contributions:

Kevin Czaplinski: FISH-STICs method, primer design, single ODN FISH-STIC experiment

Figure 10

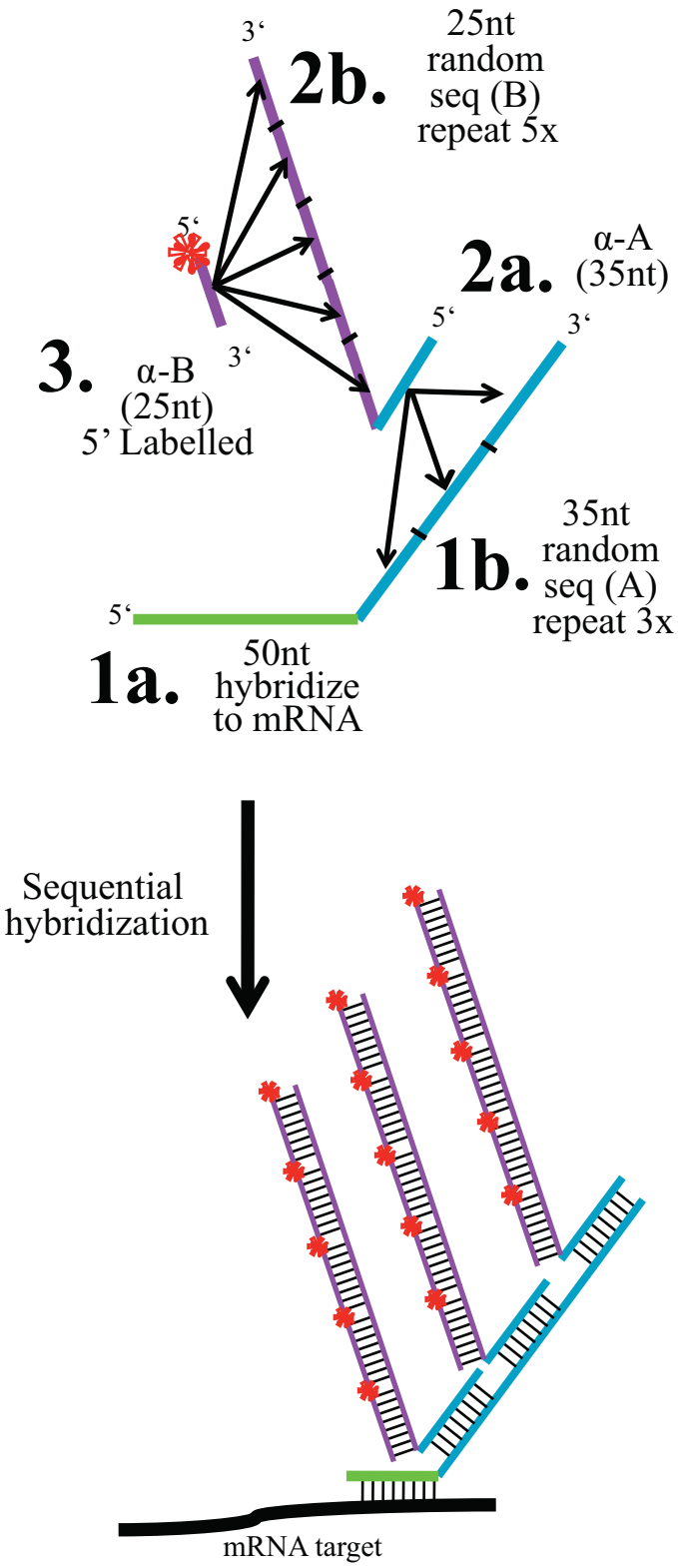

Figure 10- **FISH-STICs probe diagram.** 1a; The 50 nt at the 5’ end of the primary ODN is complementary to the RNA target (mRNA, ncRNA). 1b; 3 repeats of a unique 35 nt sequence are added at the 3’ end of the primary ODN. 2a; The 35 nt at the 5’ end of the secondary ODN is complementary to the 35 nt sequence 1b of the primary ODN. 2b; 5 repeats of a distinct unique 25 nt sequence are added at the 3’ end of the secondary ODN. 3.; A tertiary ODN is synthesized complementary to the 25 nt sequence 2b of the secondary ODN with a fluorescent dye, or any other means of detection, coupled to the 5’ end. Through sequential hybridization of these probes the individual ODN complexes can attract as many as 15 tertiary ODN, giving a bright signal for epifluorescence imaging. Multiple primary ODN against the same mRNA can incorporate common secondary and tertiary tag sequences, to increase brightness of the probes.

Figure 11

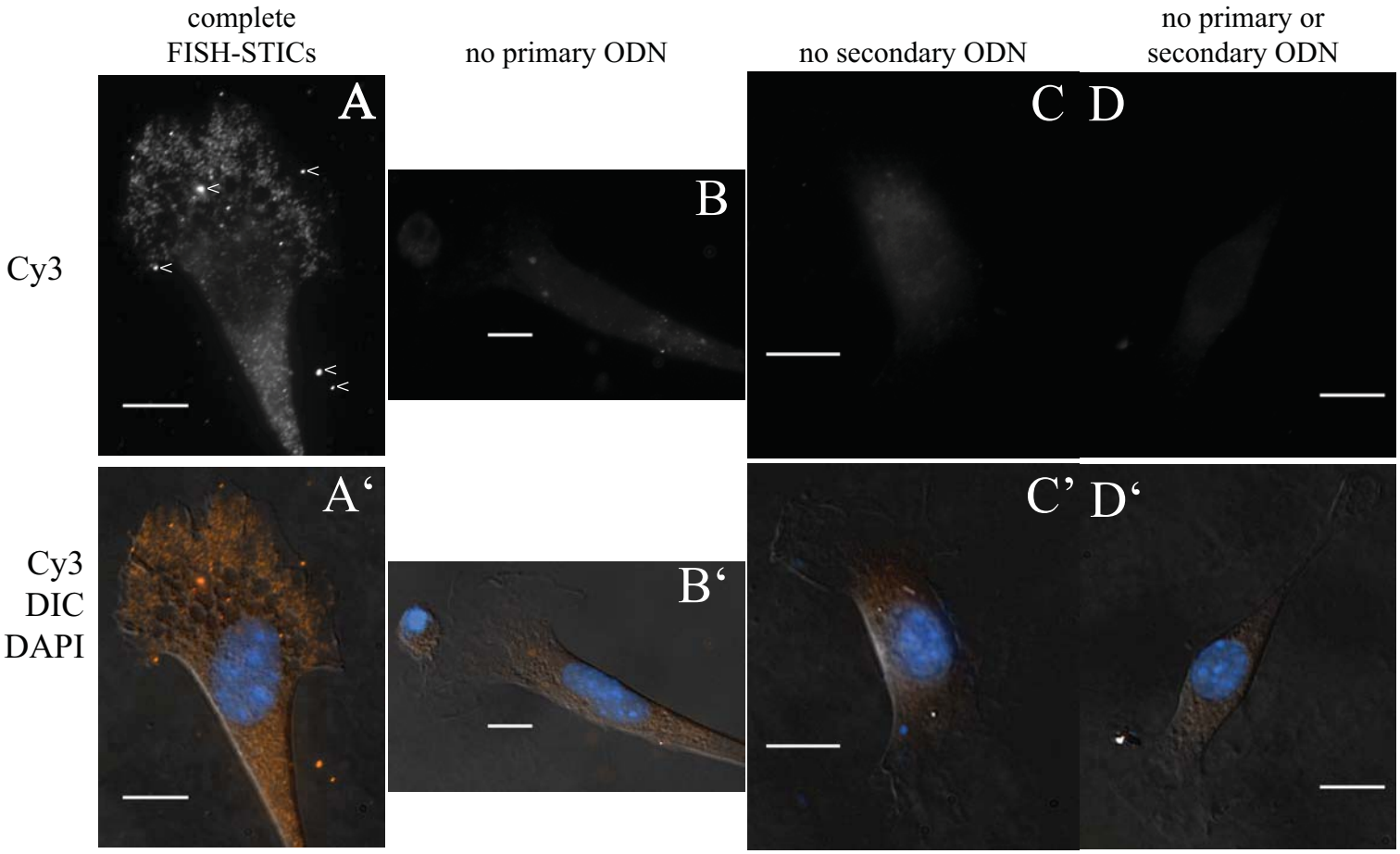

Figure 11– Detection of Actb mRNA with a single FISH-STIC probe. An Actb primary probe was hybridized to primary MEFs Top row; Normalized Cy3 images of cells after hybridization with complete FISH probes (panel A) or probes lacking one component as indicated above (panels B-D). mRNA target independent STIC complexes seen as much brighter puncta are indicated in 1A by arrowhead. Bottom row; Cy3 (orange), DAPI (blue) and DIC (grey) merged images of cells above it. Non-hybridizing STIC complexes are indicated with white arrowheads in panel A. scale bars - 10μm.

Figure 12

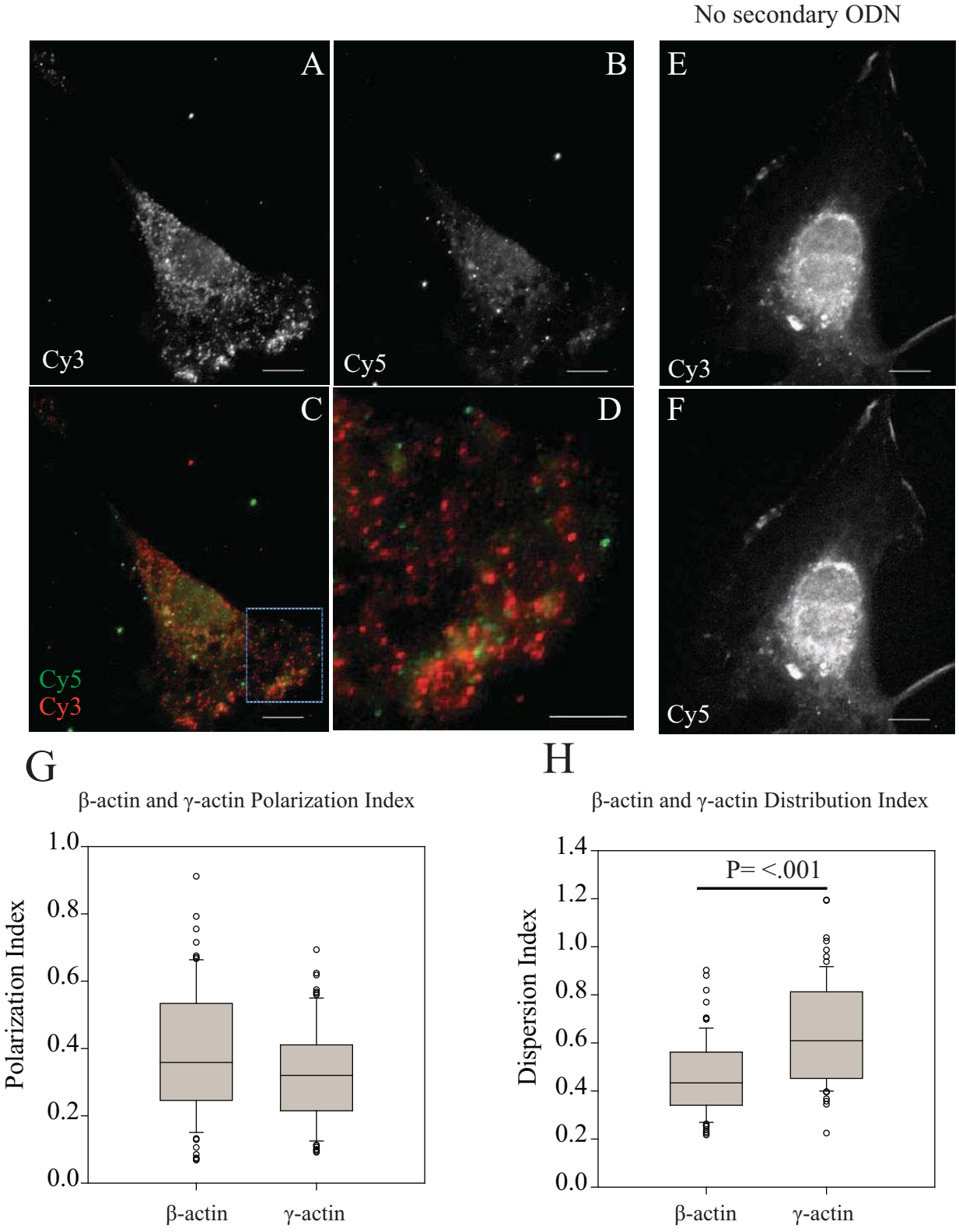

Figure 12- Actb and Actg have spatially distinct distribution in the same cells. Two Actb and two Actg primary probes were hybridized to primary MEFs and imaged with epifluorescence microscope. Representative normalized Cy3 images for Actb or Cy5 for Actg are shown in panels A and B, respectively. The merged images are shown in panel C, with the ROI indicated by the dashed box in C shown in panel D. No secondary control images are shown for Cy3 (E) and Cy5 (F). Images shown are deconvoluted from Z-series taken at 60x. Polarization index (G) and Distribution index (H) for 78 images are represented as bow-whisker plots, with the median (black line) and middle quartiles represented in the box, the highest and lowest quartiles represented in the whiskers, and outliers indicated by circles. Polarization and Distribution indexes were calculated from maximum projection images of non-deconvolved Z-series using a Mann-Whitney Rank Sum Test. Scale bars - 10μm, except for D - 2μm.

Figure 13

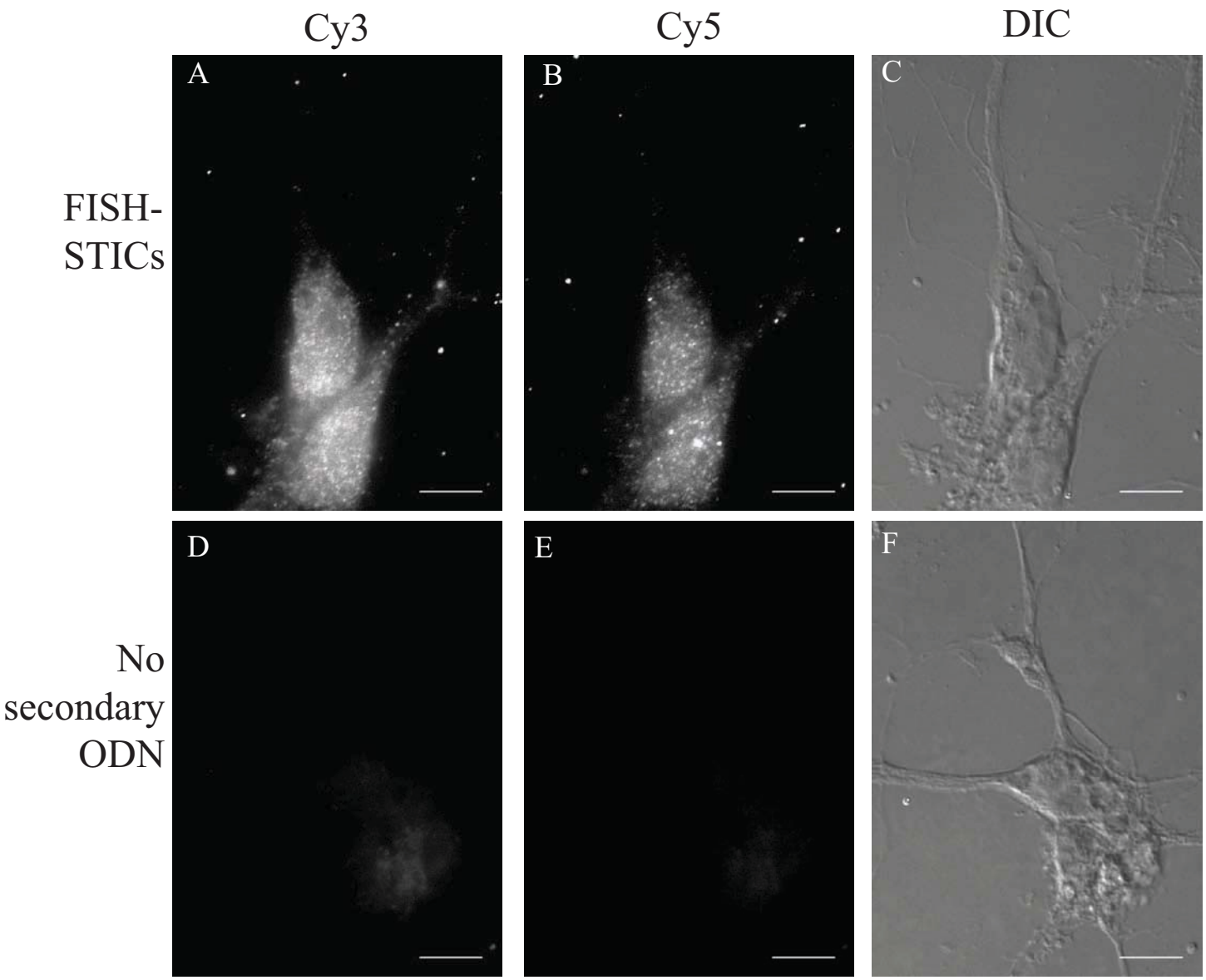

Figure 13 – FISH-STICs detection of Nrg1-III and Actg mRNA in primary neurons. Embryonic day 18 cortical neurons were plated on poly-lysine coated coverslips and maintained in culture for 10 Days in vitro (DIV). 5-Fluoro-deoxy-uridine (FDU) was added after 3DIV. Neurons were fixed, and then co-hybridized with Cy3 Nrg1-III (panel A), Cy5 Actg (panel B) primary probes and corresponding secondary probes. Normalized images from control hybridization reactions lacking any secondary probe are shown in panels D and E. DIC images of the cells imaged in Cy3 and Cy5 are shown in panel C and panel F of the hybridizations indicated. Images are single plane epifluorescence taken at 60x magnification. Scale bar -10μm

Figure 14

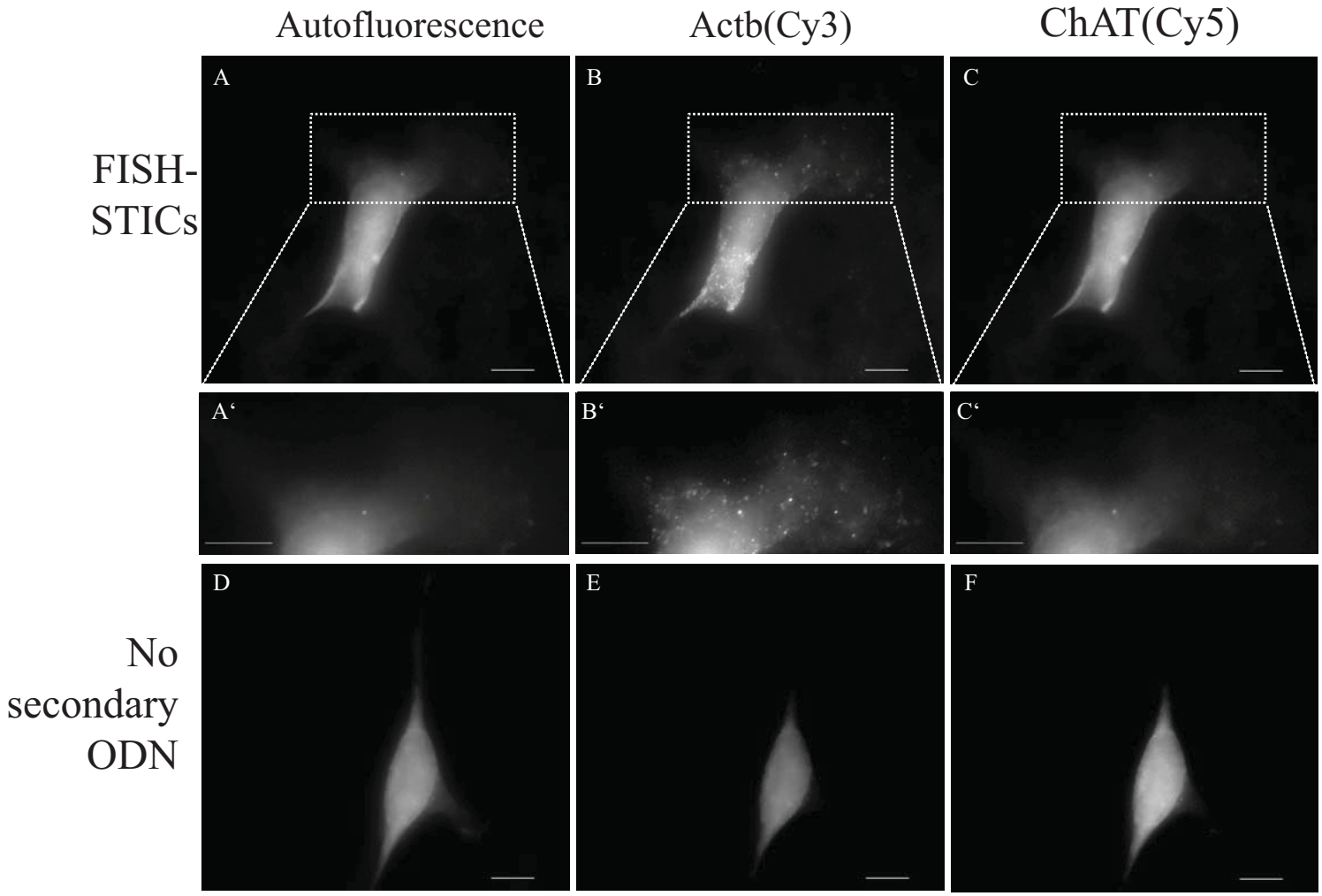

Figure 14 – FISH-STICs probe specificity. Two Actb and three mouse choline acetyl-transferase (ChAT) primary probes were synthesized to label Actb mRNA with Cy3 and simultaneously label ChAT mRNA with Cy5. Probes were hybridized to primary MEFs and imaged with epifluorescence microscope. Top row; Images of FITC autofluorescence images (A), Cy3 (B) and Cy5 (C) from one cell. Middle row; A' B' and C' correspond to and expanded view of the ROI indicated by the dashed line box in images A, B and C respectively. Bottom Row; Normalized images of FITC autofluorescence (D), Cy3 (E) and Cy5 (F) taken from one cell hybridized without a secondary ODN as an imaging control. A-F are maximum projection images of Z-series of images. Scale bars for columns A, C and D- 10μm, scale bar for column B - 2μm.

Figure 15

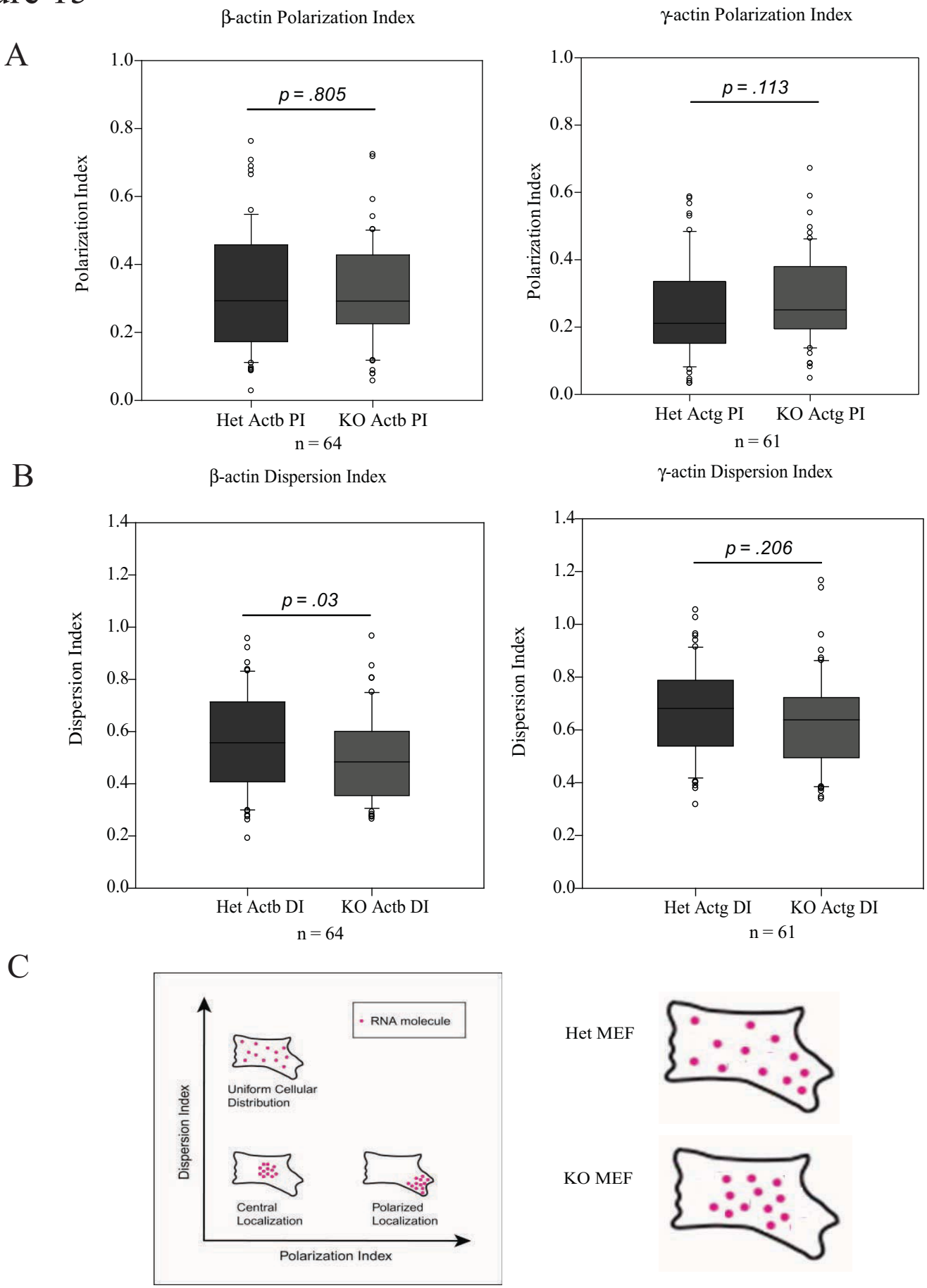

Figure 15- Hnrnpab is required for proper Actb mRNA localization. Polarization indexes (A) and Dispersion indexes (B) for Actb (64 images) and Actg (61 images) mRNA for Hnrnpab $^{+/-}$ and Hnrnpab $^{-/-}$ MEFs are represented by box and whisker plots, with the median (black line) and middle quartiles represented in the box, the highest and lowest quartiles represented in the whiskers, and outliers indicated by circles. Polarization and dispersion indexes were calculated from maximum projection images of non-deconvoluted Z-series using a Man-Whitney Rank Sum Test. The interpretation of these results are represented in the cartoons in C, the graph is taken from Hi-Yun et al. 2012.

Figure 16

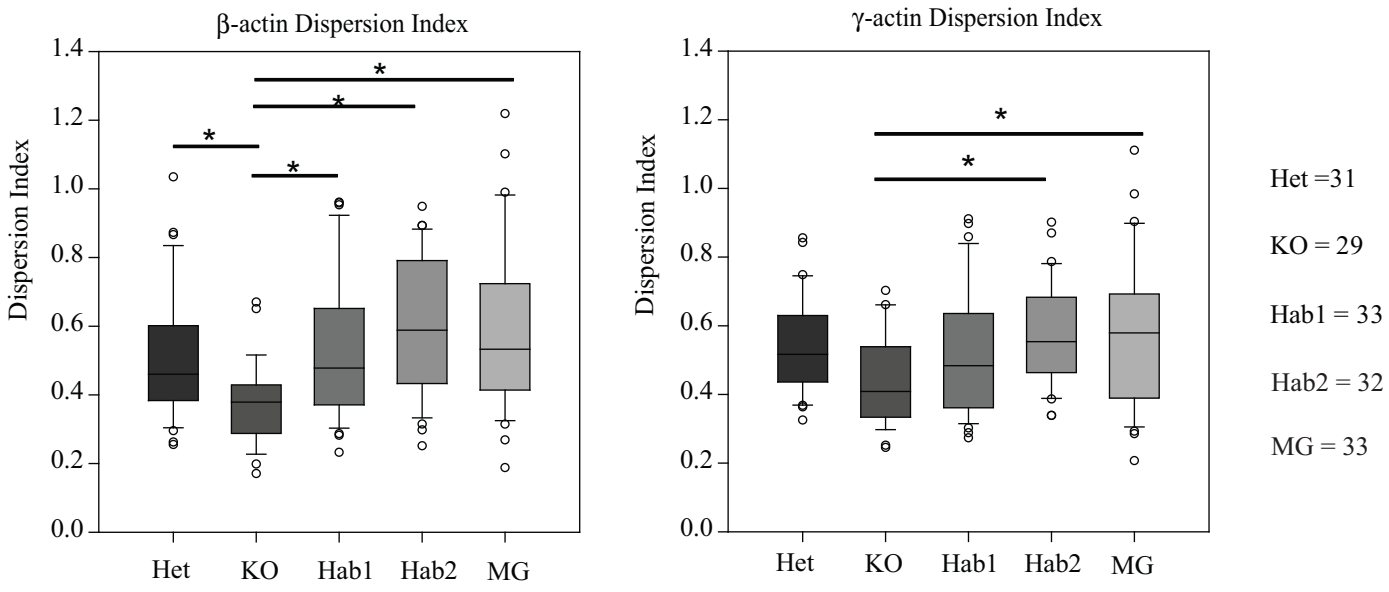

Figure 16- Hnrnpab1 rescues Actb mRNA localization. Dispersion indexes (B) for Actb and Actg mRNA from Hnrnpab $^{+/-}$, Hnrnpab $^{-/-}$, Hnrnpab1, Hnrnpab2 and Hnrnpab mini-gene MEFs are represented by box and whisker plots, with the median (black line) and middle quartiles represented in the box, the highest and lowest quartiles represented in the whiskers, and outliers indicated by circles. Dispersion indexes were calculated from maximum projection images of non-deconvoluted Z-series using a Man-Whitney Rank Sum Test. * indicates $p < .05$

Chapter 4: Hnrnpab regulates neural development and neuron cell survival in mice*

*This chapter is modified from a paper published in RNA. 2012 Apr;18(4):704-19 with permission of the authors

Abstract

To explore the role of Hnrnpab in the nervous system, the lab analyzed the genome wide protein expression profiles of mice lacking Hnrnpab. Analysis of the proteomic changes suggested an alteration in both neural development and glutamate signaling in the absence of Hnrnpab. We demonstrated that Hnrnpab$^{-/-}$ neural stem and progenitor cells undergo altered differentiation patterns in culture, Hnrnpab$^{-/-}$ neurons have an increased sensitivity to glutamate-induced excitotoxicity and longer neurites. We also show that the Hnrnpab nucleo-cytoplasmic distribution in primary neurons is regulated by developmental stage.

Results

Hnrnpab disruption alters hippocampal protein expression

Using a gene-trap embryonic stem cell line the lab generated a mouse strain with an Hnrnpab null allele (Hnrnpab$^{Gt(AV0426)Wtsi,}$, we refer to as Hnrnpab^{-}, Figure 18) [108].To gain insight into the role of Hnrnpab in the nervous system, we performed shotgun proteomics analysis to impartially quantify protein expression changes caused by the loss of Hnrnpab in the developing hippocampus. A diagram of this experiment can be seen in Figure 19. Using expression ratios of 1.5 for increased proteins, or 0.7 for decreased proteins as thresholds we identified 349 proteins increased (133 soluble, 216 insoluble, Table II) and 73 proteins decreased (26 soluble, 47 insoluble, Table III) in the Hnrnpab$^{-/-}$ hippocampus compared to Hnrnpab$^{+/-}$

hippocampus. To understand the biological significance of these differentially regulated proteins we performed pathway-based analysis on our datasets using the Ingenuity Pathway Analysis (IPA, Ingenuity@ Systems, ingenuity.com, Table IV). Results from this proteomic analysis demonstrated that Hnrnpab regulates expression of many genes that play important roles in the development of the nervous system.

Hnrnpab disruption alters differentiation of neural stem and progenitor cells

To evaluate if Hnrnpab is involved in the development of the nervous system, we used neurosphere cultures. Neurospheres contain self-renewing neural stem cells that give rise to the different neural lineages, as well as several types of lineage committed progenitor cells. These different cell types within the culture can be clearly distinguished by the expression of lineage specific marker proteins. We quantified cells representing different neural lineages within neurosphere cultures generated from Hnrnpab$^{-/-}$ and Hnrnpab$^{+/-}$ mice and observed changes in several populations. The largest was a decrease in Nestin-expressing (NES) cells in Hnrnpab$^{-/-}$ neurosphere cultures (67.2% in Hnrnpab$^{+/-}$ versus 21.6% in Hnrnpab$^{-/-}$, Figure 20). Increases in Doublecortin positive cells (DCX, a neuroblast marker, 28.8% in Hnrnpab$^{+/-}$ versus 35.3% in Hnrnpab$^{-/-}$, Figure 20) and Myelin Basic Protein positive cells (MBP, an oligodendrocyte marker, 0.8% in Hnrnpab$^{+/-}$ versus 2.1% in Hnrnpab$^{-/-}$) had p-values of 0.002 and 0.011 respectively (Figure 20). Also, a trend toward increased positive cells for an early marker of oligodendrocyte lineage cells, CNPase, was observed (7.6% in Hnrnpab$^{+/-}$ versus 9.6% in Hnrnpab$^{-/-}$, p-value 0.301) (Figure 20). A trend to slightly fewer Glial Fibrillary Accessory Protein (GFAP) positive cells was seen (27.6% in Hnrnpab$^{+/-}$ versus 24.9% in Hnrnpab$^{-/-}$, p-value 0.359, Figure 20). These data suggest involvement of Hnrnpab in neural stem cell maintenance and differentiation

of different neural lineages in neurosphere cultures, with increases in expression of some differentiation markers when Hnrnpab is disrupted, and a decrease of pluripotent cell types.

Neurons lacking Hnrnpab1 and Hnrnpab2 show increased sensitivity to glutamate excitotoxicity and longer neurites

Glutamate receptor signaling and axon guidance signaling topped the lists of affected cellular functions in Hnrnpab$^{-/-}$ hippocampus. We considered what consequences these results could have. Glutamate receptor stimulation leads to neuronal depolarization and formation of action potentials. However this activates cellular stress responses and excessive glutamate receptor stimulation leads to cell death, a process termed excitotoxicity [165]. Hypersensitivity to excitotoxicity is believed to underlie many neurodegenerative diseases [165]. We therefore tested whether Hnrnpab$^{-/-}$ neurons would demonstrate an altered sensitivity to cell death after glutamate stimulation. We plated E18 hippocampal neurons from Hnrnpab$^{+/-}$ and Hnrnpab$^{-/-}$ neurons on coverslips and treated them at 15 days in vitro (DIV) with 50 μM glutamate for 10 min, and allowed them to recover without exogenous glutamate for 6 hours prior to fixation. We quantified the percentage of dying neurons in Hnrnpab$^{+/-}$ neuron cultures versus Hnrnpab$^{-/-}$ cultures in both glutamate stimulated as well as mock stimulated cultures to control for the culture manipulations. Very few dying neurons could be found in mock stimulated Hnrnpab$^{+/-}$ or Hnrnpab$^{-/-}$ cultures (5.6% and 5.7% respectively, Figure 21). As expected, glutamate treatment increased the number of dying neurons in Hnrnpab$^{+/-}$ cultures to 24.5%, consistent with the view that glutamate application has some level of inherent toxicity (Figure 21). However, 82.8% of the Hnrnpab$^{-/-}$ neurons were dying, demonstrating that neurons lacking Hnrnpab demonstrate strongly increased sensitivity to glutamate-induced excitotoxicity (Figure 21).

Axon guidance signaling molecules were significantly up-regulated in Hnrnpab$^{-/-}$ hippocampus, so we measured the neurite length in Hnrnpab$^{+/-}$ and Hnrnpab$^{-/-}$ neurons 2 days after plating. Hnrnpab$^{-/-}$ neurons had 40% longer neurites than Hnrnpab$^{+/-}$ littermate neurons (average length of 11.56 μm for Hnrnpab$^{+/-}$ versus 16.22 μm for Hnrnpab$^{-/-}$, Figure 22). Moreover, the average length for the longest neurite of Hnrnpab$^{-/-}$ neurons was 32.5% longer than those of Hnrnpab$^{+/-}$ littermates (average length of 22.6 μm for Hnrnpab$^{+/-}$ versus 29.9 μm for Hnrnpab$^{-/-}$, Figure 22). Longer neurites of cultured neurons is consistent with up-regulation of axon guidance molecules indicated by the proteomic data.

Hnrnpab is a nucleo-cytoplasmic protein in the brain

Having established that Hnrnpab plays a functional role in the nervous system, we sought to characterize the distribution of Hnrnpab within the mature brain. We perfused and sectioned a 55-day old (postnatal Day 55 or P55) mouse brain, then immuno-stained using antigen-affinity purified antibody raised against a conserved peptide in the N terminus. This affinity-purified antibody specifically detects Hnrnpab1 and Hnrnpab2 isoforms in a western blot (Figure 23G). Hnrnpab staining is visible in throughout the brain and most cells have some level of Hnrnpab protein, only occasionally cells of unknown identity lacked detectable Hnrnpab expression. Overall we observed agreement of regional Hnrnpab protein expression with two previous FISH studies that looked at Hnrnpab RNA expression patterns in the brain [71, 166]. The most prominent Hnrnpab staining was observed within the granule cell layers of the hippocampus, dentate gyrus and cerebellum, so we acquired images within these regions at a higher magnification to observe the subcellular distribution of the protein (Figure 23). DAPI co-staining demonstrated that these regions high in Hnrnpab expression are also packed with many nuclei.

Hnrnpab immuno-reactivity is enriched in the nuclei of individual cells, although a weaker uniform cytoplasmic distribution throughout the cell soma can often be seen, particularly at the edges of these granule cell layers (Figure 23A and E). The granule cell layer of the dentate gyrus contained discrete zones of higher Hnrnpab expression at the interface between the granule layer and the polymorphic layer (Figure 23F). The tight packing of the cell bodies within these regions made cytoplasmic signal difficult to characterize in detail, however in the cerebellum the Purkinje neurons were an exception to this (Figure 23A-C). Purkinje neurons are GABA-ergic neurons at the interface of the granule cell layer and molecular layers of the cerebellum, easily distinguishable by their size and expression of parvalbumin (PV) in the cytoplasm (Figure 23B). In Purkinje neurons, Hnrnpab staining overlapped with PV, demonstrating cytoplasmic Hnrnpab staining (Figure 23A-C). While nuclear staining was always observed in Hnrnpab-expressing cells, cytoplasmic Hnrnpab was only sometimes observable in combination with the nuclear staining. Aside from Purkinje neurons, clear examples of cytoplasmic staining pattern were seen in the cells of the CA3 region in the hippocampus (Figure 23F). Based on the immuno-staining of brain slices, we conclude that at least one isoform of Hnrnpab is cytoplasmic during normal neuron function in the brain, although this Hnrnpab antibody does not determine whether different isoforms have different subcellular distributions.

A cytoplasmic pool of Hnrnpab increases during neuronal maturation

Following the pattern of immunostaining in brain sections, we wanted to understand the requirements for localization of Hnrnpab isoforms in neurons so we first immuno-stained hippocampal neuron cultures with Hnrnpab N-terminus peptide antibody and βIII tubulin as a marker for neurons. In neuron cultures 6 DIV, very prominent nuclear staining was detected in

all βIII tubulin positive cells. Weaker, but strictly nuclear signals were also detected in most cells that did not stain with βIII tubulin (Figure 24A). In these cultures, only very weak cytoplasmic signal was detectable with the N terminus antibody that detects both isoforms (Figure 24A and B). To determine whether weak cytoplasmic staining was due to Hnrnpab immuno-reactivity we blocked the Hnrnpab-dependent fluorescence by including excess immunogenic peptide in the staining reaction. This treatment effectively blocked the strong nuclear staining in all cells, however the intensity of cytoplasmic staining was unaffected by this treatment, suggesting that the very weak cytoplasmic fluorescence in these cells did not reflect a cytoplasmic pool of Hnrnpab protein (Figure 24A). Furthermore, plating neurons from Hnrnpab$^{-/-}$ mice demonstrated that the prominent nuclear stain was absent when these neurons were stained with the Hnrnpab N-terminus peptide antibody, while the same relatively weak cytoplasmic staining remained (Figure 24B). These results confirm the specificity of our antibody in immuno-staining, and suggest that the cytoplasmic appearance of at least one isoform of Hnrnpab in neurons is likely to be developmentally regulated, since both isoforms remain primarily nuclear in 6DIV cultured neurons.

To study the cytoplasmic appearance of the individual isoforms, we expressed recombinant Hnrnpab isoforms in cultured neurons. We constructed recombinant lentivirus-like particles (LVPs) designed to express either Hnrnpab1 or Hnrnpab2, and we incorporated a FLAG epitope at the amino terminus to improve our sensitivity of detection. These viruses express only full length tagged Hnrnpab1 or Hnrnpab2 by western blot as expected (data not shown). We plated hippocampal neurons from Hnrnpab$^{+/-}$ and Hnrnpab$^{-/-}$ neurons on coverslips and first infected these on day 5 with LVPs expressing Hnrnpab1 or Hnrnpab2. After 3 more days (8DIV in total), the cells were fixed, immuno-stained with an anti-flag antibody and imaged. In

Hnrnpab$^{+/-}$ cells, Hnrnpab1 and Hnrnpab2 appear nuclear, albeit a cytoplasmic pool of Hnrnpab2 is detectable in the cell body (Figure 25A and C). Quantifying the ratios of nucleus to cytoplasmic fluorescence shows that Hnrnpab$^{-/-}$ cells have the same distribution of either Hnrnpab 1 or Hnrnpab2 as Hnrnpab$^{+/-}$ cells (Figure 26). Uninfected cells do not stain with the anti-flag antibody and show only weak cytoplasmic fluorescence (auto-fluorescence) that is not apparent in normalized images (data not shown). We conclude that in immature neurons there is no detectable cytoplasmic Hnrnpab1, and only a minor pool of cytoplasmic Hnrnpab2 that our peptide antibodies could not clearly detect (compare Figure 26 panels C and D to Figure 25 A and B).

Since immuno-staining of brain sections found many neurons with clearly defined cytoplasmic Hnrnpab staining, we wanted to know if neuronal maturation influenced the localization of the Hnrnpab isoforms. We plated E18 hippocampal neurons from Hnrnpab$^{+/-}$ mice on coverslips as before, but infected these on day 7 with LVPs. At 15DIV the cells were fixed, immuno-stained with an anti-flag antibody and imaged. Hnrnpab1 was again largely nuclear, but was now detectable in the cytoplasm (compare Figure 25 A1 and A2 to Figure 26 A1 and A2, Figure 26C). Hnrnpab2 was also nuclear, but more clearly detectable in the cytoplasm (Figure 28). Interestingly, Hnrnpab2 in the cytoplasm on day 15 is more pronounced than Hnrnpab1. We examined the effect of glutamate excitation on the nucleocytoplasmic appearance of both Hnrnpab1 and Hnrnpab2. A modest increase in either Hnrnpab1 or Hnrnpab2 cytoplasmic staining was detected upon glutamate stimulation. These results suggest that the localization of Hnrnpab to the cytoplasm in brain sections is more associated with a change in stage of neuronal maturation than a state of excitation, and that a larger proportion of the cytoplasmic signal from total Hnrnpab staining is due to Hnrnpab2.

Discussion

Hnrnpab has a role in neural differentiation and excitotoxicity

We used Hnrnpab null mouse to quantify protein expression changes in the developing hippocampus at the genome wide level in their *in vivo* context. The list of the most significant changes reveals that Hnrnpab regulates levels of proteins involved in neural development. Consistent with this, neurosphere cultures showed an altered course of differentiation in the absence of Hnrnpab expression. Since nestin positive cells showed the largest decrease in neurosphere cultures and we observed an increase in neural progenitor markers, we hypothesize that Hnrnpab regulates stem cell maintenance and neural precursor differentiation. We speculate this role may continue into adulthood since Hnrnpab expression remains high in the neurogenic regions of the brain (sub-ventricular zone and rostral migratory stream) where the adult neural stem cells reside [71, 166]. Most likely Hnrnpab does not function as a master regulator of neural development since no class of neural lineage is strongly lost or favored in Hnrnpab$^{-/-}$ mice. Although the increase in the number of MBP positive cells in the absence of Hnrnpab is intriguing in light of evidence that Hnrnpab interacts with the RTS of MBP, which involved in both the localization and translation of MBP[104]. The Hnrnpab$^{-/-}$ mice give us an *in vivo* opportunity to look at the effect of this interaction by examining the G-ratio of major nerve tracts. I would predict that in the absence of Hnrnpab there would be a lower level of myelination consistent with either a decrease in trafficking or translation of MBP.

However, we think it is more likely that Hnrnpab regulates the timing of neural stem cell differentiation, possibly being involved in interpreting environmental signals that influence neural cell fate into changes in gene expression at the transcriptional and/or post-transcriptional levels. This hypothesis is supported by results from *Xenopus,* where Hnrnpab overexpression

leads to changes in neural crest behavior. Neural crest cells over-expressing Hnrnpab1 transplanted into control embryos do not migrate properly while control neural crest cells migrate properly in the presence of embryos over-expressing Hnrnpab1. This suggests that Hnrnpab is involved in controlling neural crest migration in a cell autonomous manor [167]. Cells which do not migrate properly could in turn cause changes in developmental timing. Follow up studies will be required to identify if these changes are seen *in vivo* and to determine what changes Hnrnpab directly mediates.

The proteomic results also led us to discover that Hnrnpab$^{-/-}$ neurons showed increased sensitivity to cell death induced by glutamate stimulation, suggesting that under normal conditions Hnrnpab activity prevents cell death that can result from excess neuronal activity. Excitotoxicity results from excessive release of calcium following glutamate receptor simulation, which activates cell stress response and cell death cascades [168, 169]. The table of most significantly affected genes includes an increase in Grm3/mGluR3, a G-protein coupled metabotropic glutamate receptor (Table II). A speculative explanation for glutamate excitotoxicity phenotype would be increases in glutamate stimulated calcium release to toxic levels, due to increased amount of Grm3 [170].

It is also possible that Hnrnpab is involved in a broader neuro-protective mechanism. Hypothermia is a robust neuro-protective measure against the effects of strokes. Using a rodent model and comparing gene expression of rodents where hypothermia was induced versus sham, a recent study identified Hnrnpab as significantly induced, suggesting a potential role in neuro-protection[171]. I would expect that if we expanded the *in vitro* results from this study to an *in vivo* induction of either stroke or epilepsy (which involves excitotoxicity), Hnrnpab null mice would exhibit more severe effects than wild-type littermates.

The n ucleo-cytoplasmic di stribution of H nrnpab i soforms s uggests a c hange i n t he c ellular function during neuronal maturation

The localization of Hnrnpab protein at first suggests a primarily nuclear function of Hnrnpab during development when little or no cytoplasmic signal is detected. This is most consistent with roles in transcription, or nuclear mRNA processing such as splicing, editing or cleavage and poly-adenylation. Examples of Hnrnpab binding to transcription element containing DNA have been reported, however the presence RRMs indicate that it is likely that this protein will play a role in regulating gene expression at the post-transcriptional level [172-177]. mRNA localization in the cytoplasm has been demonstrated to require nuclear RNA binding proteins, however the precise roles of these proteins in the cytoplasmic localization process remains poorly defined [1, 178]. Evidence from the previous chapters strongly suggest that Hnrnpab1 is involved in the cytoplasmic localization of Actb mRNA and similar to its ortholog in *Xenopus* may be bind to its targets in the nucleus and remain bound in the cytoplasm.

The larger increase of Hnrnpab2 in the cytoplasm after neuronal maturation raises the possibility that cytoplasmically localized Hnrnpab2 may take on a role that is distinct from Hnrnpab1, such as regulating translation or mRNA stability in this compartment. Similar to Hnrnpab, multiple isoforms of the *Drosophila* squid protein have distinct roles in mRNA localization and translation [107, 179, 180]. It will be worthwhile to delineate the mechanism of how Hnrnpab1 and Hnrnpab2 are targeted to the nucleus, how the mechanism of localization for each isoform is regulated during neuronal development and what role Hnrnpab1's unique exon 7 plays in regulating this activity.

In contrast to the cytoplasmic immuno-staining pattern observed for many other RNA binding proteins in neurons, we found no evidence for a primarily punctate localization for either Hnrnpab isoform in the cytoplasm of neurons in culture or in brain sections. In fact, the localization we observed contradicts studies using antibodies raised against the unique exon 7 sequence of Hnrnpab1, which showed very strong punctate staining throughout the cytoplasm of cells in the brain [181, 182]. We never observed punctate staining using affinity purified antibody preparations from 4 independent Hnrnpab immune-sera (all raised against the Hnrnpab N-terminus), or with recombinant lentiviral-expressed epitope-tagged Hnrnpab1 (Figures 4-7, and data not shown). Our data shows Hnrnpab1 becomes detectably cytoplasmic in mature neurons, but is always uniform in its appearance, not strongly granular or punctate.

Changes in gene expression when Hnrnpab is disrupted identifies Hnrnpab cellular function

We observed hundreds of changes in protein expression when animals develop in the absence of Hnrnpab. Classifying these changes allowed us to successfully predict a phenotype for Hnrnpab$^{-/-}$ neural cells, although we do not yet know how many of these changes are due directly to the absence of Hnrnpab regulation, either transcriptional or post-transcriptional. Hnrpab disruption favors increases in affected proteins at a 5:1 ratio over decreases. This could suggest that Hnrnpab has a widespread role in repressing transcription or translation of many transcripts, or for promoting mRNA instability. Alternatively Hnrnpab may directly regulate only one (or a few) regulatory protein that targets many other genes, making many of the changes we observe indirectly dependent on Hnrnpab function. Future experiments will be needed address the mechanism of these gene expression changes and their role in neural development and neuron activity. With a viable Hnrnpab$^{-/-}$ mouse, numerous other experiments

to explore neuronal function and survival in living mice are possible and may lead to novel insights into how regulation of gene expression influences neurological disease processes and mouse behavior. Many neurodegenerative diseases are thought to involve excitotoxicity and are largely untreatable. Therefore understanding the mechanism of Hnrnpab$^{-/-}$ sensitivity to excitotoxicity may lead to novel approaches to close this gap.

It is also interesting to consider that some of the changes we observe in fact represent a protein signature for how cells must compensate for the lack of Hnrnpab. Cellular compensation for loss of embryonic expression of many vital genes has been observed. This allows animals to develop in the absence of such genes, demonstrating that functional cellular plasticity is inherent in mammalian development, however the cellular mechanisms that adjust for this are generally unknown. If Hnrnpab indeed plays some essential role that can be compensated for, then our proteomic results indicate that the cells appear to adjust gene expression networks by altering many different pathways slightly, as opposed to strongly up-regulating one pathway.

Experimental Contributions:

John Sinnamon: genotyping Western blot, neurite length experiments, affinity purified Hnrnpab antibody, Hnrnpab immunostaining, quantification of nuclear/cytoplasmic distribution of Hnrnpab, neurosphere quantification, statistical analysis

Catherine Waddell: maintained mouse colony, genotyping, neuronal culture, glutamate sensitivity experiment, neurosphere culture, immunostaining and quantification

Sarah Nik and Emily Chen: proteomics and analysis

Kevin Czaplinski: experimental design, identification of gene-trap ES cells, proteomic sample preparation, proteomic analysis, Hnrnpab brain section immunostaining, quantification of cell death

Figure 17

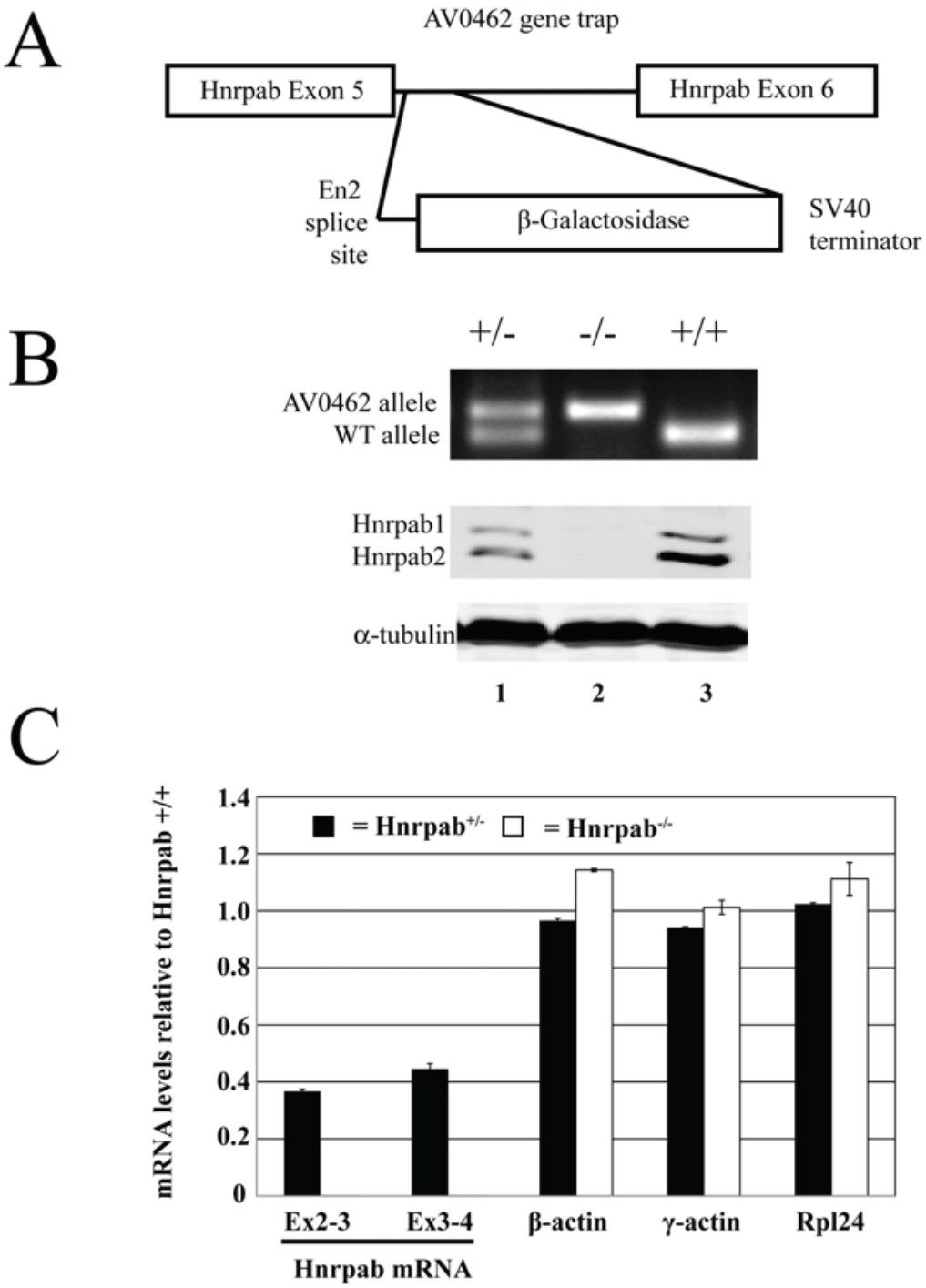

Figure 17– AV0462 ES cell gene trap disrupts Hnrpab expression. (A) A diagram of the region of the Hnrpab gene showing the location of the gene trap insertion. (B) The top panel shows typical PCR genotyping results for AV0462 gene trap heterozygous (lane 1), homozygous (lane 2) and wild type mice (lane 3). The middle panel shows western blots of protein lysates from cerebral cortex of P0 mice using antiserum raised against the N terminus of Hnrpab that recognizes both isoforms of the protein. The lower panel is the α-tubulin loading control to show equal protein loaded in all lanes. (C) The levels of mRNA in heterozygous (black box) or homozygous (white box) P0 cortex relative to wild type were determined using reverse transcription-real time-PCR (RT-RT-PCR) and plotted above. The error bars represent variation of multiple PCR measurements. Hnrpab exons 2-3 and exons 3-4 were detected in Hnrpab$^{-/-}$ samples, but their decrease was so great that that they are essentially not visible on the chart.

Figure 18

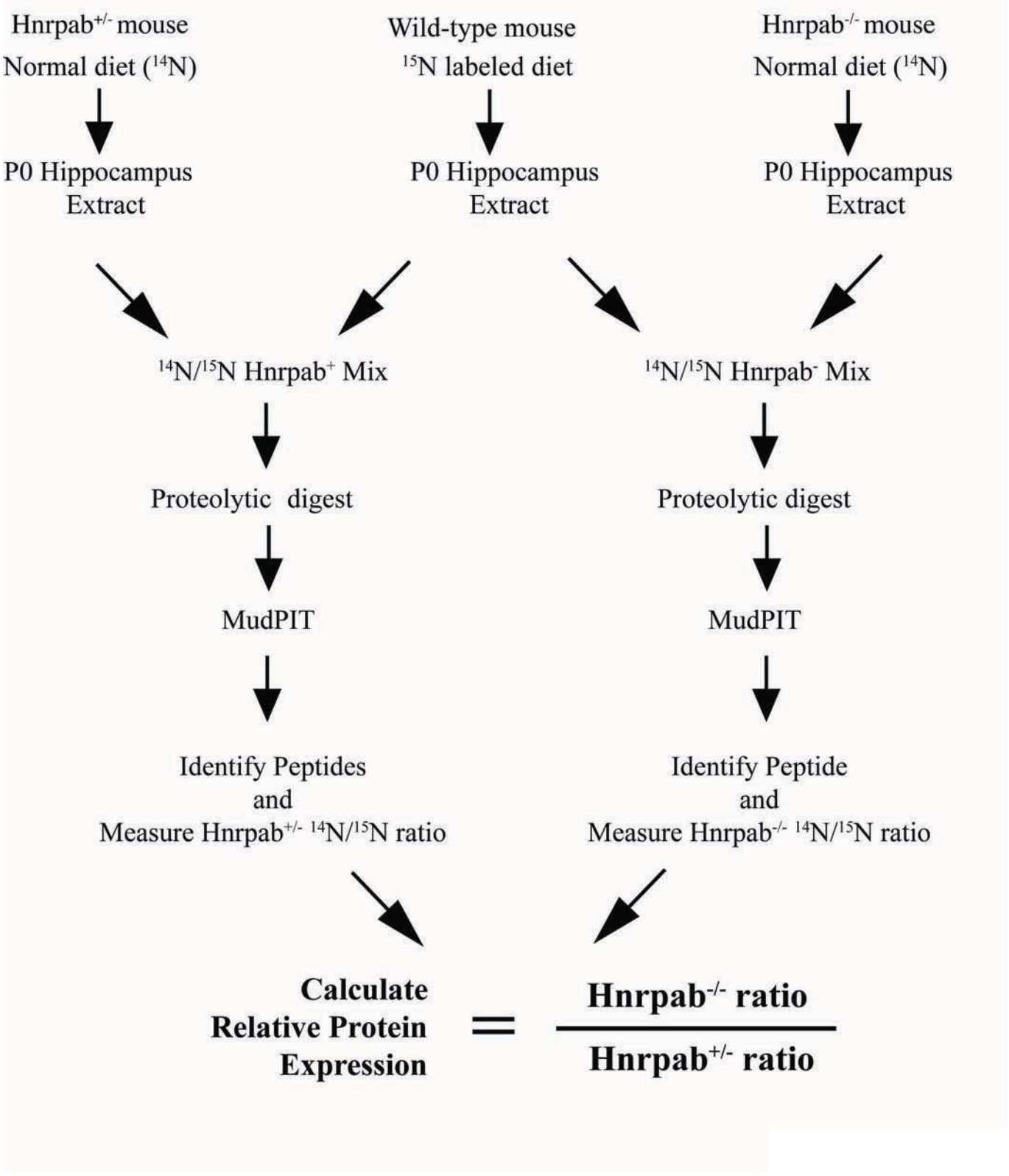

Figure 18- The workflow diagram for quantitative shotgun proteomics of Hnrpab$^{-/-}$ newborn hippocampus. The steps involved in quantifying relative protein levels at the genome wide scale are diagrammed. Brain tissue from a ^{15}N-labeled littermate was used to determine that incorporation of ^{15}N amino acids was greater than 97% by mass spectrometry. The ^{15}N sample serves as an internal reference by which to compare relative levels of protein between Hnrpab$^{+/-}$ and Hnrpab$^{-/-}$ mice after a Multidimensional Protein Identification Technology analysis (MudPIT).

This is a list of all proteins upregulated that was used for the IPA analysis in figure S2. Proteins on this list fit one of three criteria to be considered up-regulated.
First, the protein has one entry in only one fraction (either insoluble or soluble), was quantified in 2/3 animals in both genotypes and the average increase was 1.5 fold or more in Hnrpab KO animals reflected in a KO/Het ratio of 1.5 or greater.
Second, the protein has one entry in only one fraction (either insoluble or soluble) and was quantified in 2/3 Hnrpab KO animals only.These changes cannot be quantified.(found below line 154)
Third, the protein has multiple entries that all corroborate an up-regulation of the protein in the sample, only one entry is included here.

Both Soluble and Insoluble proteins are combined on this list.14N/15N ratios from Heterozygous samples are labelled in yellow. 14N/15N ratios from Homozygous samples labelled in green
The fold change that was calculated from samples of the first and third classes are labelled in orange.

		14N/15N ratio Hnrpab+/- P0 hippocampus			14N/15N ratio Hnrpab-/- P0 hippocampus						
SOLUBLE											
locus	p-value	ratio	ratio	ratio	ratio	ratio	ratio	ratio	ratio	KO/Het	description
IPI00762234	0.10573	0.55	0.29	X	X	1.08	0.94	0.42	1.01	2.4	TREMBL:Q6PAS7 Fbxw9 F-box and WD-40 domain protein 9
IPI00407339	0.11145	1.65	3.99	1.27	3.81	3.72	7.71	2.3	5.08	2.2	SWISS-PROT:P62806 Hist1h4i;Hist1h4m;Hist1h4b;Hist1h4a;Hist1h4f;Hist1h4c;Gm11275;Hist1h4k;Hist4h4;Hist1h4h;Hist2h4;4930558J22Rik;Hist1h4j;Hist1h4d Histone H4
IPI00467266	0.28228	0.71	X	0.45	X	0.72	1.08	0.58	0.9	1.6	TREMBL:Q9CQ43 Dut deoxyuridine triphosphatase isoform 2
IPI00626790	0.21378	0.87	1	X	1.68	X	1.12	0.94	1.4	1.5	SWISS-PROT:P15105 Glul Glutamine synthetase
IPI00114802	0.14935	0.64	0.96	0.7	X	1.16	0.96	0.77	1.06	1.4	SWISS-PROT:P49443 Ppm1a Protein phosphatase 1A
IPI00125267	0.08296	0.44	0.41	X	X	0.59	0.78	0.42	0.68	1.6	SWISS-PROT:Q9WV55 Vapa Vesicle-associated membrane protein-associated protein A
IPI00856140	0.3185	0.6	0.95	X	X	1.48	0.92	0.77	1.2	1.6	TREMBL:D3Z3A0 Ppp1r2 Putative uncharacterized protein Ppp1r2
IPI00720015	0.0176	0.72	0.8	1.01	1.23	1.44	1.23	0.84	1.3	1.5	REFSEQ:XP_001477847 LOC100047284 similar to CDNA sequence BC060632
IPI00116959	0.25335	X	0.34	0.73	0.98	0.6	0.91	0.54	0.83	1.5	SWISS-PROT:Q99LJ6 Gpx7 Glutathione peroxidase 7
IPI00125960	0.6659	0.93	1.11	0.97	2.88	0.9	0.71	1	1.5	1.5	SWISS-PROT:Q62433 Ndrg1 Protein NDRG1
IPI00405603	0.18588	0.67	X	0.51	1	0.75	X	0.59	0.88	1.5	TREMBL:Q8BX68 Hdlbp Putative uncharacterized protein
IPI00153660	0.08919	0.52	0.44	X	0.87	0.65	0.61	0.48	0.71	1.5	SWISS-PROT:Q8BMF4 Dlat Dihydrolipoyllysine-residue acetyltransferase component of pyruvate dehydrogenase complex, mitochondrial
IPI00474144	0.56104	X	0.86	0.79	2.05	0.86	0.72	0.82	1.21	1.5	TREMBL:D3Z613 - Putative uncharacterized protein ENSMUSP00000055939
IPI00649467	0.2872	0.48	0.49	0.63	1.03	0.54	X	0.53	0.78	1.5	SWISS-PROT:O88935-3 Syn1 Isoform 3 of Synapsin-1
IPI00404551	0.17621	0.51	0.73	X	0.71	0.86	1.03	0.62	0.87	1.4	TREMBL:Q8C243 Ctsd Putative uncharacterized protein
IPI00223661	0.29689	1	0.51	X	1.26	0.88	0.97	0.76	1.04	1.4	SWISS-PROT:Q3U487-1 Hectd3 Isoform 1 of Probable E3 ubiquitin-protein ligase HECTD3

INSOLUBLE											
locus	p-value	ratio	ratio	ratio	ratio	ratio	ratio	ratio	ratio	KO/Het	description
IPI00229824	0.24636	0.11	0.06	0.17	0.13	1.04	0.16	0.11	0.44	4.0	SWISS-PROT:Q02780-2 Nfia Nuclear factor 1
IPI00400349	0.19019	1.13	0.4	0.06	0.86	1.99	1.09	0.53	1.31	2.5	SWISS-PROT:Q80U78-2 Pum1 Isoform 2 of Pumilio homolog 1
IPI00405405	0.21348	0.83	X	0.3	X	1.66	1.09	0.56	1.38	2.5	TREMBL:Q05C65 Eif5 Putative uncharacterized protein
IPI00122489	0.33555	X	0.53	0.69	X	2.12	0.71	0.61	1.42	2.3	SWISS-PROT:Q61575 Foxn1 Forkhead box protein N1
IPI00877254	0.05737	1.23	0.65	0.95	2.26	1.74	X	0.94	2	2.1	SWISS-PROT:Q91V14-1 Slc12a5 Isoform 1 of Solute carrier family 12 member 5 KCC2 channel
IPI00323809	0.03598	0.68	0.64	0.75	0.99	2.11	1.29	0.69	1.46	2.1	SWISS-PROT:Q9Z0P4-2 Palm Isoform 2 of Paralemmin
IPI00136716	0.01696	1.23	0.83	1.15	2.27	2.23	X	1.07	2.25	2.1	SWISS-PROT:Q9QYS2 Grm3 Metabotropic glutamate receptor 3
IPI00123039	0.0132	0.67	0.68	0.73	X	1.62	1.16	0.69	1.39	2.0	SWISS-PROT:P35821 Ptpn1 Tyrosine-protein phosphatase non-receptor type 1
IPI00469207	0.22575	0.65	0.78	X	0.86	2.3	1.08	0.72	1.41	2.0	SWISS-PROT:Q6PDS3-1 Sarm1 Isoform 1 of Sterile alpha and TIR motif-containing protein 1
IPI00471006	0.22372	1.06	X	0.77	1.23	2.38	X	0.92	1.8	2.0	SWISS-PROT:Q68FM6 Elfn2 Leucine-rich repeat and fibronectin type-III domain-containing protein 6
IPI00756601	0.20621	1.38	0.7	X	2.36	1.67	X	1.04	2.01	1.9	SWISS-PROT:Q8C0I1 Agps Alkyldihydroxyacetonephosphate synthase, peroxisomal
IPI00110100	0.19536	1.11	0.64	X	2.08	1.33	X	0.88	1.7	1.9	SWISS-PROT:Q9D7A8 Armc1 Armadillo repeat-containing protein 1
IPI00469548	0.09282	1.44	0.84	0.85	1.31	2.83	1.82	1.04	1.99	1.9	SWISS-PROT:Q64332-1 Syn2 Isoform IIa of Synapsin-2
IPI00315280	0.05941	X	0.63	0.75	1.34	1.63	0.96	0.69	1.31	1.9	SWISS-PROT:Q9QUR8 Sema7a Semaphorin-7A
IPI00762435	0.32266	X	0.24	0.84	1.02	X	1.01	0.54	1.02	1.9	SWISS-PROT:P39688-1 Fyn Isoform 1 of Tyrosine-protein kinase Fyn
IPI00230290	0.02576	1.04	0.73	0.89	2.11	1.58	1.28	0.89	1.66	1.9	SWISS-PROT:P43006-3 Slc1a2 Isoform Glt-1B of Excitatory amino acid transporter 2, GLT-1, EAAT2
IPI00468697	0.12932	X	0.54	0.78	0.88	1.71	1.09	0.66	1.23	1.9	SWISS-PROT:Q71B07 Dpy19l3 Protein dpy-19 homolog 3
IPI00403079	0.0342	X	0.71	0.56	1.19	X	1.17	0.64	1.18	1.8	SWISS-PROT:O61735-1 Cd47 Isoform 1 of Leukocyte surface antigen CD47
IPI00785240	0.28604	0.69	0.42	X	X	1.3	0.7	0.55	1	1.8	SWISS-PROT:Q8BTI8-1 Srrm2 Isoform 1 of Serine/arginine repetitive matrix protein 2
IPI00137313	0.15746	1.21	0.69	X	1.77	1.65	X	0.95	1.71	1.8	SWISS-PROT:P70207 Plxna2 Plexin-A2
IPI00474660	0.16849	1.12	0.85	X	1.88	2.28	1.1	0.99	1.75	1.8	TREMBL:Q8QZS2 Rac3 Rac3 protein (Fragment)
IPI00880617	0.03221	0.66	0.46	0.53	0.73	1.16	1.01	0.55	0.97	1.8	ENSEMBL:ENSMUSP00000113502 Sec22b 19 kDa protein
IPI00262693	0.08909	1.03	0.63	1.14	X	1.74	1.55	0.93	1.64	1.8	TREMBL:Q5ICG5 Acsl6 long-chain-fatty-acid--CoA ligase 6 isoform 4
IPI00620866	0.01665	0.58	0.8	0.76	1.28	1.42	1.02	0.71	1.24	1.7	SWISS-PROT:Q7TN98-5 Cpeb4 Isoform 5 of Cytoplasmic polyadenylation element-binding protein 4
IPI00928300	0.03511	0.96	0.73	0.87	1.34	1.94	1.17	0.85	1.48	1.7	TREMBL:Q3UZD8 Rangap1 ran GTPase-activating protein 1
IPI00553593	0.01014	0.84	X	0.84	X	1.53	1.37	0.84	1.45	1.7	SWISS-PROT:Q8BYI9-2 Tnr Isoform 2 of Tenascin-R
IPI00321634	0.04644	0.98	0.61	0.6	1.01	1.49	1.28	0.73	1.26	1.7	SWISS-PROT:Q9DBH5 Lman2 Vesicular integral-membrane protein VIP36
IPI00849863	0.16329	X	0.75	0.86	1.07	1.69	X	0.8	1.38	1.7	REFSEQ:XP_001478747 LOC100047696 similar to Eukaryotic translation initiation factor 3, subunit 8
IPI00222937	0.12921	X	0.8	1.12	1.58	2.16	1.2	0.96	1.65	1.7	SWISS-PROT:Q8BM72-1 Hspa13 Isoform 1 of Heat shock 70 kDa protein 13
IPI00420919	0.27505	0.89	0.74	0.48	X	1.65	0.76	0.7	1.2	1.7	SWISS-PROT:Q6PGH0 Ubtd2 Ubiquitin domain-containing protein 2
IPI00356667	0.07735	1.03	0.74	0.9	X	1.83	1.21	0.89	1.52	1.7	TREMBL:Q3UTP0 Pcdh17 protocadherin 17 precursor
IPI00222429	0.09203	0.46	0.52	0.98	1.32	0.93	1.04	0.65	1.1	1.7	TREMBL:Q3TKZ1 Nomo1 nodal modulator 1
IPI00649344	0.43934	0.25	0.62	X	0.32	1.03	0.87	0.44	0.74	1.7	TREMBL:Q5SVW9 Tmed4 Transmembrane emp24 protein transport domain containing 4
IPI00881287	0.02158	X	0.55	0.48	0.75	1	0.87	0.52	0.87	1.7	SWISS-PROT:O35465-2 Fkbp8 Isoform 2 of Peptidyl-prolyl cis-trans isomerase FKBP8
IPI00126796	0.24184	X	0.74	0.77	0.91	1.62	X	0.76	1.27	1.7	SWISS-PROT:Q91VE0 Slc27a4 Long-chain fatty acid transport protein 4
IPI00226882	0.03719	X	0.22	0.25	0.44	X	0.37	0.24	0.4	1.7	SWISS-PROT:P61620 Sec61a1 Protein transport protein Sec61 subunit alpha isoform 1
IPI00121767	0.0742	0.75	0.51	0.68	0.91	1.25	X	0.65	1.08	1.7	SWISS-PROT:Q9JJF3 2410016O06Rik Lysine-specific demethylase NO66
IPI00666350	0.28647	0.74	0.41	0.77	X	1.42	0.7	0.64	1.06	1.7	TREMBL:A2AR01 Ppig Ppig protein
IPI00890142	0.11549	1.68	0.96	1.16	1.8	2.39	X	1.27	2.1	1.7	SWISS-PROT:A2A699-2 Fam171a2 Isoform 2 of Protein FAM171A2
IPI00113200	0.17259	1.17	0.62	0.91	X	1.73	1.18	0.9	1.46	1.6	SWISS-PROT:P56393 Cox7b Cytochrome c oxidase subunit 7B, mitochondrial
IPI00137314	0.09339	1.25	0.69	0.98	1.49	2	1.23	0.97	1.57	1.6	TREMBL:A4FVD1 Plxna3 plexin A3
IPI00850879	0.44857	X	0.57	0.66	0.6	1.41	X	0.62	1	1.6	REFSEQ:XP_001474484 Gm2991 similar to U1 snRNP-specific protein C
IPI00875068	0.11638	0.75	0.42	0.65	0.72	1.27	0.94	0.61	0.98	1.6	TREMBL:Q52L67 Tecr Gpsn2 protein (GPSN2)/trans-2,3-enoly-CoA reductase group
IPI00128905	0.04542	0.81	0.58	0.7	X	1.01	1.23	0.7	1.12	1.6	SWISS-PROT:Q91XA2 Golm1 Golgi membrane protein 1
IPI00751137	0.08588	1	0.52	0.92	1.26	1.42	1.15	0.81	1.28	1.6	TREMBL:Q3TSX8 Tomm70a Putative uncharacterized protein
IPI00119131	0.10532	1.35	0.66	0.66	1.31	1.5	1.36	0.89	1.39	1.6	SWISS-PROT:Q9DB73-1 Cyb5r1 Isoform 1 of NADH-cytochrome b5 reductase 1
IPI00224091	0.10952	0.7	0.42	0.66	0.7	1.15	0.91	0.59	0.92	1.6	SWISS-PROT:Q8C172 Lass6 LAG1 longevity assurance homolog 6
IPI00845689	0.32295	1.18	0.63	X	0.9	1.93	1.36	0.9	1.4	1.6	TREMBL:Q9CZL0 Tmed9 Putative uncharacterized protein
IPI00453798	0.03596	0.83	0.63	X	1.03	1.23	1.13	0.73	1.13	1.5	SWISS-PROT:Q8BXZ1 Tmx3 Protein disulfide-isomerase TMX3
IPI00762083	0.12536	1.23	0.87	X	1.58	1.65	X	1.05	1.62	1.5	TREMBL:Q80VM5 Dpp6 dipeptidyl aminopeptidase-like protein 6 isoform 1
IPI00230715	0.15142	1.06	0.55	0.89	1.42	1.49	0.92	0.83	1.28	1.5	SWISS-PROT:Q9ERS2 Ndufa13 NADH dehydrogenase [ubiquinone] 1 alpha subcomplex subunit 13
IPI00127237	0.29911	0.91	X	0.65	X	1.49	0.91	0.78	1.2	1.5	SWISS-PROT:Q9R0A0 Pex14 Peroxisomal membrane protein PEX14
IPI00153381	0.19668	0.96	0.55	0.61	0.91	1.56	0.79	0.71	1.09	1.5	SWISS-PROT:Q8R1I1 Uqcr10 Cytochrome b-c1 complex subunit 9
IPI00405303	0.38894	0.74	0.47	X	0.66	1.17	X	0.6	0.92	1.5	TREMBL:Q8C5J1 Aldh3a2 Putative uncharacterized protein
IPI00122826	0.19105	1.01	0.46	0.79	1.45	1.16	0.83	0.75	1.15	1.5	SWISS-PROT:Q9JKC6 Cend1 Cell cycle exit and neuronal differentiation protein 1
IPI00121131	0.16523	0.98	0.5	0.74	1.14	1.12	X	0.74	1.13	1.5	SWISS-PROT:Q62092 Nsg1 Neuron-specific protein family member 1
IPI00169845	0.12989	0.75	0.44	0.69	0.76	1.27	0.86	0.63	0.96	1.5	SWISS-PROT:Q8K273 Mmgt1 Membrane magnesium transporter 1
IPI00828929	0.33057	1.15	0.68	X	X	1.68	1.1	0.92	1.39	1.5	SWISS-PROT:Q8R0F6-2 Ilkap Isoform 2 of Integrin-linked kinase-associated serine/threonine phosphatase 2C
IPI00753292	0.0696	X	0.47	0.59	X	0.82	0.78	0.53	0.8	1.5	TREMBL:D3YU36 Gm8062 Putative uncharacterized protein ENSMUSP00000100733 (RPL22)
IPI00776142	0.46696	0.77	0.64	X	1.46	X	0.68	0.71	1.07	1.5	TREMBL:B1AVY2 Gabra3 Gamma-aminobutyric acid (GABA-A) receptor, subunit alpha 3
IPI00850413	0.17744	0.7	0.35	0.67	0.65	0.98	0.91	0.57	0.85	1.5	SWISS-PROT:Q3UUQ7-1 Pgap1 Isoform 1 of GPI inositol-deacylase
IPI00408215	0.07574	X	0.74	0.73	0.88	1.3	1.13	0.74	1.1	1.5	SWISS-PROT:P46735-1 Myo1b myosin-Ib isoform 1
IPI00896707	0.2946	X	0.51	0.74	0.84	1.28	0.65	0.62	0.92	1.5	TREMBL:B2RQA0 Gm5124 EG331392 protein
IPI00850529	0.28267	0.92	0.54	X	X	1.2	0.96	0.73	1.08	1.5	SWISS-PROT:Q3URS9-2 Ccdc51 Isoform 2 of Coiled-coil domain-containing protein 51
IPI00407312	0.25048	0.64	0.66	X	0.73	1.35	0.8	0.65	0.96	1.5	SWISS-PROT:Q922J9-3 Far1 Isoform 3 of Fatty acyl-CoA reductase 1
IPI00881090	0.31013	0.92	0.54	0.82	0.8	1.43	X	0.76	1.12	1.5	TREMBL:D3YX62 Hmox2 Putative uncharacterized protein Hmox2
IPI00229722	0.36848	X	0.71	0.81	0.8	1.45	X	0.76	1.12	1.5	SWISS-PROT:Q80U93 Nup214 Nuclear pore complex protein Nup214
IPI00515716	0.06686	0.74	0.62	X	0.94	X	1.05	0.68	1	1.5	SWISS-PROT:Q9D8B1-2 Aig1 Isoform 2 of Androgen-induced gene 1 protein
IPI00851052	0.15157	0.95	0.56	0.91	1.17	1.22	X	0.81	1.19	1.5	REFSEQ:XP_001477452 LOC100046871 similar to GPI transamidase component PIG-T precursor (Phosphatidylinositol-glycan biosynthesis class T protein) (Neuronal development-associated protein 7) isoform 2
IPI00139259	0.29964	0.94	0.41	0.66	0.68	1.43	0.84	0.67	0.98	1.5	SWISS-PROT:P62996-1 Tra2b Isoform 1 of Transformer-2 protein homolog beta
IPI00624653	0.1909	1.24	0.65	0.9	1.29	1.42	X	0.93	1.36	1.5	SWISS-PROT:Q78IK2 Usmg5 Up-regulated during skeletal muscle growth protein 5
IPI00831418	0.20233	X	0.51	1.01	1.03	1.23	1.06	0.76	1.11	1.5	TREMBL:D3Z0P9 Sdhc Putative uncharacterized protein Sdhc
IPI00754545	0.23896	1.16	0.84	1.18	1.15	1.92	X	1.06	1.54	1.5	REFSEQ:XP_001473550 Gm2423 similar to Ywhaq protein
IPI00944213	0.59047	1.24	X	0.94	0.79	X	4.54	1.09	2.66	2.4	REFSEQ:NP_001157645 Cpsf1 cleavage and polyadenylation specificity factor subunit 1 isoform 1
IPI00896093	0.13873	X	0.43	0.5	1.45	0.75	X	0.46	1.1	2.4	SWISS-PROT:Q8BGT8-2 Phyhipl Isoform 2 of Phytanoyl-CoA hydroxylase-interacting protein-like
IPI00330094	0.03802	0.46	0.42	X	0.98	1.27	0.71	0.44	0.99	2.3	SWISS-PROT:P97742 Cpt1a Carnitine O-palmitoyltransferase 1, liver isoform
IPI00775828	0.04894	X	0.74	1.04	1.81	2.03	X	0.89	1.92	2.2	SWISS-PROT:Q8C0E2-2 Vps26b Isoform 2 of Vacuolar protein sorting-associated protein 26B
IPI00323800	0.18726	1.02	0.48	0.46	0.88	1.81	X	0.65	1.34	2.1	SWISS-PROT:P08553 Nefm Neurofilament medium polypeptide
IPI00377299	0.30552	1.26	0.7	0.79	X	2.85	0.91	0.92	1.88	2.0	SWISS-PROT:Q6PGF7 Exoc8 Exocyst complex component 8
IPI00624881	0.17919	X	0.83	0.86	1.18	2.25	X	0.84	1.71	2.0	SWISS-PROT:Q3TDK6-2 Rogdi Isoform 2 of Protein rogdi homolog
IPI00515257	0.21131	X	0.37	0.86	X	1.37	1.12	0.62	1.24	2.0	SWISS-PROT:Q64152-1 Btf3 Isoform 1 of Transcription factor BTF3
IPI00655041	0.3503	X	0.88	1.07	1.14	3.53	1.15	0.98	1.94	2.0	SWISS-PROT:Q9D4H1 Exoc2 Exocyst complex component 2
IPI00309223	0.08121	0.64	0.64	X	1.08	1.77	0.94	0.64	1.26	2.0	SWISS-PROT:O70166 Stmn3 Stathmin-3
IPI00651782	0.16105	1.02	1.19	1.64	X	3.35	1.6	1.28	2.48	1.9	TREMBL:Q3TD78 Gbas glioblastoma amplified
IPI00410756	0.15013	X	0.31	0.57	X	0.82	0.87	0.44	0.84	1.9	SWISS-PROT:Q9D365 2900062L11Rik;6530401D17Rik Signal peptidase complex subunit 3
IPI00356147	0.11361	0.91	0.53	0.69	X	1.6	0.99	0.71	1.3	1.8	SWISS-PROT:O8K4G5-4 Ablim1 Ablim1 protein
IPI00378480	0.20833	0.07	0.02	0.05	0.09	0.12	0.05	0.05	0.09	1.8	SWISS-PROT:Q9QZQ8-1 H2afy Isoform 2 of Core histone macro-H2A.1
IPI00230383	0.02797	1.17	0.89	1.03	X	2.09	1.59	1.03	1.84	1.8	SWISS-PROT:Q03137-2 Epha4 Isoform Short of Ephrin type-A receptor 4
IPI00404970	0.25209	0.61	0.87	X	1.37	1.84	0.74	0.74	1.32	1.8	SWISS-PROT:Q5FWK3 Arhgap1 Rho GTPase-activating protein 1
IPI00751955	0.22844	X	0.49	0.82	0.91	1.43	X	0.66	1.17	1.8	TREMBL:D3Z2J6 Tmx2 Putative uncharacterized protein Tmx2
IPI00281011	0.14245	1.1	0.78	1.05	1.46	2.64	1.09	0.98	1.73	1.8	SWISS-PROT:P28667 Marcksl1 MARCKS-related protein
IPI00624863	0.5216	0.98	0.86	1.32	0.78	2.91	X	1.05	1.85	1.8	TREMBL:Q9CQ38 Paics Putative uncharacterized protein
IPI00876027	0.15673	0.89	0.76	0.85	0.97	1.96	X	0.83	1.46	1.8	SWISS-PROT:Q3TPX4 Exoc5 Exocyst complex component 5
IPI00315463	0.0933	0.73	0.62	1	1	1.85	1.14	0.78	1.33	1.7	SWISS-PROT:Q60870 Reep5 receptor expression-enhancing protein 5
IPI00757771	0.15528	X	0.83	0.94	1.83	X	1.18	0.88	1.5	1.7	TREMBL:D3YW67 Nptn Putative uncharacterized protein Nptn
IPI00623890	0.24286	X	1.04	1.19	1.12	2.65	1.94	1.12	1.9	1.7	TREMBL:Q52KF7 Dlg3 Dlgh3 protein (SAP102)
IPI00775844	0.07858	1.15	0.82	0.88	1.51	2.18	1.14	0.95	1.61	1.7	TREMBL:D3YXG6 Arpc2 Putative uncharacterized protein Arpc2
IPI00269408	0.0973	1.13	0.73	0.9	1.14	2.08	1.31	0.92	1.51	1.6	SWISS-PROT:Q8R570-1 Snap47 Isoform 1 of Synaptosomal-associated protein 47
IPI00319965	0.29073	0.88	0.67	1.16	1.57	2.11	0.74	0.9	1.47	1.6	SWISS-PROT:Q99JI4 Psmd6 26S proteasome non-ATPase regulatory subunit 6
IPI00129548	0.17277	1.44	1.45	0.96	1.55	2.62	X	1.28	2.08	1.6	SWISS-PROT:Q8VIM9 Irgq Immunity-related GTPase family Q protein
IPI00928212	0.22019	0.63	0.66	0.61	0.63	1.54	0.83	0.63	1	1.6	TREMBL:D3YTP4 Scamp1 Putative uncharacterized protein Scamp1
IPI00113606	0.10513	0.89	0.56	0.9	1.19	1.25	X	0.78	1.22	1.6	SWISS-PROT:Q9ESW4-1 Agk Isoform 1 of Acylglycerol kinase, mitochondrial
IPI00751569	0.14043	1.35	0.66	0.9	1.24	1.92	1.32	0.97	1.49	1.5	TREMBL:A2AUE1 Dnajc5 DnaJ (Hsp40) homolog, subfamily C, member 5
IPI00473582	0.22094	X	0.82	1.16	X	1.76	1.26	0.99	1.51	1.5	TREMBL:Q9D586 Cntfr ciliary neurotrophic factor receptor subunit alpha isoform 2
IPI00313841	0.34008	0.89	X	0.93	1.25	2.02	0.87	0.91	1.38	1.5	SWISS-PROT:P51863 Atp6v0d1 V-type proton ATPase subunit d 1
IPI00128692	0.04974	0.82	0.57	0.72	0.92	1.29	0.98	0.7	1.06	1.5	SWISS-PROT:O9R1J0 Nsdhl Sterol-4-alpha-carboxylate 3-dehydrogenase, decarboxylating
IPI00880589	0.20052	1.01	0.62	0.82	1.11	1.77	0.85	0.82	1.24	1.5	ENSEMBL:ENSMUSP00000121852 Auh Protein AU RNA binding protein/enoyl-Coenzyme A hydratase (AUH)
IPI00856480	0.16073	1.43	X	0.98	1.72	1.93	X	1.2	1.82	1.5	ENSEMBL:ENSMUSP00000109088 Nrxn2 177 kDa protein
IPI00226727	0.18234	1.1	1.27	0.86	1.75	2.08	1.04	1.08	1.62	1.5	SWISS-PROT:Q91XM9-2 Dlg2 Isoform 2 of Disks large homolog 2
IPI00128973	0.08318	0.99	0.64	0.96	1.17	1.59	1.12	0.86	1.29	1.5	SWISS-PROT:P06837 Gap43 Neuromodulin
IPI00461500	0.36242	X	0.3	0.49	0.45	X	0.74	0.4	0.6	1.5	TREMBL:D3YTZ1 Gm5443 Putative uncharacterized protein Gm5443 (RPL29)
IPI00850413	0.17744	0.7	0.35	0.67	0.65	0.98	0.91	0.57	0.85	1.5	SWISS-PROT:Q3UUQ7-1 Pgap1 Isoform 1 of GPI inositol-deacylase
IPI00719927	0.01556	1.06	0.83	1.01	1.54	1.51	1.26	0.97	1.44	1.5	TREMBL:Q2TJI9 Pcdh1 Protocadherin 1 isoform 2
IPI00621229	0.26576	0.94	0.52	0.79	X	1.37	0.85	0.75	1.11	1.5	TREMBL:D3Z6G6 Rps8-ps1 Putative uncharacterized protein Gm6998
IPI00515319	0.37856	1.35	0.37	0.28	X	0.96	1.02	0.67	0.99	1.5	TREMBL:O54696 Ptgfrn prostaglandin F2 receptor negative regulator precursor
IPI00855186	0.30792	1.24	0.9	1.02	1.01	2.4	1.24	1.05	1.55	1.5	TREMBL:Q99JZ9 Srp54c signal recognition particle 54C
IPI00877282	0.12584	0.81	0.54	0.86	1.16	X	1.02	0.74	1.09	1.5	SWISS-PROT:Q5SS80-2 Dhrs13 Dehydrogenase/reductase (SDR family) member 13
IPI00120984	0.1278	1.05	0.61	0.93	1.27	1.51	1	0.86	1.26	1.5	SWISS-PROT:Q9DCJ5 Ndufa8 NADH dehydrogenase [ubiquinone] 1 alpha subcomplex subunit 8
IPI00652694	0.18397	1.14	0.94	0.73	1.11	1.62	X	0.94	1.37	1.5	TREMBL:Q3TP95 Psmd3 Putative uncharacterized protein
IPI00849044	0.39379	0.97	0.96	0.86	0.85	2.21	1	0.93	1.35	1.5	TREMBL:Q3TDU1 Arcn1 Putative uncharacterized protein (coatamer subunit delta)
IPI00654180	0.214	0.75	X	1.03	1.14	1.71	X	0.89	1.42	1.6	TREMBL:A0PJ98 Ppp2r5e Putative uncharacterized protein

These proteins belong to the second class of entries, and are provided in a separate list because their fold regulation could not be quantified.

SOLUBLE

IPI00480321	SWISS-PROT:Q91YM2 Grlf1 Glucocorticoid receptor DNA-binding factor 1
IPI00551347	SWISS-PROT:Q8CBW3-3 Abi1 Isoform 3 of Abl interactor 1
IPI00407158	SWISS-PROT:Q9QZX7-2 Srr Isoform 2 of Serine racemase
IPI00929839	TREMBL:Q3TT18 Actr10 ARP10 actin-related protein 10
IPI00943373	TREMBL:B1ATT5 Fn3krp ketosamine-3-kinase
IPI00750256	SWISS-PROT:Q9R0Y5-2 Ak1 Isoform 2 of Adenylate kinase isoenzyme 1
IPI00830172	SWISS-PROT:Q9D6T0-2 Nosip Isoform 2 of Nitric oxide synthase-interacting protein
IPI00315463	SWISS-PROT:O60870 Reep5 receptor expression-enhancing protein 5

IPI00117733 SWISS-PROT:Q99MI1-2 Erc1 Isoform 2 of ELKS/Rab6-interacting/CAST family member 1
IPI00661414 SWISS-PROT:Q9CVB6 Arpc2 Actin-related protein 2/3 complex subunit 2
IPI00467104 SWISS-PROT:Q9JJZ8 Flii Protein flightless-1 homolog
IPI00658779 REFSEQ:XP_905039 Gm6563 hypothetical protein isoform 2
IPI00129132 SWISS-PROT:P97789-1 Xrn1 5'-3' exoribonuclease 1
IPI00652635 SWISS-PROT:P70303-2 Ctps2 Isoform 2 of CTP synthase 2
IPI00406442 SWISS-PROT:Q9WUM5 Suclg1 Succinyl-CoA ligase [GDP-forming] subunit alpha, mitochondrial
IPI00116877 SWISS-PROT:Q99LG2 Tnpo2 transportin-2
IPI00759938 SWISS-PROT:P17710-4 Hk1 Isoform HK1-SC of Hexokinase-1
IPI00122273 SWISS-PROT:Q62165 Dag1 Dystroglycan
IPI00458109 REFSEQ:XP_485435 Gm12844;LOC631743 similar to Rho family GTPase RhoA
IPI00111117 SWISS-PROT:Q9DB98 Arpc5l Actin-related protein 2/3 complex subunit 5-like protein
IPI00269408 SWISS-PROT:Q8R570-1 Snap47 Isoform 1 of Synaptosomal-associated protein 47
IPI00648157 TREMBL:A2ALE9 Dnajc8 Dna1 (Hsp40) homolog, subfamily C, member 8
IPI00109401 SWISS-PROT:Q9D706 Rpap3 RNA polymerase II-associated protein 3
IPI00469231 TREMBL:Q3U5J8 Adrbk1 Adrenergic receptor kinase, beta 1
IPI00877282 SWISS-PROT:Q5SS80-2 Dhrs13 Dehydrogenase/reductase (SDR family) member 13
IPI00462899 SWISS-PROT:Q920Q6-2 Msi2 Isoform 2 of RNA-binding protein Musashi homolog 2
IPI00459329 SWISS-PROT:P97300-4 Nptn Isoform 4 of Neuroplastin
IPI00831544 SWISS-PROT:Q7TMB8-2 Cyfip1 Isoform 2 of Cytoplasmic FMR1-interacting protein 1
IPI00880589 ENSEMBL:ENSMUSP00000121852 Auh Protein
IPI00124820 SWISS-PROT:Q9WUM4 Coro1c Coronin-1C
IPI00816895 TREMBL:D3Z7J2 Pycrl Putative uncharacterized protein Pycrl
IPI00407764 SWISS-PROT:Q9CSH3 Dis3 Exosome complex exonuclease RRP44
IPI00108811 SWISS-PROT:P17439 Gba Glucosylceramidase
IPI00461314 TREMBL:Q9EP83 Lsm2 SnRNP core protein SMX5b
IPI00271453 SWISS-PROT:P97792-2 Cvadr Isoform 2 of Coxsackievirus and adenovirus receptor homolog
IPI00816922 SWISS-PROT:Q6A4J8-3 Usp7 Isoform 3 of Ubiquitin carboxyl-terminal hydrolase 7
IPI00135150 TREMBL:Q9CT07 Kpna3 Putative uncharacterized protein (Fragment)
IPI00323079 SWISS-PROT:P12023-2 App Isoform APP695 of Amyloid beta A4 protein (Fragment)
IPI00117632 SWISS-PROT:Q99ME2 Wdr6 WD repeat-containing protein 6
IPI00387422 TREMBL:Q3TCR9 Zyx zyxin
IPI00126072 SWISS-PROT:Q62465 Vat1 Synaptic vesicle membrane protein VAT-1 homolog
IPI00356147 SWISS-PROT:Q8K4G5-4 Ablim1 Ablim1 protein
IPI00153656 SWISS-PROT:Q8BP71-5 Rbm9 Isoform 5 of RNA-binding protein 9 (AKA FOX2)
IPI00756747 TREMBL:A2AR56 Fam129b Novel PH domain containing protein
IPI00221845 SWISS-PROT:Q8BHE3 Atcay Caytaxin
IPI00312101 SWISS-PROT:Q8RS50-3 Sh3kbp1 Isoform 3 of SH3 domain-containing kinase-binding protein 1
IPI00624876 SWISS-PROT:P70460 Vasp Vasodilator-stimulated phosphoprotein
IPI00623890 TREMBL:Q52KF7 Dlg3 Dlg3 protein
IPI00460653 TREMBL:Q6AXD2 Abi2 Abi2 protein
IPI00620988 ENSEMBL:ENSMUSP00000081137 Clstn1 115 kDa protein (a psd protein)
IPI00882382 TREMBL:D3Z1V3 Eftud1 Putative uncharacterized protein Eftud1
IPI00458056 SWISS-PROT:Q3UYV9 Ncbp1 Nuclear cap-binding protein subunit 1
IPI00856297 TREMBL:Q3U8U9 Lrpap1 Putative uncharacterized protein
IPI00136252 SWISS-PROT:Q4VBE8 Wdr18 WD repeat-containing protein 18
IPI00420589 SWISS-PROT:Q6ZQA6 Igsf3 Immunoglobulin superfamily member 3
IPI00133928 SWISS-PROT:O9D1M4 Eef1e1 Eukarvotic translation elonzation factor 1 epsilon-1
IPI00131056 SWISS-PROT:O88477 Igf2bp1 Insulin-like growth factor 2 mRNA-binding protein 1
IPI00225719 SWISS-PROT:Q8C570 Rae1 mRNA export factor
IPI00884555 TREMBL:O3TCN0 Pelo protein pelota homoloo
IPI00762036 ENSEMBL:ENSMUSP00000096180 Aplp1 73 kDa protein
IPI00857879 TREMBL:D3Z0C2 Asns Putative uncharacterized protein Asns (upregulated in UPR)
IPI00875943 ENSEMBL:ENSMUSP00000108806 Asrgl1 36 kDa protein
IPI00378156 SWISS-PROT:A2AWA9-1 Rabgap1 Isoform 1 of Rab GTPase-activating protein 1
IPI00130589 SWISS-PROT:P08228 Sod1 Superoxide dismutase [Cu-Zn]
IPI00719908 SWISS-PROT:Q2M3X8-1 Phactr1 Isoform 1 of Phosphatase and actin regulator 1
IPI00625151 SWISS-PROT:Q3TRR0-2 Mtap9 Isoform 2 of Microtubule-associated protein 9
IPI00267661 SWISS-PROT:Q9D219 Bcl9 B-cell CLL/lymphoma 9 protein
IPI00648476 SWISS-PROT:P32020-2 Scp2 Isoform SCP2 of Non-specific lipid-transfer protein
IPI00626986 SWISS-PROT:Q80U49-2 AW555464 Isoform 2 of Protein KIAA0284 (related to a centrosomal protein170kd)
IPI00757916 REFSEQ:XP_001474216 LOC100045699 similar to Electron transferrino flavoprotein, beta polvpeptide isoform 1
IPI00876172 TREMBL:D3YU46 - Putative uncharacterized protein ENSMUSP00000100709 (RPL23/25?)
IPI00750883 SWISS-PROT:Q9CRZ9-2 Ccdc43 Isoform 2 of Coiled-coil domain-containing protein 43
IPI00128240 SWISS-PROT:Q8VHC3 Selm Selenoprotein M
IPI00927993 VEGA:OTTMUSP00000046115 Asl 49 kDa protein (argininosuccinate lyase)
IPI00225349 TREMBL:Q542X2 Gmpr2 GMP reductase 2
IPI00755905 TREMBL:A2AIX1 Sec16a SEC16 homolog A
IPI00607928 SWISS-PROT:O8DO30-1 2310014H01Rik Isoform 1 of Phostensin (actin capping, pp1 targeting)
IPI00380989 TREMBL:Q9D7X2 2210016F16Rik hypothetical protein LOC70153
IPI00308498 SWISS-PROT:P70677 Casp3 Caspase-3
IPI00620834 SWISS-PROT:Q78YZ6-2 Scoc Isoform 2 of Short coiled-coil protein
IPI00651987 SWISS-PROT:Q3ULW6-1 Ccdc33 Isoform 1 of Coiled-coil domain-containing protein 33
IPI00469565 SWISS-PROT:Q62059-3 Vcan versican core protein isoform 3
IPI00466186 SWISS-PROT:Q8CDG3-2 Vcpip1 Isoform 2 of Deubiquitinating protein VCIP135
IPI00875057 TREMBL:O54716 Slc4a1ap Kanadaptin
IPI00169622 SWISS-PROT:Q8K0S0 Phyhip Phytanoyl-CoA hydroxylase-interacting protein
IPI00165711 SWISS-PROT:Q3UI43 5430437P03Rik BRCA1-A complex subunit MERIT40
IPI00322610 SWISS-PROT:Q9DBL7 Coasy Bifunctional coenzyme A synthase
IPI00857041 TREMBL:D3Z3T5 Pcyt1a Putative uncharacterized protein Pcyt1a
IPI00762238 SWISS-PROT:Q8C525 1600021P15Rik Uncharacterized protein C3orf59 homolog
IPI00228306 SWISS-PROT:Q9WUA6-2 Akt3 Isoform 2 of RAC-gamma serine/threonine-protein kinase
IPI00129479 SWISS-PROT:Q91XU3 Pip4k2c Phosphatidylinositol-5-phosphate 4-kinase type-2 gamma
IPI00229349 TREMBL:Q8CFP7 Ate1 Putative uncharacterized protein (arginyl transferase)
IPI00473209 TREMBL:Q8R0Z4 Snx6 Snx6 protein
IPI00131287 SWISS-PROT:Q91ZP9-1 Necab2 Isoform 1 of N-terminal EF-hand calcium-binding protein 2
IPI00621975 REFSEQ:XP_001476702 LOC100046698 similar to Probable ATP-dependent RNA helicase DDX46
IPI00223757 SWISS-PROT:P45376 Akr1b3 Aldose reductase
IPI00137831 SWISS-PROT:Q05186 Rcn1 Reticulocalbin-1
IPI00330551 SWISS-PROT:Q59J78 Ndufaf2 Mimitin, mitochondrial
IPI00121271 SWISS-PROT:Q9DCS2 0610011F06Rik UPF0585 protein C16orf13 homolog
IPI00756773 REFSEQ:XP_001474704 LOC100045629 similar to myocardial ischemic preconditioning upregulated protein 2 isoform 1
IPI00752921 TREMBL:A2AH27 Nudt9 Nudix (Nucleoside diphosphate linked moiety X)-type motif 9
IPI00311476 SWISS-PROT:Q8BVF2 Pdcl3 Phosducin-like protein 3
IPI00858299 TREMBL:D3YYK0 Abhd11 Putative uncharacterized protein Abhd11 (abhydrolase domain containing 11)
IPI00226726 SWISS-PROT:O8C7K6 Pcvox1l Prenvlcvsteine oxidase-like
IPI00172022 SWISS-PROT:Q8CFC7-2 Sfrs16 Isoform 2 of Splicing factor, arginine/serine-rich 16
IPI00608077 SWISS-PROT:Q6URW6-2 Myh14 Isoform 2 of Myosin-14
IPI00130475 SWISS-PROT:Q91Z38 Ttc1 Tetratricopeptide repeat protein 1
IPI00957058 SWISS-PROT:B2RXR6 Ankrd44 Serine/threonine-protein phosphatase 6 regulatory ankyrin repeat subunit B
IPI00457619 SWISS-PROT:Q3UJD6-2 Usp19 Isoform 2 of Ubiquitin carboxyl-terminal hydrolase 19
IPI00653141 SWISS-PROT:Q91WG4-2 Elp2 Isoform 2 of Elongator complex protein 2
IPI00116529 SWISS-PROT:O70274 Ptp4a2 Protein tyrosine phosphatase type IVA 2
IPI00874436 SWISS-PROT:Q9DB27-1 Mcts1 Isoform 1 of Malignant T cell-amplified sequence 1
IPI00125135 SWISS-PROT:P62838 Ube2d2 Ubiquitin-conjugating enzyme E2 D2
IPI00113408 SWISS-PROT:P47968 Rpia Ribose-5-phosphate isomerase
IPI00330933 SWISS-PROT:Q9WVQ5 Apip Probable methylthioribulose-1-phosphate dehydratase
IPI00342382 SWISS-PROT:P56960 Exosc10 Exosome component 10
IPI00881096 TREMBL:D3Z4B2 Napg Putative uncharacterized protein Napg (N-ethylmaleimide-sensitive factor attachment protein)
IPI00753434 REFSEQ:XP_001478674 LOC100047333 similar to Ena-VASP-like isoform 1
IPI00652521 TREMBL:Q3TVD9 Mccc1 Putative uncharacterized protein (methylcrotonoyl-CoA carboxylase 1)
IPI00673016 TREMBL:D3Z3C1 Gm6432 similar to Fas apoptotic inhibitory molecule
IPI00654224 SWISS-PROT:Q2YDW2-2 Msto1 Isoform 2 of Protein misato homolog 1
IPI00229392 SWISS-PROT:Q80X95 Rraga Ras-related GTP-binding protein A

INSOLUBLE

IPI00466992 SWISS-PROT:Q6VNB8-2 Wdfy3 Isoform 2 of WD repeat and FYVE domain-containing protein 3
IPI00465884 SWISS-PROT:P60670-1 Nploc4 Isoform 1 of Nuclear protein localization protein 4 homolog
IPI00849688 REFSEQ:XP_001473949 LOC100045228 similar to neuroligin 3
IPI00869359 SWISS-PROT:Q8CI71-1 Ccdc132 Isoform 1 of Coiled-coil domain-containing protein 132
IPI00128915 SWISS-PROT:Q8VHY0-1 Cspg4 Isoform 1 of Chondroitin sulfate proteoglycan 4
IPI00268433 TREMBL:Q27PY9 Slc8a1 Solute carrier family 8 sodium/calcium exchanger member 1 splicing variant 1.41
IPI00471176 SWISS-PROT:Q640R3 Hepacam Hepatocyte cell adhesion molecule
IPI00276926 TREMBL:Q3TDH6 Slc25a1 solute carrier family 25, member 1 (citrate carrier)
IPI00876343 TREMBL:Q3UJ14 Hip1r huntingtin-interacting protein 1-related protein
IPI00875833 SWISS-PROT:Q3V3R1 Mthfd1l Monofunctional C1-tetrahydrofolate synthase, mitochondrial
IPI00551412 SWISS-PROT:P61327 Magoh Protein mago nashi homolog
IPI00407938 SWISS-PROT:Q9CRD0-2 Ociad1 Isoform 2 of OCIA domain-containing protein 1
IPI00224168 SWISS-PROT:P10711-2 Tceal Isoform 1 of Transcription elongation factor A protein 1
IPI00857720 SWISS-PROT:A6X919-1 Dpy19l1 Isoform 1 of Protein dpy-19 homolog 1
IPI00462424 SWISS-PROT:Q99M28-1 Rnps1 Isoform 1 of RNA-binding protein with serine-rich domain 1
IPI00312101 SWISS-PROT:Q8RS50-3 Sh3kbp1 Isoform 3 of SH3 domain-containing kinase-binding protein 1
IPI00338327 TREMBL:Q8VCV2 Ndrg3 protein NDRG3 isoform 1
IPI00606398 REFSEQ:XP_620562 - similar to glutamate dehydrogenase (Glud2)
IPI00750192 REFSEQ:XP_001002936 LOC677374 similar to Carboxypeptidase E
IPI00621806 SWISS-PROT:P11798-1 Camk2a Isoform Alpha CaMKII of Calcium/calmodulin-dependent protein kinase type II subunit alpha
IPI00662007 TREMBL:A6H5Z3 Exoc5b SEC15-like 2
IPI00228045 SWISS-PROT:Q923T9-3 Camk2g Isoform 3 of Calcium/calmodulin-dependent protein kinase type II subunit gamma
IPI00110918 SWISS-PROT:Q9CXW2 Mrps22 28S ribosomal protein S22, mitochondrial
IPI00719919 TREMBL:Q3TPN0 Nid2 nidogen 2 precursor
IPI00556840 TREMBL:Q6GTG6 Acsl1 long-chain-fatty-acid--CoA ligase 1
IPI00856469 TREMBL:Q8VBX2 Spnb4;Shkbp1 spectrin beta 4
IPI00136683 SWISS-PROT:Q9QYR9 Acot2 Acyl-coenzyme A thioesterase 2, mitochondrial
IPI00380338 SWISS-PROT:Q7TNR6 Igsf21 Immunoglobulin superfamily member 21
IPI00845558 SWISS-PROT:Q6PD19-1 9130011E15Rik Isoform 1 of UPF0668 protein C10orf76 homolog
IPI00461120 SWISS-PROT:Q8CEC0-2 Nup88 Isoform 2 of Nuclear pore complex protein Nup88
IPI00312673 SWISS-PROT:Q9DB16-2 Cab39l Isoform 2 of Calcium-binding protein 39-like
IPI00798614 SWISS-PROT:Q9CPR5-1 Mrpl15 Isoform 1 of 39S ribosomal protein L15, mitochondrial
IPI00221614 SWISS-PROT:P61205 Arf3 ADP-ribosylation factor 3
IPI00315620 SWISS-PROT:O35681 Syt3 Synaptotagmin-3
IPI00317599 SWISS-PROT:Q9DSV6 Syap1 Synapse-associated protein 1
IPI00751689 SWISS-PROT:Q6PHS9-4 Cacna2d2 Isoform 4 of Voltage-dependent calcium channel subunit alpha-2/delta-2
IPI00121359 SWISS-PROT:Q9DCU6 Mrpl4 39S ribosomal protein L4, mitochondrial
IPI00828569 SWISS-PROT:Q8BNA6-1 Fat3 Isoform 1 of Protocadherin Fat 3
IPI00463493 TREMBL:A0JLN9 Gbf1 Golgi-specific brefeldin A-resistance factor 1
IPI00129610 TREMBL:Q3UTK9 Pcdhgc4;Pcdhga12 Protocadherin gamma subfamily C, 4
IPI00556823 SWISS-PROT:Q5EG47 Prkaa1 5'-AMP-activated protein kinase catalytic subunit alpha-1
IPI00133179 SWISS-PROT:Q9CQV5 Mrps24 28S ribosomal protein S24, mitochondrial
IPI00653835 SWISS-PROT:Q4PJX1-3 BC003331 Isoform 3 of Protein odr-4 homolog
IPI00136098 SWISS-PROT:Q9QYF1 Rdh11 Retinol dehydrogenase 11
IPI00875924 TREMBL:Q56A00 Dnpep aspartyl aminopeptidase isoform b
IPI00229287 SWISS-PROT:Q8CFE4-1 Scyl2 Isoform 1 of SCY1-like protein 2
IPI00462749 SWISS-PROT:Q9JKL4 Ndufaf3 NADH dehydrogenase (ubiquinone) 1 alpha subcomplex assembly factor 3

IPI00474370	TREMBL:Q8R581 Rhot2 Arht2 protein
IPI00310533	TREMBL:Q8C3M7 Gna14 guanine nucleotide-binding protein subunit alpha-14
IPI00653256	TREMBL:Q3TSS7 Sqle Putative uncharacterized protein
IPI00675407	SWISS-PROT:Q6ZQA0-1 Nbeal2 similar to FLJ00341 protein isoform 3
IPI00221411	SWISS-PROT:Q8BG02 Ppp2r2c Serine/threonine-protein phosphatase 2A 55 kDa regulatory subunit B gamma isoform
IPI00828824	TREMBL:Q3UKZ9 Ash2l set1/Ash2 histone methyltransferase complex subunit ASH2 isoform b
IPI00351315	SWISS-PROT:Q9R049-2 Amfr Isoform 2 of Autocrine motility factor receptor
IPI00315302	SWISS-PROT:Q9CQ75 Ndufa2 NADH dehydrogenase [ubiquinone] 1 alpha subcomplex subunit 2
IPI00122589	SWISS-PROT:Q8VCV1 Fam108c Abhydrolase domain-containing protein FAM108C1
IPI00462204	TREMBL:D3YY61 Gm5520 Putative uncharacterized protein Gm5520 (RPL13)
IPI00761979	TREMBL:D3Z499 Mdga1 Putative uncharacterized protein Mdga1
IPI00649471	TREMBL:A2A9I0 Gosr2 Golgi SNAP receptor complex member 2, isoform CRA_a
IPI00606219	TREMBL:Q3UYN7 Fut8 Alpha-(1,6)-fucosyltransferase
IPI00133215	SWISS-PROT:Q9CR61 Ndufb7 NADH dehydrogenase [ubiquinone] 1 beta subcomplex subunit 7
IPI00474802	TREMBL:Q8BLD9 Grm7 Putative uncharacterized protein
IPI00111931	SWISS-PROT:Q9D8S3 Arfgap3 ADP-ribosylation factor GTPase-activating protein 3
IPI00380220	SWISS-PROT:Q6VNS1-1 Ntrk3 Isoform 1 of NT-3 growth factor receptor
IPI00124700	SWISS-PROT:Q62351 Tfrc Transferrin receptor protein 1
IPI00119466	SWISS-PROT:O70579 Slc25a17 Peroxisomal membrane protein PMP34
IPI00884508	TREMBL:Q3TD17 Slc2a1 solute carrier family 2, facilitated glucose transporter member 1
IPI00267596	SWISS-PROT:Q8BJ03-2 Cox15 Isoform 2 of Cytochrome c oxidase assembly protein COX15 homolog
IPI00229762	SWISS-PROT:Q3UN04 Usp30 Ubiquitin carboxyl-terminal hydrolase 30
IPI00849598	REFSEQ:XP_001477392 Gm3405 similar to QM protein
IPI00131584	SWISS-PROT:Q9Z2Z6 Slc25a20 Mitochondrial carnitine/acylcarnitine carrier protein
IPI00928374	TREMBL:Q3T9E5 Ncstn nicastrin precursor (gamma secretase complex)
IPI00320303	SWISS-PROT:Q8R0G9 Nup133 Nuclear pore complex protein Nup133
IPI00890234	TREMBL:Q3THF5 Dbt lipoamide acyltransferase component of branched-chain alpha-keto acid dehydrogenase complex, mitochondrial
IPI00330122	SWISS-PROT:Q6DFY8 Fam5b Protein FAM5B
IPI00856157	ENSEMBL:ENSMUSP00000119470 Parl 19 kDa protein
IPI00605077	TREMBL:D3YZ47 - Putative uncharacterized protein 100048210
IPI00124593	SWISS-PROT:P63166 Sumo1 Small ubiquitin-related modifier 1
IPI00331527	TREMBL:Q3TC91 Cpsf3 cleavage and polyadenylation specificity factor subunit 3
IPI00380738	TREMBL:Q69ZP8 Sfrs15 Splicing factor, arginine/serine-rich 15
IPI00133441	SWISS-PROT:P31360 Pou3f2 POU domain, class 3, transcription factor 2
IPI00653189	TREMBL:Q3UWI3 Slc33a1 Putative uncharacterized protein (acetyl CoA transporter)
IPI00222929	REFSEQ:XP_001479768 LOC100048049 similar to Regulatory factor X, 3 (influences HLA class II expression) isoform 1
IPI00669709	SWISS-PROT:Q6A026 Pds5a Sister chromatid cohesion protein PDS5 homolog A
IPI00458851	TREMBL:D3Z3S1 - Putative uncharacterized protein ENSMUSP00000082625 (HMG family pseudogene GM5518)
IPI00136555	SWISS-PROT:O88967 Yme1l1 ATP-dependent metalloprotease YME1L1
IPI00648776	TREMBL:A2AIR2 Rnf20 Ring finger protein 20
IPI00649369	SWISS-PROT:Q9QWH1-2 Phc2 Isoform 2 of Polyhomeotic-like protein 2
IPI00117771	SWISS-PROT:Q99MJ9 Ddx50 ATP-dependent RNA helicase DDX50
IPI00469443	SWISS-PROT:A2ABV5-3 Med14 Isoform 3 of Mediator of RNA polymerase II transcription subunit 14
IPI00830717	TREMBL:Q3UES8 Sox2 transcription factor SOX-2
IPI00396739	SWISS-PROT:Q91ZW3 Smarca5 SWI/SNF-related matrix-associated actin-dependent regulator of chromatin subfamily A member 5
IPI00874810	TREMBL:Q3TSR2 Top1 Putative uncharacterized protein
IPI00135443	SWISS-PROT:Q64511 Top2b DNA topoisomerase 2-beta
IPI00282848	ENSEMBL:ENSMUSP00000089303 Hist1h3b;Hist2h3b;Hist2h3c1;Hist1h3e;Hist1h3c;Hist1h3d;Hist1h3f;Hist2h3c2 histone H3.2

This is a list of all proteins downregulated that was used for the IPA analysis in figure S3. Proteins on this list fit one of three criteria to be considered down-regulated.
First, the protein is found in only one fraction (either insoluble or soluble), was quantified in 2/3 animals in both genotypes and the average decrease was 1.4 fold or more in Hnrpab KO animal. The decrease is reflected in a KO/Het ratio of 0.7 or less.
Second, the protein has one entry that is unique to only one fraction (either insoluble or soluble) and was quantified in 2/3 Hnrpab Het animals only. These changes cannot be quantified. (Listed separately below line 27)
Third, the protein has multiple entries that all corroborate an down-regulation of the protein in the sample, only one entry is included.

Both Soluble and Insoluble proteins are combined on this list.14N/15N ratios from Heterozygous samples are labelled in yellow. 14N/15N ratios from Homozygous samples labelled in green
The fold change that was calculated from samples of the first and third classes are labelled in orange.
The Hnrpab entry corroborating the lack of detectable expression in Hnrpab$^{-/-}$ mice is highlighted with bold text.

SOLUBLE PROTEINS

		14N/15N ratio			14N/15N ratio						
		Hnrpab+/- P0 hippocampus			Hnrpab-/- P0 hippocampus						
locus	variance p-value	sample 1 ratio	sample 2 ratio	sample 3 ratio	sample 1 ratio	sample 2 ratio	sample 3 ratio	average Het ratio	average KO ratio	KO/Het	description
IPI00320484	0.03955	0.9	1.04	X	X	0.56	0.64	0.97	0.6	0.6	SWISS-PROT:P70188-1 Kifap3 Isoform KAP3A of Kinesin-associated protein 3
IPI00648960	0.19911	0.85	0.94	X	0.85	0.29	0.26	0.9	0.47	0.5	TREMBL:B1AUN3 Eif2b3 eukaryotic translation initiation factor 2B, subunit 3 gamma isoform 2
IPI00877236	0.32434	1.86	4.28	X	X	1.93	1.17	3.07	1.55	0.5	TREMBL:O08855 Apoa1 apolipoprotein A-I preproprotein

INSOLUBLE PROTEINS

locus	variance p-value	sample 1 ratio	sample 2 ratio	sample 3 ratio	sample 1 ratio	sample 2 ratio	sample 3 ratio	average Het ratio	average KO ratio	KO/Het	description
IPI00131695	0.18251	2.22	1.97	2.83	1.4	2.34	1.47	2.34	1.74	0.7	SWISS-PROT:P07724 Alb Serum albumin
IPI00227582	0.20379	1.28	X	0.95	0.76	0.87	X	1.12	0.82	0.7	SWISS-PROT:O35375-4 Pard3b;Nrp2 neuropilin-2 isoform 1 precursor
IPI00116929	0.39096	1.23	0.54	1.02	0.69		0.58	0.93	0.64	0.7	SWISS-PROT:Q99LI7 Cstf3 Cleavage stimulation factor subunit 3
IPI00757909	0.88152	3	0.51	0.77	0.87	1.2	0.87	1.43	0.98	0.7	SWISS-PROT:Q9D0L7-1 Armc10 Isoform 1 of Armadillo repeat-containing protein 10
IPI00831643	0.26695	0.98	X	1.57	0.54	X	0.94	1.28	0.74	0.6	TREMBL:D3Z3S1 Preb Putative uncharacterized protein Preb - prolactin regulatory element binding (PREB) protein
IPI00134137	0.27275	1.41	X	1.3	0.27	X	0.98	1.36	0.62	0.5	SWISS-PROT:O88741-1 Gdap1 Isoform 1 of Ganglioside-induced differentiation-associated protein 1

These proteins belong to the second class of entries, and are provided in a separate list because their fold regulation could not be quantified.

SOLUBLE PROTEINS

IPI00466593	SWISS-PROT:Q8BTW3 Exosc6 Exosome complex exonuclease MTR3
IPI00109326	SWISS-PROT:Q9EP97 Senp3 Sentrin-specific protease 3
IPI00649674	SWISS-PROT:Q80YV2-2 Zc3hc1 Isoform 2 of Nuclear-interacting partner of ALK
IPI00754444	TREMBL:Q6P0X1 Pfdn4 Prefoldin 4
IPI00776080	SWISS-PROT:Q91XI1-2 Dus3l Isoform 2 of tRNA-dihydrouridine synthase 3-like
IPI00762035	SWISS-PROT:Q3TEI4-2 1700017B05Rik Isoform 2 of Uncharacterized protein C15orf39 homolog
IPI00111343	SWISS-PROT:Q9QZH3 Ppie Peptidyl-prolyl cis-trans isomerase E
IPI00605090	ENSEMBL:ENSMUSP00000087012 - 22 kDa protein
IPI00274226	SWISS-PROT:Q811B3-1 Adamts12 Isoform 1 of A disintegrin and metalloproteinase with thrombospondin motifs 12
IPI00227451	SWISS-PROT:Q8BZA9 9630033F20Rik;LOC677429 Probable fructose-2,6-bisphosphatase TIGAR
IPI00229768	SWISS-PROT:Q8CI70 Lrrc20 Leucine-rich repeat-containing protein 20
IPI00135630	TREMBL:Q8VD12 Zfp385a zinc finger protein 385A
IPI00121105	SWISS-PROT:Q61425 Hadh Hydroxyacyl-coenzyme A dehydrogenase, mitochondrial
IPI00117016	SWISS-PROT:P49717 Mcm4 DNA replication licensing factor MCM4
IPI00467914	SWISS-PROT:P10922 H1f0 Histone H1.0
IPI00122312	SWISS-PROT:Q8VCM7 Fgg Putative uncharacterized protein
IPI00856964	TREMBL:Q1WWN0 Ppp1r12c Ppp1r12c protein
IPI00121071	SWISS-PROT:Q61411 Hras1 GTPase HRas
IPI00673239	SWISS-PROT:A2CG49-8 Kalrn Isoform 8 of Kalirin
IPI00467495	SWISS-PROT:Q9CQI3 Gmfb Glia maturation factor, beta
IPI00277066	**TREMBL:Q20BD0 Hnrnpab heterogeneous nuclear ribonucleoprotein A/B isoform 1**

IPI00848617	REFSEQ:XP_001474175 9930104M19Rik hypothetical protein LOC320788
IPI00453947	SWISS-PROT:Q6PCX7-1 Rgma Isoform 1 of Repulsive guidance molecule A
IPI00227928	SWISS-PROT:P31648 Slc6a1 Sodium- and chloride-dependent GABA transporter 1
IPI00849457	REFSEQ:XP_001475586 Gm15365 similar to Translocase of outer mitochondrial membrane 20 homolog
IPI00475158	REFSEQ:XP_894449 Gm12251 similar to NADH dehydrogenase (ubiquinone) Fe-S protein 3
IPI00918598	TREMBL:D3YV19 5033414D02Rik RIKEN cDNA 5033414D02, isoform CRA_a
IPI00126548	SWISS-PROT:O35083 Agpat1 Putative uncharacterized protein
IPI00136253	SWISS-PROT:Q9QYJ3 Dnajb1 DnaJ homolog subfamily B member 1
IPI00620207	TREMBL:Q8JZV5 Epb4.9 Putative uncharacterized protein
IPI00954338	TREMBL:C9W8L2 Tert Telomerase reverse transcriptase (Fragment)
IPI00331654	SWISS-PROT:Q8K2T8 Paf1 RNA polymerase II-associated factor 1 homolog
IPI00221616	SWISS-PROT:P62331 Arf6 ADP-ribosylation factor 6
IPI00130489	SWISS-PROT:Q6PHN9 Rab35 Ras-related protein Rab-35
IPI00466200	SWISS-PROT:Q9D6K8 Fundc2 FUN14 domain-containing protein 2
IPI00338458	SWISS-PROT:Q14C51 Ptcd3 Putative uncharacterized protein
IPI00408556	REFSEQ:XP_001472285 Gm5578 similar to RIKEN cDNA 0610010K06 gene
IPI00848816	REFSEQ:XP_001480334 LOC100048522 similar to Cofilin-1
IPI00128425	SWISS-PROT:Q91X51 Gorasp1 Golgi reassembly-stacking protein 1
IPI00221921	SWISS-PROT:P40240 Cd9 CD9 antigen
IPI00918622	TREMBL:D3YU49 Gm8994 predicted gene, EG668137 (a dead-box helicase)
IPI00470178	SWISS-PROT:P97314 Csrp2 Cysteine and glycine-rich protein 2
IPI00311509	SWISS-PROT:P58742 Aaas Aladin (causes Algrovesyndrome)
IPI00309285	TREMBL:Q6P5G5 Hccs cytochrome c-type heme lyase
IPI00875492	ENSEMBL:ENSMUSP00000110510 Gpc4 70 kDa protein
IPI00830486	TREMBL:D3YU80 Cirbp Putative uncharacterized protein Cirbp (cold inducible RNA binding protein)
IPI00310220	SWISS-PROT:P29387 Gnb4 Guanine nucleotide-binding protein subunit beta-4 (G beta4)
IPI00658339	REFSEQ:XP_914557 LOC634666 similar to transmembrane protein 1
IPI00928223	ENSEMBL:ENSMUSP00000122215 Slc35e1 26 kDa protein
IPI00330763	SWISS-PROT:Q80XP8-1 Fam76b Isoform 1 of Protein FAM76B
IPI00316431	SWISS-PROT:Q9D0I4 Stx17 Syntaxin-17
IPI00459797	REFSEQ:XP_913143 Gm6236 similar to Peptidylprolyl isomerase D
IPI00420158	SWISS-PROT:Q9Z1X2-2 Ptdss2 Isoform 2 of Phosphatidylserine synthase 2
IPI00132099	SWISS-PROT:Q9CPW7 Zmat2 Zinc finger matrin-type protein 2
IPI00900431	SWISS-PROT:Q921E6-2 Eed Isoform 2 of Polycomb protein EED
IPI00761648	REFSEQ:XP_001480768 Gm9029 similar to Cell division cycle 5-like
IPI00134804	SWISS-PROT:P53784 Sox3 transcription factor SOX-3
IPI00459269	TREMBL:Q8C5F4 Hmgcs1 Putative uncharacterized protein
IPI00875107	TREMBL:Q9QYT9 Prnd Major prion protein
IPI00471224	SWISS-PROT:Q8BIV3 Ranbp6 Ran-binding protein 6
IPI00753951	TREMBL:Q3V344 Epha5 Putative uncharacterized protein
IPI00351266	SWISS-PROT:Q8VHK9 Dhx36 Probable ATP-dependent RNA helicase DHX36

Ingenuity Pathway Analysis of Proteins increased in Hnrpab-/- hippocampus relative to Hnrpab+/+

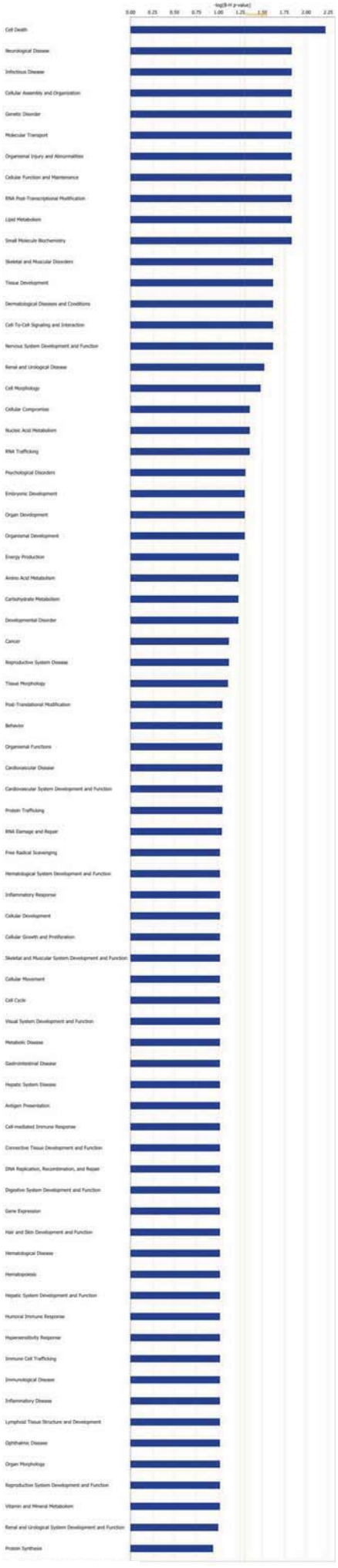

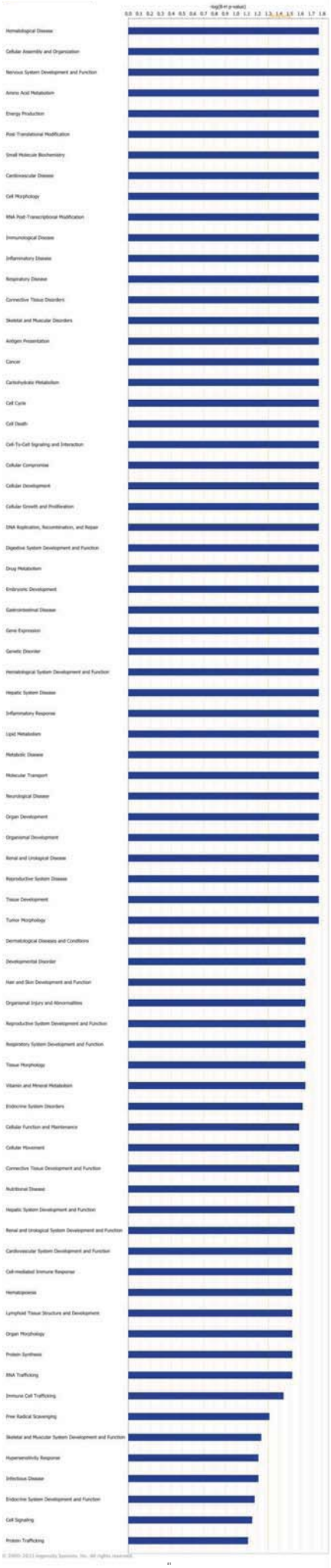

Ingenuity Pathway Analysis of proteins increased in Hnrpab$^{-/-}$ hippocampus relative to Hnrpab$^{+/-}$ with p-value of <0.1

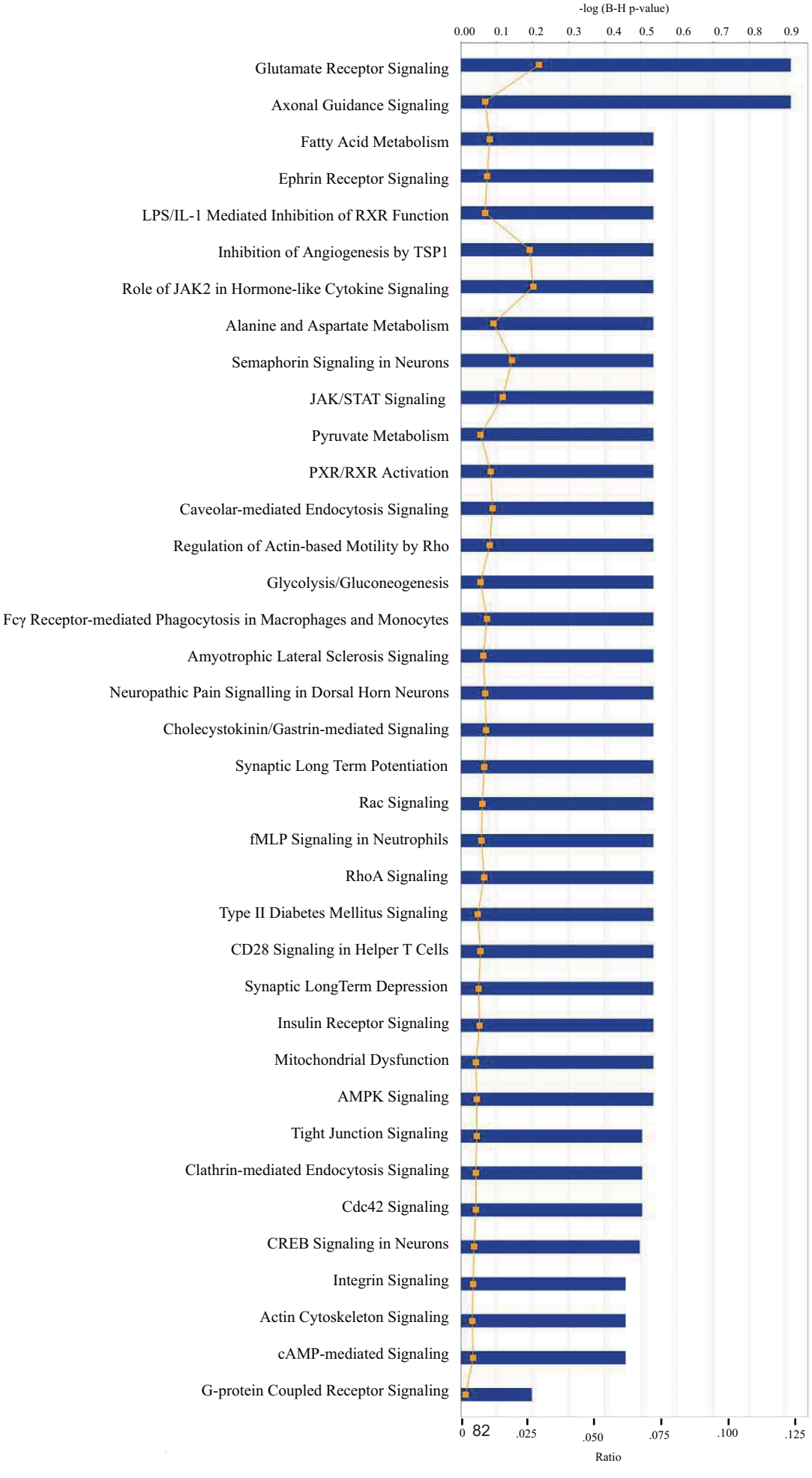

Figure 19

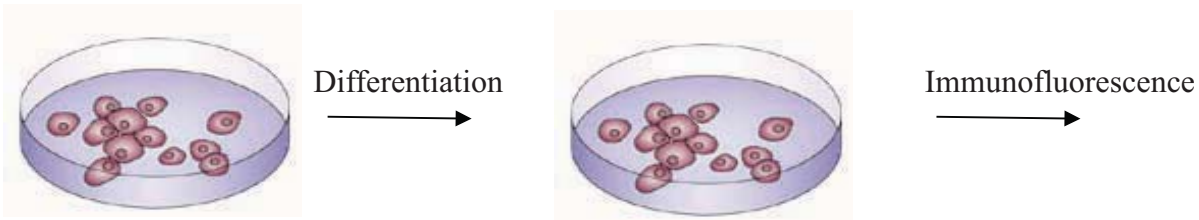

	DCX[1]	βIII tubulin[1]	Nestin[1]	CNPase[1]	MBP[2]	GFAP[2]
Hnrpab+/-	28.8%	3.4%	67.2%	7.6%	0.8%	27.6%
Hnrpab-/-	35.3%	3.7%	21.6%	9.6%	2.1%	24.9%
p-value	0.002	0.797	<0.001	0.301	0.011	0.359*

[1] Mann-Whitney Rank Sum Test; medians reported
[2] T-test; means reported
* Low power
The percent of total cells expressing each marker is reported in the table.
For Dcx n=2000 cells. For the rest of the markers, n=1000 cells.

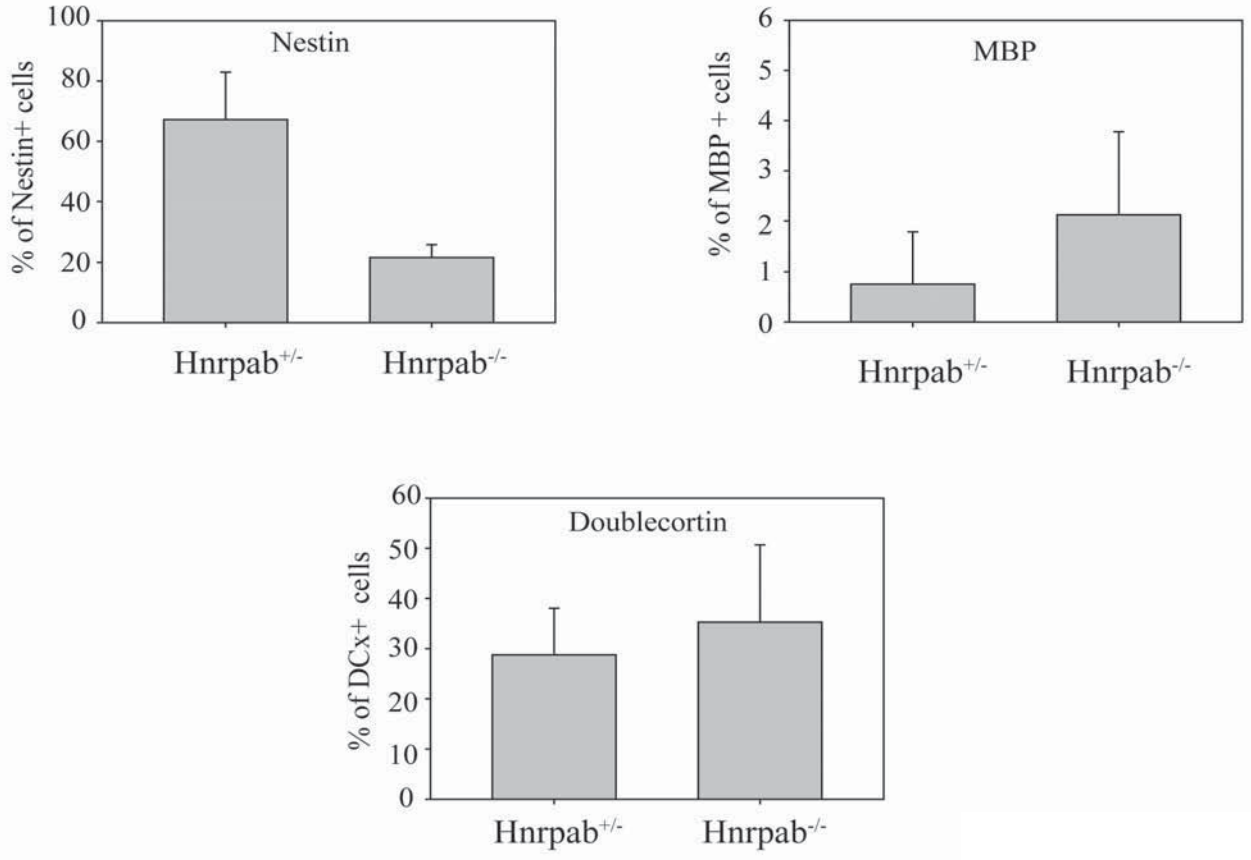

Figure 19– Hnrpab disruption affects the differentiation of neural lineage cells in neurosphere cultures. Neurosphere cultures at the second passage were dissociated, plated on coverslips and grown for 6 days under differentiation conditions, then fixed and immuno-stained with indicated markers for different neural lineages. For each image, the total number of cells was counted by DAPI staining and the percentage of these cell that were positive for each marker was calculated. The data represents the average percentage per image field over all the fields imaged (at least 30 fields per marker). This represented a minimum of 1000 cells for all markers, 2000 for Doublecortin. Graphs of the three differences with a p value of <0.011 are included to illustrate the results. Abbreviations: DCX – Doublecortin; CNPase - 2', 3'-cyclic nucleotide 3'-phosphodiesterase; MBP – Myelin Basic Protein, GFAP- Glial Fibrillary Accessory Protein.

Figure 20

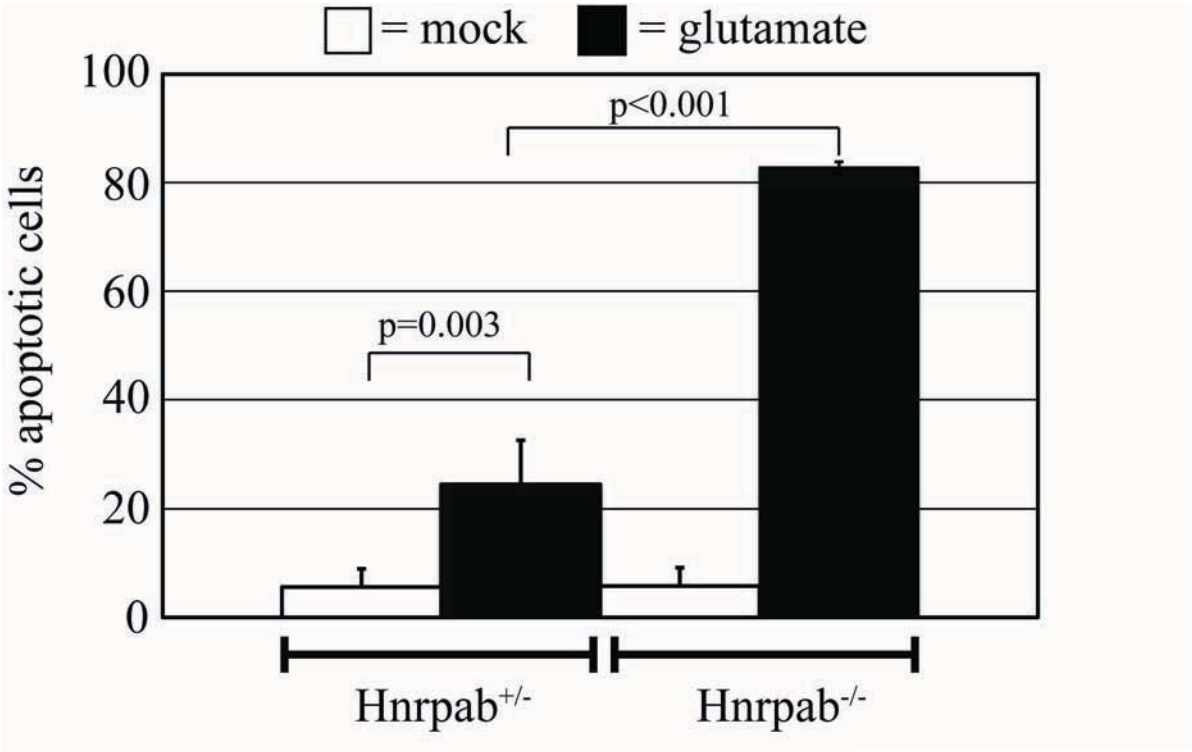

Figure 20– Hnrpab disruption increases sensitivity of cells to glutamate-stimulated excitotoxicity. At 15DIV, Hnrpab$^{+/-}$ and Hnrpab$^{-/-}$ neurons were treated with 50μM glutamate for 10 minutes, or mock treated with the same media changes lacking glutamate, and allowed to recover for 6 hours. Cells were then fixed and imaged using 60x magnification, and cell death was scored visually through shrinkage of the nucleus in the DAPI channel and morphology of neurons using DIC microscopy. Error bars represent the standard deviation over three independent experiments. P values were determined using a two-way ANOVA followed by the Tukey test for multiple comparisons.

Figure 21

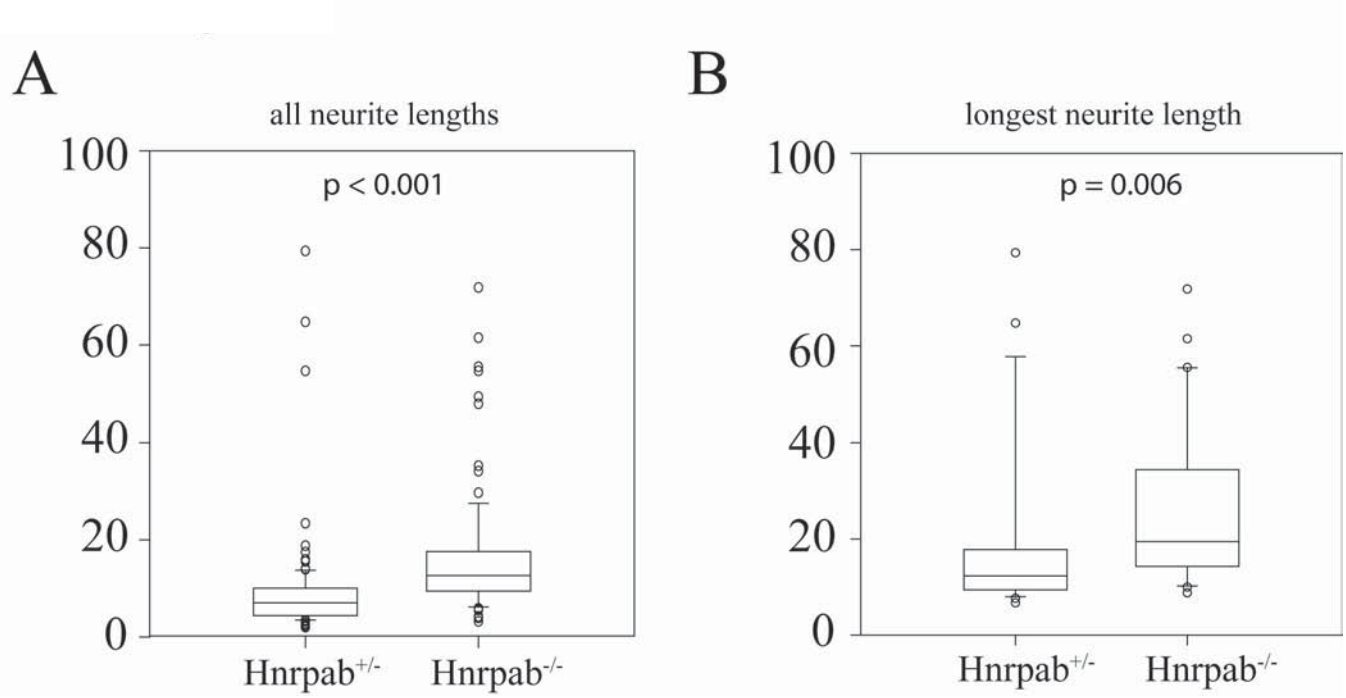

Figure 21– Hnrpab disruption leads to increased neurite length. Primary neurons from Hnrpab$^{+/-}$ and Hnrpab$^{-/-}$ E18 mouse hippocampus were dissociated and plated then maintained in culture for 2 days prior to fixation. Cells were immunostained for βIII-tubulin and distance that β-III tubulin extended from the cell body was measured as neurite length. All neurite lengths (A) or longest neurite lengths (B) were plotted with a box-whisker plot and statistics were performed using the Mann-Whitney rank sum test on the median values.

Figure 22

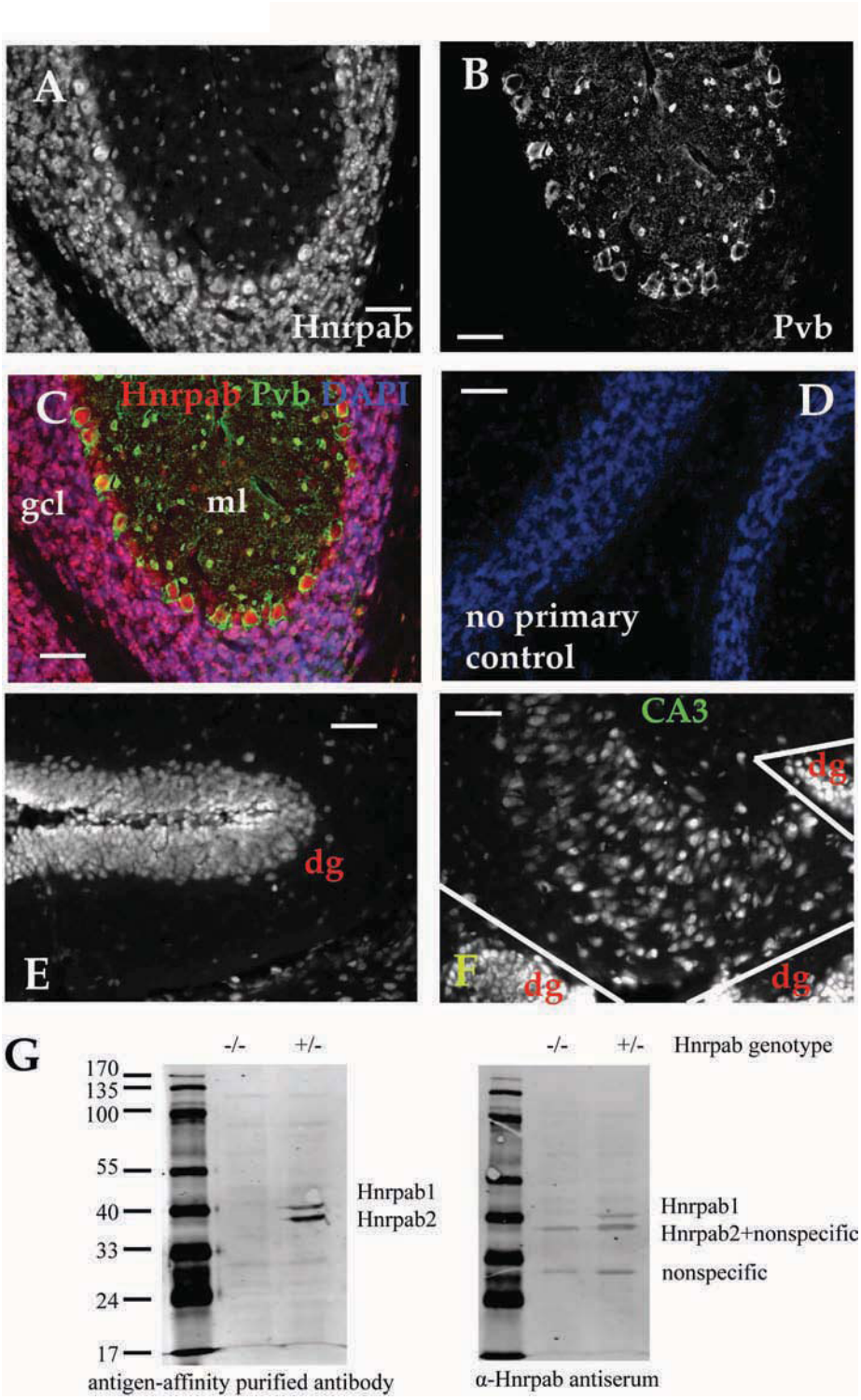

Figure 22- Immunofluorescence of Hnrpab in the brain of adult mice. (A) Brain sections were immuno-stained with N-terminal peptide antibody that recognizes both isoforms of Hnrpab. (B) Co-immuno-staining with a parvalbumin monoclonal antibody confirms the cytoplasmic localization of Hnrpab in the cytoplasm of cerebellar Purkinje neurons. (C) A merge of these images pseudo-colored together with DAPI. (D) A pseudo colored, normalized then merged image from an adjacent brain section that was processed for immuno-staining without primary antibodies. (E and F) Hnrpab immuno-stained fluorescence image from the dentate gyrus (dg) and the CA3 region of the hippocampus, with the adjacent dg regions indicated are shown in panels E and F, respectively. The polymorphic layer of the dg in panel E lies in between the two branches of the granule layer that fold back to about 180 degrees in this image. Scale bar in all images is 50μm. (G) Hnrpab$^{+/-}$ and Hnrpab$^{-/-}$ protein lysate was separated on a 10% PAGE gel and probed with Hnrpab peptide-affinity purified antibody or antiserum as indicated.

Figure 23

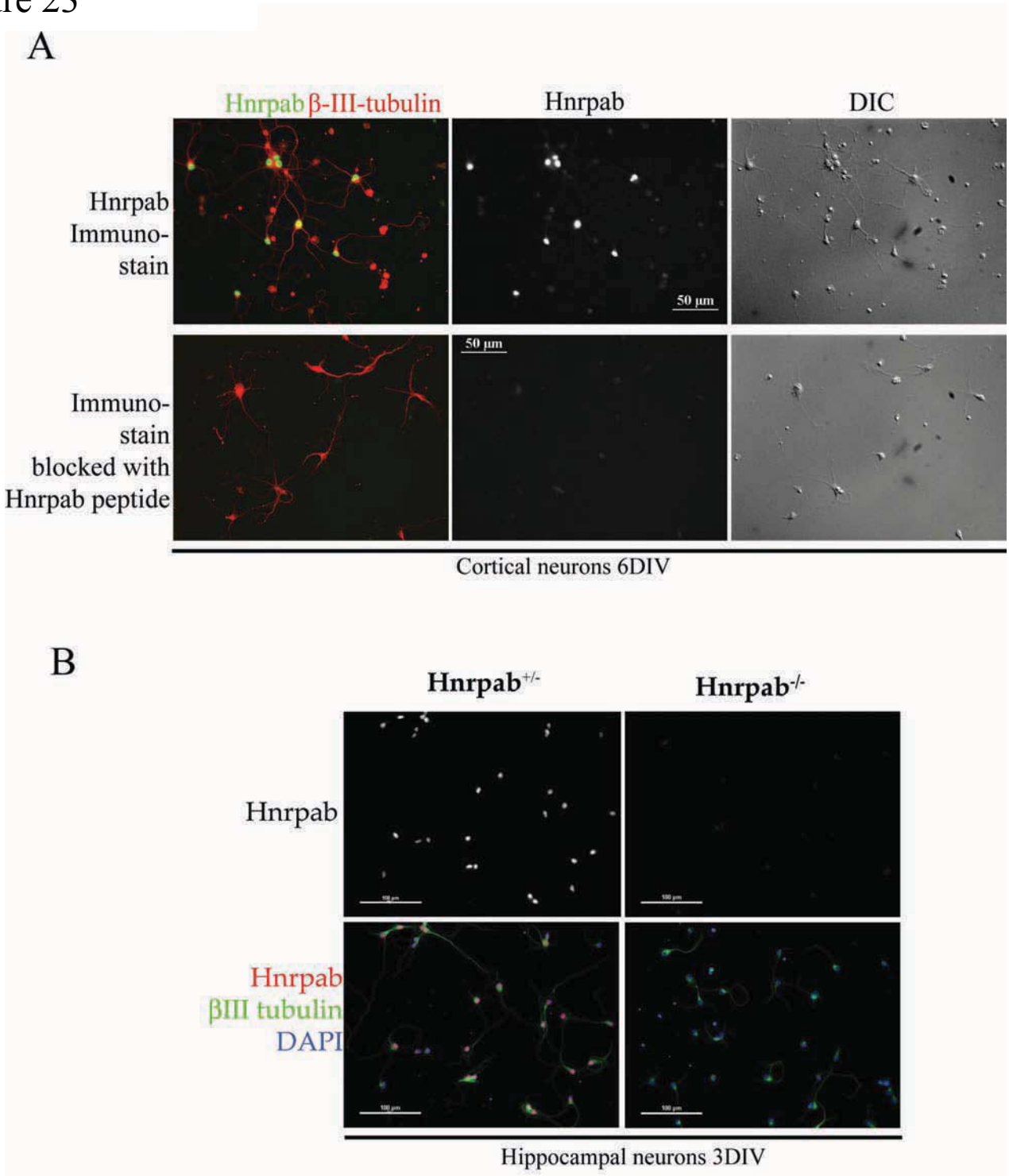

Figure 23–Hnrpab localizes to the nucleus in early primary neuron cultures. (A) Primary cortical neurons from an E18 Hnrpab$^{+/-}$ mouse brain were dissociated and plated then maintained in culture for 6 days. These were immuno-stained with N-terminus peptide Hnrpab antibody, in the absence (top panels) or presence (bottom panels) of the immunogenic peptide. βIII-tubulin was co-stained as a marker for neurons. Normalized Hnrpab images (center panels) are shown together with pseudo-colored Hnrpab/βIII-tubulin merge images (left panels) and DIC images (right panels). All images were taken on the same magnification and the scale bars in the center images are 50µm. Cell bodies that are βIII-tubulin^{+} but Hnrpab^{-} in the top panel always coincide with dead neurons in the DIC images. (B) Primary hippocampal neurons from Hnrpab$^{+/-}$ and Hnrpab$^{-/-}$ E18 mouse brains were dissociated and plated then maintained in culture for 3 days. These were immuno-stained with N-terminus peptide Hnrpab antibody, βIII-tubulin and DAPI. Normalized images of Hnrpab immunofluorescence (Top panels) and pseudo-colored Hnrpab/βIII-tubulin/DAPI merged images (bottom panels) are shown. Scale bars in these images represent 100µm.

Figure 24

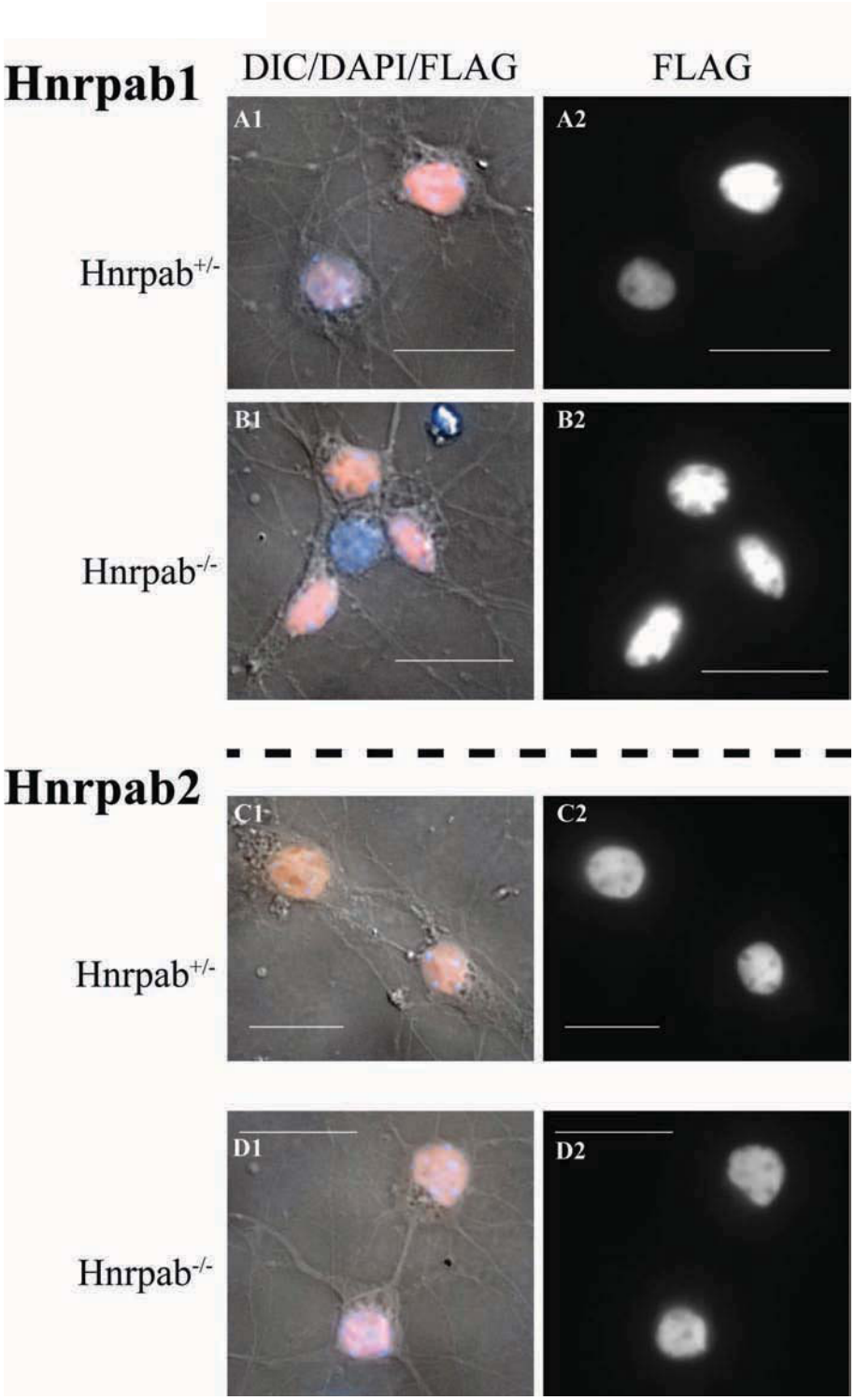

Figure 24 – Hnrpab isoforms are predominantly nuclear in developing neurons. Primary hippocampal neurons from Hnrpab$^{+/-}$ (panels a and c) and Hnrpab$^{-/-}$ (panels b and d) E18 mouse brains were dissociated and plated then maintained in culture for 5 days before infection with recombinant LVPs to express Flag-epitope tagged either Hnrpab1 (panels a and b) or Hnrpab2 (panels c and d). These were fixed and processed for immuno-staining 3 days later (8DIV), using anti-Flag epitope antibodies, and DAPI for the nucleus. Pseudo-colored Flag immunofluorescence (orange) merged with DAPI (blue) and DIC images (gray) (panels labelled 1) are shown next to the Flag immuno-fluorescence images alone (panels labelled 2). Scale bars represent 20μm.

Figure 25

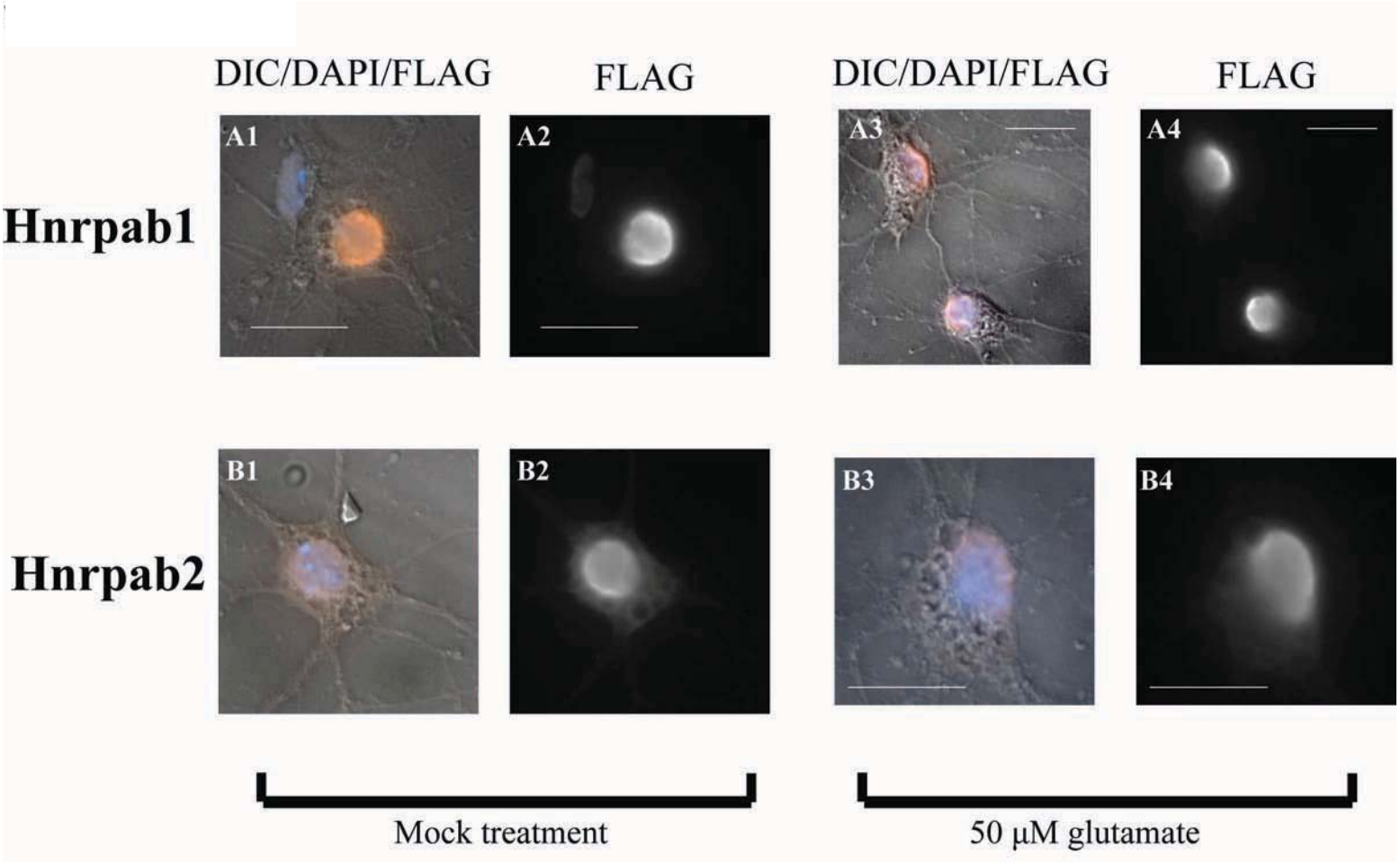

Figure 25 – Hnrnpab isoforms appear in the cytplasm of mature neurons. Primary hippocampal neurons from E18 Hnrpab$^{+/-}$ mouse brains were dissociated and plated on coverslips then maintained in culture for 8 days before infection with recombinant LVPs to express Flag-epitope tagged either Hnrnpab1 (panel a) or Hnrnpab2 (panels b). O 15DIV Cultures were treated with 50μm glutamate (panels labelled 3 and 4) or mock treated (panels labelled 1 and 2) for 10 minutes and then glutamate removed and incubation continued for 6 hours. These were fixed and processed for immuno-staining using anti-Flag epitope antibodies, and DAPI for the nucleus. Pseudo-colored Flag immunofluorescence (orange) merged with DAPI (blue) and DIC images (panels labelled 1 and 3) are shown next to the Flag immuno-fluorescence images alone (panels labelled 2 and 4). Scale bars represent 20μm.

Figure 26

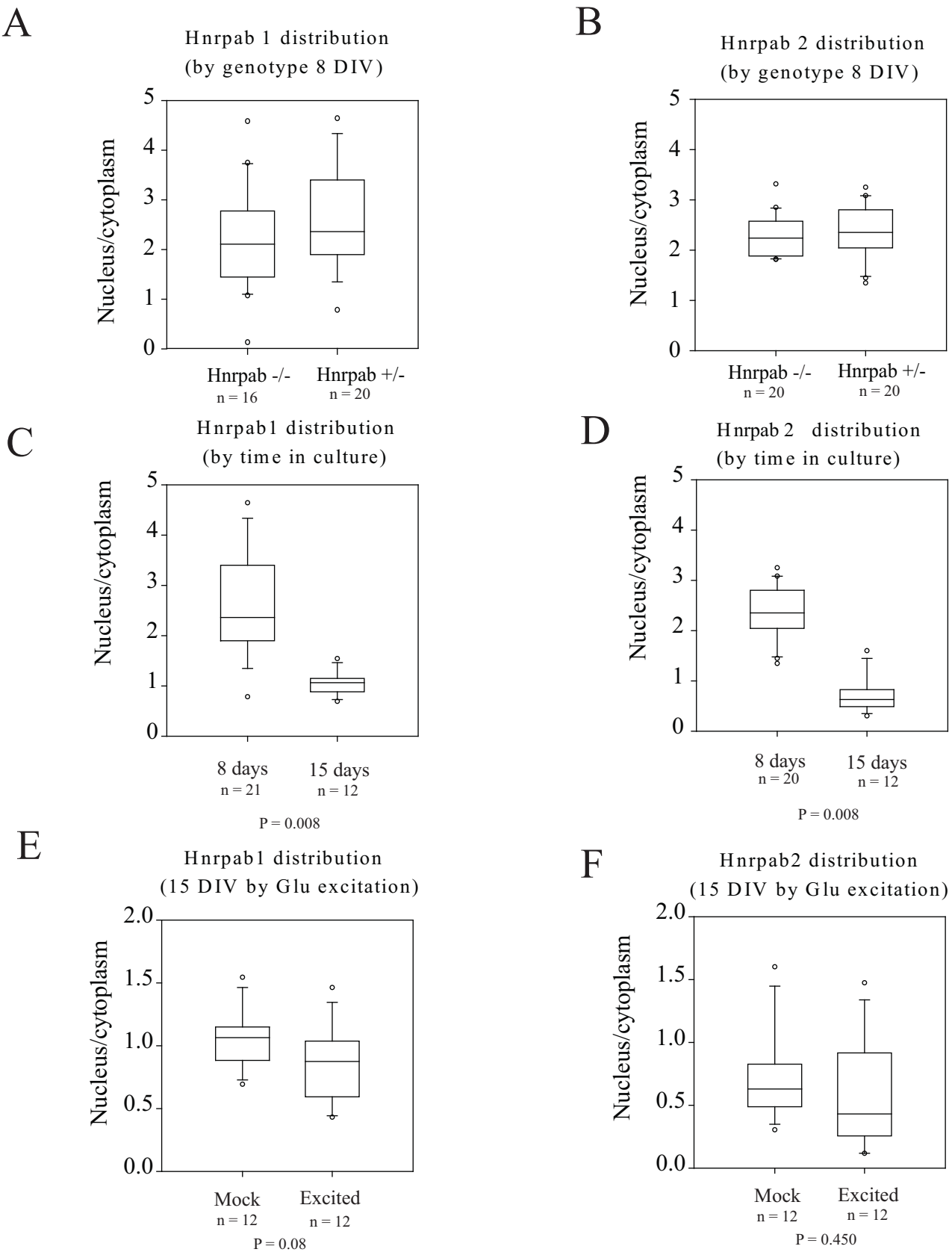

Figure 26 – Quantification of the nuclear and cytoplasmic localization of Hnrpab1 and Hnrpab2 isoforms. Total fluorescence intensity measurements were extracted from the nuclear and cytoplasmic regions of fluorescence micrographs and expressed as ratios. These measurements were combined for each condition and used to determine how the ratios changed in response to different experimental variables. Panels A and B show how genotype affects distribution of Hnrpab1 (A) or Hnrpab2 (B) at 8DIV. Panels C and D show how time in culture affects distribution of Hnrpab1 (C) or Hnrpab2 (D). Panels E and F show how glutamate stimulation of 15DIV neurons affects distribution of Hnrpab1 (E) or Hnrpab 2 (F). Data is plotted in box-whisker-plots of the ratio of the nucleus versus the cytoplasm. All statistical comparisons were done using the Mann-Whitney Rank Sum Test, followed by a Bonferroni Adjustment for multiple comparisons. The lower boundary of the box represents the 25th percentile, the upper boundary represents the 75th percentile and the line in the middle of the box represents the median. The whiskers represent the 90th and 10th percentiles.

Chapter 5: Discussion

Hnrnpab 1 and 2 function in regulating Actb mRNA

While I have established Hnrnpab is required for the proper localization of Actb mRNA, many questions remain about the exact function of Hnrnpab1 in this process and the possible function of Hnrnpab2 in Actb mRNA regulation. One of the next logical steps is to determine the Hnrnpab1 and 2 binding sites on the Actb mRNA. I would extend the RIP assay I used in chapter 2 to map Hnrnpab1 and 2 binding sequences within Actb mRNA. mCherry is a commonly used reporter mRNA not endogenously expressed in mammalian cells and so I would clone different regions of the Actb mRNA zipcode into the 3' UTR of a mCherry reporter creating mCherry-Actb mRNA fusions. Transfecting these fusions into Hnrnpab1 and 2 expressing cells and performing RIP-PCR for mCherry will determine what region of the Actb mRNA each isoform binds. Once the minimal binding elements are established I would express the sequences in the opposite orientation to establish if Hnrnpab is binding is sequence or a structurally mediated. To confirm direct binding to these sequences I would then perform UV-crosslinking of radiolabeled RNA using both cell extracts and purified protein. Preliminary experiments from the lab have already determined the RRMs of Hnrnpab bind to the zipcode A element with a high affinity but I think with the questions raised about the different binding of the two isoforms this systematic approach will yield even more information.

It is important to determine if Hnrnpab is involved in other aspects of Actb mRNA regulation other than trafficking. To study Actb translation, the lab already plans to pulse label methionine starved Hnrnpab$^{+/+}$ and Hnrnpab$^{-/-}$ MEFs with ^{35}S methoinine and then immunoprecipitate Actb protein with Actb specific antibodies at defined times after the addition

of ^{35}S methionine. If Hnrnpab is involved in the translation of Actb then there should be a change in the amount of protein produced in Hnrnpab$^{-/-}$ compared to Hnrnpab$^{+/+}$ MEFs. If there is a change then we will repeat the assay but also compare MEFs expressing each isoform of Hnrnpab to determine which isoform is responsible for the change in translation. To establish a possible role for Hnrnpab in transcription or mRNA stability we will quantify the Actb and Actg mRNA levels in Hnrnpab$^{+/+}$ and Hnrnpab$^{-/-}$ MEFs by northern blot. If there is a change in mRNA levels then the mRNA half-life will be measured using northern blots following addition of Actinomycin D to block transcription.

I have established Hnrnpab effects the distribution of Actb mRNA and this result is rescued by the addition of Hnrnpab1. However, I think it is important to repeat the studies I performed in primary neurons. Neurons are more polarized than MEFs and may possibly show a larger affect than MEFs. In addition to these studies, the lab has already begun crossing the Hnrnpab$^{-/-}$ mice with those containing the Actb MBS knock-in allele. By categorizing Actb mRNA movements in live cells we will be able to determine any effect on Actb mRNA kinetics such as the speed or directionality of the mRNA. The use of Hnrnpab1 and 2 viral vectors can then determine if any kinetic affects are due to one isoform or the other.

Defining the Actb L-RNP

Hnrnpab likely functions as part of a larger L-RNP complex in trafficking Actb mRNA. The GRNA chromatography I performed gave some insight to what proteins may be part of this complex, however, more experiments are necessary to define the required components for Actb localization. I would propose repeating the GRNA chromatography but instead of using brain lysate, I would utilize lysate made from isolated axons in culture. Actb mRNA is highly

expressed in cells but only a small population is trafficked. I believe this experiment would eliminate factors which are involved in regulation of Actb mRNA in the cell body and tell us what proteins associate with the zipcode when it is being trafficked. I know many of the proteins required for the formation of the trafficking L-RNP would not be included in the results of this assay, however it would give us a snapshot of the Actb mRNA interactome in axons.

Only ZBP1, ZBP2, PTB and Hnrnpab bind to the zipcode of Actb mRNA and affect Actb mRNA localization. After the studies described above we will be able to determine and mutate the binding sites for each of these factors on the Actb mRNA zipcode. To determine additional zipcode binding proteins I would use GRNA chromatography using this mutated zipcode and the WT zipcode sequence. Any factors which bind independently of ZBP1, ZBP2, PTB and Hnrnpab can be studied for their ability to bind to the zipcode directly and possibly mediate Actb mRNA localization. The binding of ZBP1, PTB and Hnrnpab1 to the Actb mRNA zipcode is interesting because these three proteins also regulate the trafficking of Vg1 mRNA in *Xenopus* oocytes. I think it will be important to determine if these factors affect the binding of one another as they do in *Xenopus* by performing RIP-PCR using cells from ZBP1, Hnrnpab1 and PTB$^{-/-}$ mice [103, 150].

Exploring other functions of Hnrnpab

It is unlikely the changes we see in the Hnrnpab$^{-/-}$ mice are all due to Actb mRNA regulation. Therefore to determine other functions of the Hnrnpab isoforms I have attempted to establish the process of high throughput sequence of cross-linked mRNAs (HITS-CLIP) in the lab. The ability of Hnrnpab deletion constructs to cross-link in Figure 8, demonstrate the feasibility of this process. I have been successfully able to isolate Hnrnpab1-RNA complexes in this manner but have been unable to succeed in isolating a library. The advantage to using HITS-

CLIP is that it can establish a binding site on a given mRNA and you know that the binding to the mRNA is direct. By comparing the binding sites on the various mRNAs you can establish a consensus site if one exists. An alternative to this method is to perform micro-array analysis on Hnrnpab1 and 2 immune-complexes (RIP-Chip). This assay yields slightly different information since the bound targets could be due to protein-protein interactions rather than a direct Hnrnpab-mRNA interaction. However, since I am able to successfully isolate immune-complexes for RIP-PCR, this may be the easiest option moving forward. Comparing the list of bound mRNAs to the list of proteomic differences seen in the Hnrnpab $^{-/-}$ hippocampus would help to establish if the proteomic changes are due to direct post-transcriptional regulation by Hnrnpab and which isoform may be responsible for these changes. Pathway analysis would also help to direct behavioral assays to establish any behavioral phenotypes in the Hnrnpab $^{-/-}$ mice. Initially these high throughput experiments will be performed cell lines expressing Flag-Hnrnpab1 and Hnrnpab2. But once the protocol is established we can express Hnrnpab1 and 2 using *in utero* electroporation and determine the *in vivo* targets of each isoform of Hnrnpab.

Materials and Methods

Embryonic rat brain extract

A timed pregnant female rat was sacrificed using CO_2 when the pups were embryonic day 21 (E21). The embryos were isolated and placed in ice cold PBS. The brain was isolated and placed in ice cold PBS with 1mM PMSF and minced with a razor blade. The tissue chunks were pelleted by spinning for 3 minutes at 300xg and resuspended in ice cold PBS with 1 mM PMSF. Following 5 washes in PBS with 1 mM PMSF, the pellet was resuspended in 1.5 tissue volume of hypotonic lysis buffer (10 mM HEPES pH 7.5, 10 mM KOAc, 0.5 mM $MgSO_4$, 0.5 mM PMSF, 1x protease inhibitor cocktail and 200 Units/ml RNAse OUT) and transferred to a dounce homogenizer. The tissue was passed through with the loose fitting pestle 5 times, followed by a5 minute incubation on ice. The tissue was then passed through with the loose fitting pestle 25 times and then the tight homogenizer 25 times. NaCl was added to a final concentration of 200 mM and the lysate incubated for 10 minutes on ice. The lysate was spun at 1000 x g for 1 minute and then 15,000 x g for 10 minutes. The supernatant was dialyzed against a 20 fold excess of cold storage buffer (10 mM HEPES pH 7.5, 50 mM NaCl, 0.5 mM $MgSO_4$, 0.5mM PMSF and 5% (v/v) glycerol) for 2 hours. The lysate was spun for 5 minutes at 15,000 x g and the supernatant snap frozen using liquid nitrogen and stored at -80 degrees Celsius.

GRNA Chromatography

The GRNA columns were made by incubating 50 ul glutathione sepharose with 26 µg of lamdaH2 protein with 100 pmol of either the 5' UTR or zipcode of human β-actin containing BoxB hairpins for 1 hour at 4 degrees C. RNA was transcribed using a T7 transcription vector and the MEGAscript T7 kit (Invitrogen, AM1334). Embryonic rat brain extract was pre-cleared for 1 hour at 4 degrees using glutathione sepharose resin that had been resuspended in GRNA

buffer (50mM HEPES, 50 mM NaCl, 1.5mM $MgSO_4$, 1µg/ml Heparain, 2mM DTT, 0.05% NP40, 0.1mg/ml tRNA and 10% glyercol). 3mg of pre-cleared extract along with RNAse inhibitor was added to the column and the volume brought up to 1 ml with GRNA buffer. The extract and column were incubated for 45 minutes at 15 degrees C, washed 5 times with buffer and added to moBi columns (Mo Bi Tec). Protein was eluted using three times with buffer containing 0.1% SDS in 2.5 mM Tris pH 6.8 with 5mM DTT. All three fractions were run on a 12-25% gradient SDS-PAGE gel and silver-stained.

To identify proteins bound to RNA, 32 select bands were excised individually from silver stained gradient SDS-PAGE gels of the GRNA chromatography fractions. Some bands were combined for digestion and analysis. Peptides from 20 tryptic digestions were analyzed by tandem mass spectrometry by the Proteomics Center at Stony Brook University as described elsewhere [183]. The MS/MS data was searched with Inspect against a Uniprot rat database (downloaded 5/26/2013), containing 27253 rat proteins plus 84 common contaminants, with modifications: fixed +57 on Cysteine, +16 on Methionine, and possible phosphorylations on Serine, Threonine, Tyrosine [184]. Only peptides with at least a p value of 0.01 were analyzed further.

Generation of immortalized neural cells (INCs)

Cortices from Hnrnpab null and heterozygous P0 mice were collected, dispersed and plated in 10 cm dishes coated with ECM gel (Sigma, E1270). Following attachment, cells were transfected with the SV40 T antigen using Lipofectamine 2000 and continually passaged in DMEM containing 10% FBS with 10µg/ml gentamicin. Once successful immortalization was observed individual clones were selected, grown up and examined for Hnrnpab expression by both Western Blot and immunofluoresence.

Creation of putative bZBP expression vectors and bZBP cell lines

Putative bZBPs were cloned by add-on PCR into a Tat and Rev dependent lentiviral vector (pHAGE-UbC-GIR) [185]. The open reading frames of the bZBPs were amplified from P0 mouse brain cDNA with the exception of HnrnpD/AUF1, SET1 and 2 and the IMP proteins. The Hnrnpd isoforms were cloned from plasmids expressing each isoform, which were kind gifts from Gary Brewer. The SET proteins were cloned from plasmids graciously provided by Maarten Fornerod. The human IMP 1, 2, 3 ORFs were amplified from plasmids described previously [186]. The primers for each protein are provided in the table below.

After LVP infection, target cells use the human Ubiquitin C promoter to transcribe an mRNA that will translate three tandem Flag epitopes at the N terminus and an Internal Ribosomal Entry Site (IRES) followed by Green Fluorescent Protein from *Zoanthus* species as a marker for infection of living cells. LVPs are produced by co-transfection of these vectors individually into HEK 293-T cells with Tat, Rev, Gag-pol and VSV-G envelope protein expressing vectors as described [185]. Virus-containing culture supernatant is harvested on the first, second and third days after transfection. Debris is cleared from the virus containing supernatant at 3000xg for 10 minutes. This supernatant from the first and second day is stored on ice until the third day post transfection. On the third day, all three days of debris-cleared supernatant are combined and filtered with a 0.4μm PES-syringe filter. LVPs are concentrated by ultracentrifugation at 100,00xg for 2 hours. After removal of the supernatant, the pellet is resuspended in 1.2 ml of DMEM (no serum), and aliquoted into 100μl aliquots and stored at -80°C. For infection, one aliquot is thawed on ice and infection performed by addition of the appropriate amount of viral stock solutions directly to the culture medium.

Cloning Primers

Open Reading Frame	**Species**	**Primer**	**Restriction Site**	**Sequence**
HnrnpA0	Mouse	Fwd	Pci1	gcgcgacatgtccatggagaactcgcagctc
HnrnpA0	Mouse	Rev	Xho1	gcgcgctcgagctagaacgagcctccgc
HnrnpD	Human	Fwd	Pci1	gcgcgacatgtcggaggagcagttc
HnrnpD	Human	Rev	Xho1	gcgcgctcgagttagtatggtttgtagctattttga
HuR	Mouse	Fwd	Nco1	gactgaccatggccatgtctaatggttatgaagaccac a
HuR	Mouse	Rev	Xho1	gcgcgctcgagtatttgtgggacttgttggt
IMP1	Mouse	Fwd	Nco1	gcgcgccatggccatgaacaagctttacatcgg
IMP1	Human	Rev	Xho1	cgcgcctcgagtcacttcctccgtgcctg
IMP2	Human	Fwd	Pci1	gcgcgacatgtccatgaacaagctttacatcgg
IMP2	Human	Rev	Xho1	cgcgcctcgagtcacttgctgcgctgtga
IMP3	Human	Fwd	Nco1	gcgcgccatggccatgaacaaactgtatatcggaaac c
IMP3	Human	Rev	Xho1	cgcgcctcgagttatttccgtcttgactgaggt
NonO	Mouse	Fwd	Nco1	gcgcgccatggccatgcagagcaataaagcctt
NonO	Mouse	Rev	Xho1	gcgcgctcgagctaatatcggcggcgttta
Npm1	Mouse	Fwd	Nco1	gcgcgccatggaagactcgatggatatg
Npm1	Mouse	Rev	Xho1	gcgcgctcgagcttaaagagatttcctcca
PKR	Mouse	Fwd	Nco1	gcgcgccatggccagtgataccccagg
PKR	Mouse	Rev	Xho1	gcgcgctcgagctaacatgtgtttcttttcttttttc
PSPC1	Mouse	Fwd	Pci1	gcgcgacatgtccatgatgttaagaggaaacct
PSPC1	Mouse	Rev	Xho1	ctctcctcgagttaatatctccgacgcttattagg
SET1	Human	Fwd	Nco1	gcgcgccatggcccctaaacgcca
SET2	Human	Fwd	Nco1	gcgcgccatggccatgtcggcgcaggc

SET	Human	Rev	Xho1	gcgcgctcgagttagtcatcttctccttcatcctcc
SFPQ	Mouse	Fwd	Pci1	gcgcgacatgtctcgggatcggttccg
SFPQ	Mouse	Rev	Xho1	aaataaaaaaaccccgattttagctcgaggcgcg

Cell culture

All cell lines were grown in Dulbecco's Modification of Eagle's Medium (DMEM, Cellgro) containing 4.5 g/L glucose, L-glutamine and sodium pyruvate supplemented with 10% fetal bovine serum and 10μg/mL of gentamicin (GIBCO). N2A cells were passaged every other day at a density of 1x10^ cells per 10cm plate. INCs were passaged every other day at a density of 250,000 cells per 10cm plate.

Preparation of bZBP soluble extract

Cells lines were allowed to grow to 80% confluency, were detached from the dish using 1x Trypsin-EDTA (Sigma) and spun at 0.5xg for 5 minutes. The pellet was washed 3X with ice cold PBS with 1mM PMSF and resuspended in polysome lysis buffer containing 100mM KCl, 5mM $MgCl_2$, 10mM HEPES, 0.5% NP40, 1mM β-mercaptoethanol, 100 units/mL RNase Out and 1X EDTA free protease inhibitor. Lysate was spun at 4 degrees C at 10,000 rpm for 10 minutes and the supernatant was collected and stored at -80 degrees Celsius. Protein concentration was determined using the Pierce BCA Protein kit according to manufacturer's instructions.

RNP Immunoprecipitation (RIP)

50 μl of packed protein G agarose beads were washed 3x in NT2 buffer containing 50 mM Tris-HCl, 150 mM NaCl, 1mM $MgCl_2$ and 0.5% NP40. The beads were resuspended in 100 μl of NT2 buffer and 2 μg of Flag-antibody (Sigma). The beads were rotated at 4 degrees for 3

hours and then washed 3x in NT2 buffer. 2 mg of soluble extract from non-FACS-sorted cells or 1mg of soluble extract from FACS sorted cells was added to the beads and the beads and extract were rotated at 4° C for 3 hours. The beads were separated by spinning at 500 rpm for 5 minutes and the unbound supernatant was collected to determine the immunoprecipitation efficiency. The beads were washed 5x with NT2 buffer, resuspended in NT2 buffer containing 0.1% SDS and placed at 55° C for 30 minutes. The beads were separated from the eluate using mobicols (Mo Bi Tec) and 1/5 of the elution was kept for immunoblot while the remaining amount was set aside for phenol/chloroform extraction. RNA was extracted from the eluate and 100 μg of extract using phenol:chloroform extraction and precipitated using glycogen, 3M sodium acetate and ethanol.

Reverse Transcription and PCR

The amount of RNA for the extract and IP were determined using a Nanodrop Spectrophotometer. 100ng of IP RNA and 200ng of total RNA were reverse transcribed using Dynamo cDNA synthesis kit (Thermo Scientific). 1 μl of cDNA from each sample was then amplified using *Taq* polymerase (NEB) and primers against the transcript of interest. The primers used are listed in the primers section. The resulting PCR products were run on a 1% agarose gel containing ethidium bromide and imaged using a gel dock system.

Construction of Hnrnpab deletions

PCR primers amplified regions of mouse Hnrnpab as follows: Hnrnpab N-teriminus amino acids 1-76, Hnrnpab del N amino acids 69-332, Hnrnpab C Terminus amino acids 240-332, RRMs amino acids 69-246. These PCR products were designed to be cloned in frame with pHAGE-3xFLAG-IR for deltaN, deltaC and RRMs. The N terminus was cloned into the pHAGE vector by a three piece ligation so that it expressed The N-terminus fused to the amino terminus

of Cerulean Fluorescent protein (CFP) that contained a triple Flag tag at the C terminus. The C-terminus of Hnrnpab1 was cloned by three piece ligation to create a CFP with an amino terminal triple-Flag epitope and the Hnrnpab C terminus at the CFP C-terminus.

Cross-linking immunoprecipitation (CLIP)

50 µl of packed protein G agarose beads were washed 3x with CLIP lysis buffer containing 50mM Tris-HCl, 100mM NaCl, 1% NP40, 0.1% SDS, 0.5% deoxycholate and 5mM EDTA. The beads were resuspended in 100 µl of lysis buffer with 2 µg of Flag antibody and rotated at 4 ° C for 3 hours. Beads were then washed 3X with lysis buffer and were kept in the last wash until needed for immunoprecipitation.

INCs were placed in a Stratalinker and exposed to 400,000 µj of UV-light at a distance of approximately 9cm from the bulb. After collection, the cells were resuspended in 1mL CLIP lysis buffer, spun at 10,000 rpm for 10 minutes, the supernatant collected and the protein concentration determined using the Pierce BCA protein assay kit. 1mg of extract was then treated with a 1:15,000 dilution of RNAse A and Turbo DNase for 5 minutes at 37 ° C. The digested extract was then added to the prepared agarose beads and rotated at 4 ° C for 3 hours. The beads were then separated by spinning at 500 rpm for 5 minutes. The beads were washed 5x with wash buffer containing 20 mM Tris-HCl, 10 mM $MgCl_2$ and 0.2% Tween, resuspended in hot T4 poly-nucleotide kinase (NEB, M0201) and incubated at 37 C for 5 minutes. The PNK and unbound nucleotide was removed, the beads washed with wash buffer and resuspended in SDS-PAGE loading buffer. The sample was then loaded on a 10% Bis-Tris gel, transferred to a nitrocellulose membrane, washed with PBS pH 7.4 and exposed to film.

FISH Primer Design

Primary ODNs consisted of a 45 to 50mer sequence antisense to a gene specific mRNA at the 5' end of a DNA oligo, followed by 3 copies of a random 35-mer sequence. Multiple primary ODNs to the same mRNA were designed with 50-mers complementary to different sequences within the same transcript but containing the same 35mer repeated sequence. The secondary ODNs contain a 35-mer complementary to the 35-mer of the primary ODN at the 5'end, followed by 5 copies of a distinct random 25-mer. The tertiary or dye ODN is a 25-mer complementary to the 25-mer in the secondary ODN and contains a fluorescent dye at the 5' end (Cy3 for the Actb probes and Cy5 for the Actg probes). All DNA sequences were targeted to consist of 50% G-C base pairs, with actual ratios varying between 40% and 60%. Individual antisense 50-mer and randomly generated 35-mer and 25-mer sequences were subjected to BLAST search to minimize the potential to cross-hybridize to other mRNA sequences in the genome. Typically 14-16 continuous bases were the largest stretch of complementary sequence found in secondary targets. Primary and secondary oligonucleotides were purchased as standard-desalted Ultramers from Integrated DNA Technologies (IDT), dye oligo was ordered with the dye at the 5'end from synthesis with purification standard for labeled ODN (IDT).

FISH Oligonucleotides

Mouse Actb primary1	5'caacgaaggagctgcaaagaagctgtgctcgcgggtggacgcgactcTCGTTGGCCCCC GACCGTTACAGACTGTTCTCAGTtcgttggcccccgaccgttacagactgttctcagt TCGTTGGCCCCCGACCGTTACAGACTGTTCTCAGT
Mouse Actb primary2	5'ggtggcttttgggagggtgagggacttcctgtaaccacttatttcatggaTCGTTGGCCCCC GACCGTTACAGACTGTTCTCAGTtcgttggcccccgaccgttacagactgttctcagt TCGTTGGCCCCCGACCGTTACAGACTGTTCTCAGT
Mouse Actg primary1	5'ctccccagcccccaagtgaccgagccacatgaactaaggactaaatcaagTCTATAAACG AGCAATTACATAAGACATCCGTAGAtctataaacgagcaattacataagacatcc gtagaTCTATAAACGAGCAATTACATAAGACATCCGTAGA
MouseActg primary2	5'tgacgagtgcggcgatttcttcttccattgcgatcggcgaaggacTCTATAAACGAGCA ATTACATAAGACATCCGTAGAtctataaacgagcaattacataagacatccgtagaT

	CTATAAACGAGCAATTACATAAGACATCCGTAGA
Secondary1 (for Actb)	5'ACTGAGAACAGTCTGTAACGGTCGGGGGCCAACGAacgcgattgactaccagactatacgACGCGATTGACTACCAGACTATACGacgcgattgactaccagactatacgACGCGATTGACTACCAGACTATACGacgcgattgactaccagactatacg
Secondary2 (for Actg)	5'TCTACGGATGTCTTATGTAATTGCTCGTTTATAGAtaccaattctgacatatgtgactcaTACCAATTCTGACATATGTGACTCAtaccaattctgacatatgtgactcaTACCAATTCTGACATATGTGACTCAtaccaattctgacatatgtgactca
Tertiary1 (for Actb)	/Cy3/5' CGTATAGTCTGGTAGTCAATCGCGT
Tertiary2 (for Actg)	/Cy5/ 5'TGAGTCACATATGTCAGAATTGGTA
Nrg1-III primary1	5'tatgttccgctgccggaagcccatcgagagatgggtctgcactcagctgaTCGTTGGCCCCCGACCGTTACAGACTGTTCTCAGTtcgttggcccccgaccgttacagactgttctcagtTCGTTGGCCCCCGACCGTTACAGACTGTTCTCAGT
Nrg1-III primary2	5'agatcttctcggagttgaggcaccctctgagacgctccgcttccaggcTCGTTGGCCCCCGACCGTTACAGACTGTTCTCAGTtcgttggcccccgaccgttacagactgttctcagtTCGTTGGCCCCCGACCGTTACAGACTGTTCTCAGT
Nrg1-III primary3	5'cccccagggtcaaggtgggtaggagagtcgtattcgaatatcttgtccacTCGTTGGCCCCCGACCGTTACAGACTGTTCTCAGTtcgttggcccccgaccgttacagactgttctcagtTCGTTGGCCCCCGACCGTTACAGACTGTTCTCAGT
Mouse ChAT primary1	5'ctcgctcccaccgcttctgcaaactccacagatgaggtctctttgcagccTCTATAAACGAGCAATTACATAAGACATCCGTAGAtctataaacgagcaattacataagacatccgtagaTCTATAAACGAGCAATTACATAAGACATCCGTAGA
Mouse ChAT primary2	5'aacatgccagcttcatgtgagcccccaaggataggggagcagcaacaagcTCTATAAACGAGCAATTACATAAGACATCCGTAGAtctataaacgagcaattacataagacatccgtagaTCTATAAACGAGCAATTACATAAGACATCCGTAGA
Mouse ChAT primary3	5'gggggttataacaggctccatacccattgggtaccacagggccataacTCTATAAACGAGCAATTACATAAGACATCCGTAGAtctataaacgagcaattacataagacatccgtagaTCTATAAACGAGCAATTACATAAGACATCCGTAGA

Cell culture for FISH

Primary fibroblasts were isolated from E14 mouse embryos by standard procedures and maintained in DMEM with 10% FBS with gentamicin (D10). SV40 Large T antigen

immortalized mouse embryonic fibroblasts were plated at a density of 25,000 cells on coated 18 mM coverslips in a 12 well culture dish in D10. The coverslips were coated using 50μg/ml poly (l) lysine in boric acid buffer (50mM boric acid, 5 mM sodium tetraborate, pH 8.5) over-night at room temperature) then washed in sterile water prior to adding cells. The cells were allowed to attach and grow over-night before being fixed using four two-fold dilutions of 4% paraformaldehyde with 1mM $MgSO_4$. Cells were allowed to fix in the final dilution for 20 minutes. The cells were then washed in PBS with 0.1M glycine (PBSG) for 10 minutes and then permeabilized and stored in 80% methanol at -20 degrees C overnight.

Neuronal cultures were maintained according to the procedure described previously [187]. Briefly, embryonic day 18 timed pregnant mice were sacrificed using CO2 in accordance with IACUC protocols. Cortices were isolated from the pups, trypsinized, dissociated and plated in neurobasal supplemented with B27, primocin, and glutamax. After two days in vitro cultures were treated with 3μM FDU. Following the indicated days in culture the cells were fixed using four two-fold dilutions of 4% paraformaldehyde with 1mM $MgSO_4$. Cells were allowed to fix in the final dilution for 20 minutes. The cells were then washed in PBS with .1M glycine for 10 minutes and then permeabilized and stored in 80% methanol over-night at -20 degrees C.

Expression of Hnrnpab1, Hnrnpab2 and Hnrnpab Mini-gene in MEFs

A lentiviral expression vector to express Flag tagged Hnrnpab from the ubiquitin C promoter was created by subcloning PCR. Three repeats of the Flag epitope tag were added to the open reading of Hnrnpab, and these were cloned into a pHAGE lentiviral transfer vector that includes an IRES followed by a fusion of the fluorescent protein mcherry linked by a self-cleaving 2A peptide sequence to the sequence encoding for puromycin resistance. The open reading frames of Hnrnpab1 and Hnrnpab2 were cloned into this vector and confirmed by

sequencing. Lentiviral particle infection of Hnrnpab -/- MEFs was confirmed by the presence of mcherry signal under a fluorescent microscope. Infected cells were then selected for using puromycin selection for 5 days. An Hnrnpab minigene construct to express both alternatively spliced isoforms under their endogenous splicing context was created by using the cDNA from the amino half of Hnrnpab (Exons 1 through 5) and the genomic DNA from the carboxyl half of Hnrnpab (from exon 5 to the end of exon 8). The minigene construct differs from the Hnrnpab1 and Hnrnpab2 vectors by using the UbC promoter in the opposite orientation so that the lentiviral genomic RNAs are transcribed with the antisense Hnrnpab mRNA (to retain the introns) and adding the BGH polyadenylation sequence to its 3' end. A YFP ORF behind the UbC promoter in this construct is produced at detectable levels so that it can be used as a marker for Hnrnpab expression.

FISH probe preparation

Probe mixes are 50µl per coverslip and assembled for each experiment from concentrated stocks. Once probe mixes were assembled, they were heated to 65 °C for a minute immediately prior to use. **Primary Probe** Mix contained 2X SSC (300mM NaCl, 30mM Sodium Citrate), 10% dextran sulfate, 40% formamide, 0.1uM of each primary ODN for each gene hybridized, 20 µg/ml sheared salmon sperm DNA, 20 µg/ml *E. coli* RNAse free tRNA, 0.4% SDS. **Secondary Probe** Mix contained 2X SSC, 10% dextran sulfate, 35% formamide, 0.1µM each secondary probe corresponding to the primary probes used, 20 µg/ml sheared salmon sperm DNA, 20 µg/ml *E. coli* RNAse free tRNA, 0.4% SDS. **Tertiary Probe** Mix contained 2X SSC, 10% dextran sulfate, 20% formamide, 0.1uM of each tertiary probe used.

Assembly of a humidified chamber

A piece of parafilm was spread in the bottom of a plastic culture dish. 50µl probe solution was placed on the parafilm without creating air bubbles with enough distance between probes so that coverslips will not contact each other during incubation. The cover-slips were then placed face-down on the drop of probe. A conical tube top was placed inside the chamber full of and then the vessel was sealed with parafilm.

Hybridization

Coverslips with fixed cells in 80% methanol from above were warmed to room temperature, and serially rehydrated by 5 successive 2-fold dilutions with 2X SSC/40% formamide, followed by one complete change into 2X SSC/40% Formamide. After 5-mintues coverslips were placed into primary probe (prepared as above) cells-side down in a humidified chamber as above and incubated 37 °C overnight. All steps from here forward were performed in a 37°C warm room, and all reagents kept at 37°C. The coverslips were gently pried off the parafilm, individually placed cells-side up into separate wells of a 6-well culture dish with 3 ml of 2X SSC/40% formamide and then rocked gently in a 2D shaker for 15 minutes. This wash was repeated for three 15-minute intervals, then buffer changed to 2X SSC, 35% formamide to equilibrate the coverslips for the secondary hybridization. Coverslips were placed cells-side down on a drop of secondary probe mixture (prepared as above) in a hybridization chamber. The chamber was sealed with parafilm and incubated 3 hours. The coverslips were gently pried off the parafilm, individually placed cells-side up into separate wells of a 6-well culture dish with 3 ml of 2X SSC/40% formamide and then rocked gently in a 2D shaker for 15 minutes. This wash was repeated for three 15 minute intervals, and then the buffer changed to 2X SSC, 20% formamide to equilibrate the cover-slips for the tertiary hybridization. Coverslips were placed cells-side down on a drop of tertiary probe mixture (prepared as above) in a hybridization

chamber. The chamber was sealed with parafilm, covered with aluminum foil and incubated 3 hours. The coverslips were gently pried off the parafilm, individually placed cells-side up into separate wells of a 6-well culture dish with 3 ml of 2X SSC/40% formamide and then rocked in a 2D shaker for 15 minutes. This wash was repeated for three 15 minute intervals then the buffer changed to 1x SSC, 0.05% Tween 20 and 300nM DAPI and rocked in a 2D shaker for 15 minutes. Cells were rinsed two times in 1xSSC, then mounted in hard set anti-fade microscopy mounting medium according to manufacturer's recommendations, and used for microscopy.

Image acquisition and analysis of mRNA dispersion and polarization

Epifluorescence micrographs were obtained using a standard epifluorescence microscope (Nikon TiE). Single plane images were acquired using a Cool Snap HQ2 or QuantEM digital camera. To be able to compare images shown, fluorescence micrographs of the same wavelengths (Cy3 or Cy5) within an individual experiment were acquired with the same exposure time, and the display scales of the representative images from each condition were equalized. For mRNA distribution analysis, serial Z-sections (0.5μm steps, between 5-7 μm total distance) were acquired in the Cy3, Cy5 and FITC channels and a maximum projection image was generated using the Nikon Elements software. For quantification of the polarization and distribution of mRNAs, a manual mask was generated using the autofluorescent image generated in the FITC channel using ImageJ and the dispersion and polarization indexes were calculated using the script described[161]. Cells that contained bright STIC probe aggregates were not imaged for mRNA distribution analysis.

Raising Hnrnpab$^{-/-}$ mice

Gene trap AV0462 ES cells in the Wellcome Trust Sanger Institute collection harbored a putative insertion of the pGT01xr gene trap vector into intron 5 of the Hnrnpab gene. ES cell line

expansion, gene trap verification, blastocyst injection and germ line screening of chimeras were all performed using standard techniques by the Mutant Mouse Regional Resource Center facility at University of California at Davis. We designed a single PCR reaction to genotype, with a sense strand primer to exon 4 (5' ggtggcttgtttcttcttg) in combination with two antisense primers that bind either to intron 5 (to amplify the wild type allele, 5' gaagagccagctgtttccag), or the En2 intron of pGT01xr (5' ggctaccggctaaaacttga). The wild type allele produces a band of 429 nucleotides (nt) and the Gt(AV0462)Wtsi allele produces a band of 745 nt. 15µl reactions with Sigma Jump Start Taq PCR mix are used with 1µl of genomic DNA from mouse tail, prepared with DNeasy Blood and tissue kit (Qiagen). A 58° annealing and 1 minute extension time is used. Homozygous males and females breed normally on the mixed genetic background of the germ line transmitted mice and this colony is maintained inbred. We routinely mate a heterozygous female with a homozygous male to generate a 1:1 ratio of Hnrnpab$^{+/-}$ and Hnrnpab$^{-/-}$ mice in each litter.

Hnrnpab antisera and affinity purified antibodies

Amino acids 6-24 of mouse Hnrnpab (NH_2-EEQPMETTGATENGHEAAP-COOH) were used to raise polyclonal rabbit antibodies (ProteinTech Group). This peptide is present in both isoforms of Hnrnpab and is 100% conserved in mouse, rat, and most other mammalian Hnrnpab orthologs. We also purified recombinant 6his-tagged human Hnrnpab N-terminus protein (amino acids 1-71) and ProteinTech Group raised polyclonal antisera to this. To affinity purify antibodies, either the peptide or 6his-Hnrnpab1-71 was attached to a NHS-sepharose to a high concentration as per manufacturer's instructions. Immune serum was reacted with resin in batch then poured into a column for washing (PBS-0.5 M NaCl) before the antigen purified antibodies

were eluted with 0.1M glycine pH2.5, 500mM NaCl and immediately neutralized with 1/10 volume 1M Tris pH 8.0. This was dialyzed against PBS, then concentrated in Dialysis tubing (MWCO 3000) covered in PEG powder (MW 30,000), then dialyzed extensively against PBS-20% glycerol in new dialysis tubing with 10,000 MWCO. This antibody (approximately 100μg/ml) was aliquoted and stored at -80 for long- term storage, or at 4°C for short-term use. Both serum and affinity purified antibody recognized the expected two isoforms of Hnrnpab on western blots.

Immuno-staining of Brain sections

A 55-day-old mouse was perfused with PBS-4%PFA and the brain dissected, cryo-protected, frozen and mounted in tissue mounting medium. Saggital sections were prepared, and post-fixed on the slides with PBS-4%PFA and permeabilized with PBS-1%TritonX-100. After washing in PBS, blocking was performed in CAS block (Zymed) for 1 hour and primary antibodies diluted in CAS block. Hnrnpab N-terminal peptide affinity purified antibody was used at 1:50 and Mouse anti-parvalbumin (Sigma P3088) was also used 1:50 and these primary antibodies were incubated with sections overnight at 4°C. After washing in PBS, secondary antibodies (anti-mouse IgG FITC and anti Rabbit IgG-Cy3, Jackson Immunoresearch) were diluted to 1:500 in PBS and incubated for an hour. After several washes, DAPI was included in the final PBS wash at 300-600nM. And brain sections were mounted in Pro-long Gold anti-fade (molecular probes). Microscopy was performed on a Nikon TiE widefield fluorescence microscope with appropriate fluorescence filters, and images acquired using a Photometrics cool snap HQ2 camera.

Neuron culture and immunofluorescence

Culture methods are based on routine practices for embryonic neuron cultures [182, 188, 189]. Hnrnpab$^{+/Gt(AV0462)Wtsi}$ mothers are mated with Hnrnpab $^{Gt(AV0462)Wtsi / Gt(AV0462)Wtsi}$ males and embryonic day 18 (E18) mouse pups are dissected from the pregnant females and transferred and extensively washed in ice cold sterile PBS. Brains are dissected in ice cold Hanks Basal Salt Solution, w/o Mg^{++} or Ca^{++} (HBSS) with 5mM HEPES pH 7.5 and hippocampi are removed without meninges from individual animals, and tails are kept separate and quickly processed for genotyping. Brain tissue is treated with 0.25% trypsin in HBSS at 37° for 20 minutes. Trypsin is inactivated by adding Ovomucoid Inhibitor to 1 mg/ml and DNAseI added to 0.2 mg/ml and cells incubated for 5 minutes at room temperature. Tissue pieces are rinsed 3 times with room temperature Hibernate-E (BrainBitsLLC) containing 2mM Glutamax and 1x B27 and then dissociated carefully by 10 passes through a flame polished Pasteur pipette. Cultures are filtered with a 0.4μm mesh and stored on ice in the dark until genotyping is completed (typically within 24 hours). Equal numbers of neurons from animals of the same genotype are then pooled prior or plating 75,000 to 100,000 viable cells on 18mm glass coverslips coated with 50μg/ml Poly-L-Lysine hydrobromide in boric acid buffer (50mM Boric Acid, 12.5mM Sodium Borate, decahydrate). The hippocampal neurons are diluted in in Neurobasal 1xB27 and 2mM glutamax with 25μM glutamate for plating. Coverslips are maintained within one well of a 12 well dish. And after cells attach to coverslips (typically within 1 hour) the media is changed to remove cell debris. Media half changes occur every 4 days using a 1:1 mixture of fresh Neruobasal-B27-2mM Glutamax and glia-conditioned medium [188]. Cells were maintained at 37°C with 5% CO_2 in a humidified incubator.

For glutamate stimulation, complete medium change to fresh Neurobasal-B27-1mM Glutamax was very carefully performed, and after 10 minutes cells were rinsed once in plain Neurobasal and then changed back to fresh Neurobasal-B27-Glutamax and incubation continued for 6 hours. All media for glutamate stimulation was equilibrated in 5% CO_2 at 37 degrees prior to application to the cells. Fixation was performed by 3 serial 3-fold dilutions of culture medium with PBS-4% PFA, followed by a last complete change with PBS-4% PFA. After 20 minutes, coverslips were changed into PBS-0.1M Glycine for 20 min. For storage cells were changed into 80% methanol and kept at -20. Stored coverslips were rehydrated by 6 2-fold serial dilutions of the storage solution with PBS followed by a final wash with PBS. These were permeabilized with PBS-0.5% IGEPAL-60 for 5 minutes. Coverslips were rinsed in PBS and blocked for 30 minutes with CAS block (Zymed). Hnrnpab antibody was diluted 1:50 in CAS block for immuno-staining, anti-Flag M2 monoclonal mouse antibody was diluted into TBST (50mM Tris pH 8.0, 150mM NaCl, 0.1% Tween 20) at a concentration of 10-20 μg/ml. Primary antibodies were incubated with samples overnight at 4°C in a humidified chamber. Coverslips were washed for 1 hour with 4 changes of PBS. Coverslips were incubated with secondary antibody at 1:500 in CAS block for 1 hour at room temperature (anti-rabbit IgG –Cy3 or anti-mouse IgG-Alexa 546 for Hnrnpab and FlagM2 respectively). Coverslips were washed for 1 hour with 4 changes of PBS, 300nM DAPI included in the last wash. Coverslips were mounted and imaged as described for brain sections above, with the exception that a QuantEM camera with 512x512 pixel chip with the multiplier off was used for image acquisition of the virus infected neurons.

For neurite length measurements, embryonic day 18 cortical neurons were prepared as described above and allowed to grow for 2 days *in vitro*. The cells were then fixed with 4% PFA and permeabilized with NP40. The cells were immunostained using β–III tubulin (Sigma T8660)

in the presence of CAS block (Invitrogen 00-8120) to block non-specific interactions. A total number of 26 Heterozygous and 30 KO cells with 117 and 99 neurites (respectively) were analyzed using the Nikon NIS Elements Software. A neurite was defined as anti-III β tubulin positive extension from the cell body. The lengths of individual neurites per cell were recorded and the longest neurite from each cell determined. Statistics were performed using a Mann-Whitney Rank Sum Test on the median values of the lengths of each neurite and the longest neurite per cell.

To quantify Nuclear/Cytoplasmic Ratios of Flag-tagged Hnrnpab isoforms at least 12 cells per condition were analyzed using the Nikon NIS Elements Software. The sum intensity Flag staining in the nucleus was determined along with the sum intensity of the total cell soma. The cytoplasmic distribution of the Hnrnpab isoforms was calculated by subtracting the nuclear intensity from the total intensity. The ratio of nuclear signal to cytoplasmic signal was then calculated. Statistical analyses of the nuclear to cytoplasmic ratios were performed using the Mann-Whitney Sum Rank Test or students t-test, controlling for multiple comparisons with the Bonferroni adjustment.

Proteomic Methods

Materials

Invitrosol^{TM} was purchased from Invitrogen (Carlsbad, CA). Trypsin (modified, sequencing grade) was obtained from Promega, WI. Other laboratory reagents were purchased from Sigma-Aldrich (St. Louis, MO) and Thermo Fisher Scientific (Waltham, MA) unless noted otherwise.

Sample Preparation.

An entire litter from Hnrnpab$^{+/-}$ and Hnrnpab$^{-/-}$ animals was dissected within several hours of birth. Hippocampi from each mouse were combined and fractionated into soluble fractions and insoluble fractions, and the corresponding tails used to genotype the samples. Hippocampus tissues were homogenized in the first mass spectrometry-compatible lysis buffer (50mM Ammonium Bicarbonate,, 0.5X invitrosol, protease and phosphatase inhibitors (Roche)) using the Precellys 24 tissue homogenizer (Bertin Technologies). After homogenization, tissue lysates were cleared by centrifugation. The cleared supernatant was collected as the soluble fraction. The remaining pellet was solubilized in the second mass spectrometry-compatible lysis buffer (50mM Ammonium Bicarbonate, 8M Urea, 1X invitrosol, protease and phosphatase inhibitors) and collected as the insoluble fraction. The protein concentration from each fraction was determined using the EZQ protein assay (Invitrogen, CA).

For quantitative global protein analysis, we used brain lysates from metabolically labeled mice as internal protein standards. C57BL/6 mice were labeled metabolically using stable isotope-labeled (^{15}N) amino acids (SILAM, Silantes, Germany) according to the feeding regimen established in the Chen laboratory. The isotopic incorporation was to greater than 97% of ^{15}N amino acids into proteins in the brain tissue as determined by LC-MS/MS. Age-matched ^{15}N labeled hippocampus tissues were homogenized and fractionated using the same method described above, and the protein concentration was determined using the EZQ protein assay.

Trypsin Digestion.

30μg of unlabeled soluble or insoluble hippocampus lysates were mixed with 30μg of corresponding ^{15}N labeled hippocampus lysates and diluted in 50mM Ammonium Bicarbonate for trypsin digestion. Trypsin was added to each sample at a ratio of 1:30 enzyme/protein along

with 2 mM $CaCl_2$ and incubated for 16 hours at 37°C. Following digestion, all reactions were acidified with 90% formic acid (2% final) to stop proteolysis. Then, samples were centrifuged for 30 minutes at 14,000 rpm to remove insoluble material. The soluble peptide mixtures were collected for LC-MS/MS analysis.

Multidimensional chromatography and tandem mass spectrometry

Peptide mixtures were pressure-loaded onto a 250 μm inner diameter (i.d.) fused-silica capillary packed first with 3 cm of 5 μm strong cation exchange material (Partisphere SCX, Whatman), followed by 3 cm of 10 μm C18 reverse phase (RP) particles (Aqua, Phenomenex, CA). Loaded and washed microcapillaries were connected *via* a 2 μm filtered union (UpChurch Scientific) to a 100 μm i.d. column, which had been pulled to a 5 μm i.d. tip using a P-2000 CO_2 laser puller (Sutter Instruments), then packed with 13 cm of 3 μm C18 reverse phase (RP) particles (Aqua, Phenomenex, CA) and equilibrated in 5% acetonitrile, 0.1 % formic acid (Buffer A). This split-column was then installed in-line with a NanoLC Eskigent HPLC pump. The flow rate of channel 2 was set at 300 nl/min for the organic gradient. The flow rate of channel 1 was set to 0.5μl/min for the salt pulse. Fully automated 11-step chromatography runs were carried out. Three different elution buffers were used: 5% acetonitrile, 0.1 % formic acid (Buffer A); 98% acetonitrile, 0.1% formic acid (Buffer B); and 0.5 M ammonium acetate, 5% acetonitrile, 0.1% formic acid (Buffer C). In such sequences of chromatographic events, peptides are sequentially eluted from the SCX resin to the RP resin by increasing salt steps (increase in Buffer C concentration), followed by organic gradients (increase in Buffer B concentration). The last chromatography step consists in a high salt wash with 100% Buffer C followed by acetonitrile gradient. The application of a 2.5 kV distal voltage electrosprayed the eluting peptides directly

into a LTQ-Orbitrap XL mass spectrometer equipped with a nano-LC electrospray ionization source (ThermoFinnigan). Full MS spectra were recorded on the peptides over a 400 to 2000 m/z range by the Orbitrap, followed by five tandem mass (MS/MS) events sequentially generated by LTQ in a data-dependent manner on the first, second, third, and fourth most intense ions selected from the full MS spectrum (at 35% collision energy). Mass spectrometer scan functions and HPLC solvent gradients were controlled by the Xcalibur data system (ThermoFinnigan, San Jose, CA).

Database search and interpretation of MS/MS datasets

Tandem mass spectra were extracted from raw files, and a binary classifier - previously trained on a manually validated data set - was used to remove the low quality MS/MS spectra. The remaining spectra were searched against a *mouse* protein database containing 56,871 protein sequences downloaded as FASTA-formatted sequences from EBI-IPI (database version 3.75, released on August, 19, 2010) [190] and 124 common contaminant proteins, for a total of 56,995 target database sequences. To calculate confidence levels and false positive rates, we used a decoy database containing the reverse sequences of 56,995 proteins appended to the target database [191], and the SEQUEST algorithm [192, 193] to find the best matching sequences from the combined database.

SEQUEST searches were done using the Integrated Proteomics Pipeline (IP2, Integrated Proteomics Inc., CA) on Intel Xeon X5450 X/3.0 PROC processor clusters running under the Linux operating system. The peptide mass search tolerance was set to 50ppm. No differential modifications were considered. No enzymatic cleavage conditions were imposed on the database

search, so the search space included all candidate peptides whose theoretical mass fell within the 50ppm mass tolerance window, despite their tryptic status.

The validity of peptide/spectrum matches was assessed in DTASelect2 [194] using SEQUEST-defined parameters, the cross-correlation score (XCorr) and normalized difference in cross-correlation scores (DeltaCN). The search results were grouped by charge state (+1, +2, and +3) and tryptic status (fully tryptic, half-tryptic, and non-tryptic), resulting in 9 distinct sub-groups. In each one of the sub-groups, the distribution of XCorr and DeltaCN values for (a) direct and (b) decoy database hits was obtained, and the two subsets were separated by quadratic discriminant analysis. Outlier points in the two distributions (for example, matches with very low Xcorr but very high DeltaCN were discarded. Full separation of the direct and decoy subsets is not generally possible; therefore, the discriminant score was set such that a false positive rate of 1% was determined based on the number of accepted decoy database peptides. This procedure was independently performed on each data subset, resulting in a false positive rate independent of tryptic status or charge state.

In addition, a minimum sequence length of 7 amino acid residues was required, and each protein on the final list was supported by at least two independent peptide identifications unless specified. These additional requirements – especially the latter - resulted in the elimination of most decoy database and false positive hits, as these tended to be overwhelmingly present as proteins identified by single peptide matches. After this last filtering step, the false identification rate was reduced to below 1%.

Quantitative global protein analysis

SEQUEST identified ^{14}N and ^{15}N labeled peptides based on their fragmentation spectra. CenSus, an algorithm-based quantification software [195] was used to identify co-eluting ^{14}N and ^{15}N peptide peaks from the MS based on MS/MS identifications, generate ratios of co-eluting ^{14}N and ^{15}N peptides based on the measured ion intensities, and perform statistical analysis (R^2 correlation, ratio distribution of peptides, and etc). Only co-eluting ^{14}N and ^{15}N peptides with R^2 scores greater than 0.5 were used for protein quantification. Relative expression level between ^{14}N labeled (Hnrnpab$^{+/-}$ or Hnrnpab$^{-/-}$) and ^{15}N labeled (wildtype) for each protein was calculated by averaging the ratio of ^{14}N to ^{15}N labeled peptides among animals of a the same genotype. Differential protein expression between Hnrnpab$^{+/-}$ or Hnrnpab$^{-/-}$ hippocampus lysates was calculated by dividing the Hnrnpab$^{-/-}$ ^{14}N /^{15}N ratios by Hnrnpab$^{+/-}$ ^{14}N/^{15}N ratios.

Functional Analysis of an Entire Data Set

Network analysis using ingenuity pathway analysis software can organize gene expression changes into groups of genes, which highly influence one another governing specific biological functions. Proteins whose expression was changed by Hnrnpab disruption were uploaded into ingenuity software (www.ingenuity.com) to perform network analysis. The software scans the input gene expression data to provide networks by using the Ingenuity Pathway Knowledge Base, which is a data base created from data mining for expression and functional relationships between molecules extracted from previously published peer reviewed papers found in NCBI Pubmed, Medline, and several other databases. These proteins were associated with biological pathways using Ingenuity's Knowledge Base. Right-tailed Fisher's exact test with the Benjamini-Hochberg multiple correction to control for false positives was used to calculate a p-value determining the probability that each biological function and/or disease assigned to that data set is due to chance alone.

References

1. Czaplinski, K. and R.H. Singer, *Pathways for mRNA localization in the cytoplasm.* Trends Biochem Sci, 2006. **31**(12): p. 687-93.
2. Ainger, K., et al., *Transport and localization elements in myelin basic protein mRNA.* J Cell Biol, 1997. **138**(5): p. 1077-87.
3. Ferrandon, D., et al., *RNA-RNA interaction is required for the formation of specific bicoid mRNA 3' UTR-STAUFEN ribonucleoprotein particles.* Embo J, 1997. **16**(7): p. 1751-8.
4. Macdonald, P.M. and G. Struhl, *cis-acting sequences responsible for anterior localization of bicoid mRNA in Drosophila embryos.* Nature, 1988. **336**(6199): p. 595-8.
5. Mori, Y., et al., *Two cis-acting elements in the 3' untranslated region of alpha-CaMKII regulate its dendritic targeting.* Nat Neurosci, 2000. **3**(11): p. 1079-84.
6. Miller, S., et al., *Disruption of dendritic translation of CaMKIIalpha impairs stabilization of synaptic plasticity and memory consolidation.* Neuron, 2002. **36**(3): p. 507-19.
7. Blichenberg, A., et al., *Identification of a cis-acting dendritic targeting element in the mRNA encoding the alpha subunit of Ca2+/calmodulin-dependent protein kinase II.* Eur J Neurosci, 2001. **13**(10): p. 1881-8.
8. Huang, Y.S., et al., *Facilitation of dendritic mRNA transport by CPEB.* Genes Dev, 2003. **17**(5): p. 638-53.
9. Subramanian, M., Rage, F., Tabet, R., Flatter, E., Mandel, JL., Moine, H., *G-quadruplex RNA structure as a signal for neurite mRNA targeting.* Embo J, 2011. **12**: p. 697-704.
10. Otero, L.J., A. Devaux, and N. Standart, *A 250-nucleotide UA-rich element in the 3' untranslated region of Xenopus laevis Vg1 mRNA represses translation both in vivo and in vitro.* Rna, 2001. **7**(12): p. 1753-67.
11. Moore, M., *From Birth to Death: The Complex Lives of Eukaryotic mRNAs.* Science, 2005. **309**: p. 1514-1518
12. Gonsalvez, G.B., C.R. Urbinati, and R.M. Long, *RNA localization in yeast: moving towards a mechanism.* Biol Cell, 2005. **97**(1): p. 75-86.
13. Gu, W., et al., *A new yeast PUF family protein, Puf6p, represses ASH1 mRNA translation and is required for its localization.* Genes Dev, 2004. **18**(12): p. 1452-65.
14. Chartrand, P., et al., *Asymmetric sorting of ash1p in yeast results from inhibition of translation by localization elements in the mRNA.* Mol Cell, 2002. **10**(6): p. 1319-30.
15. Estrada, P., et al., *Myo4p and She3p are required for cortical ER inheritance in Saccharomyces cerevisiae.* J Cell Biol, 2003. **163**(6): p. 1255-66.
16. Kruse, C., et al., *Ribonucleoprotein-dependent localization of the yeast class V myosin Myo4p.* J Cell Biol, 2002. **159**(6): p. 971-82.
17. Takizawa, P.A., et al., *Actin-dependent localization of an RNA encoding a cell-fate determinant in yeast.* Nature, 1997. **389**(6646): p. 90-3.
18. Zimyanin, V.L., et al., *In vivo imaging of oskar mRNA transport reveals the mechanism of posterior localization.* Cell, 2008. **134**(5): p. 843-53.
19. Hachet, O. and A. Ephrussi, *Splicing of oskar RNA in the nucleus is coupled to its cytoplasmic localization.* Nature, 2004. **428**(6986): p. 959-63.
20. Hachet, O. and A. Ephrussi, *Drosophila Y14 shuttles to the posterior of the oocyte and is required for oskar mRNA transport.* Curr Biol, 2001. **11**(21): p. 1666-74.
21. Le Hir, H. and B. Seraphin, *EJCs at the heart of translational control.* Cell, 2008. **133**(2): p. 213-6.
22. Ishigaki, Y., Li, X., Serin, G., Maquat, LE., *Evidence for a pioneer round of mRNA translation: mRNAs subject to nonsense-mediated decay in mammalian cells are bound by CBP80 and CBP20.* Cell, 2001. **106**: p. 607-617.

23. Lejeune, F., Ishigaki, Y., Li, X., Maquat, LE., *The exon-junction complex is detected on CBP80-bound but not eIF4E-bound mRNA in mammalian cells; dynamics of mRNA remodeling.* Embo J, 2002. **21**: p. 3236-3545.
24. Wilkie, G.S. and I. Davis, *Drosophila wingless and pair-rule transcripts localize apically by dynein-mediated transport of RNA particles.* Cell, 2001. **105**(2): p. 209-19.
25. Dienstbier, M., Boehl, F., Li, X., Bullock, S.L., *Egalitarian is a selective RNA-binding protein linking mRNA localization signals to the dynein motor.* Genes and Development, 2009. **23**: p. 1546-1558.
26. Navarro, C., Puthalakath, H., Adams, J.M., Strasser, A., Lehmann, R., *Egalitarian binds dynein light chain to estbalish oocyte polarity and maintain cell fate.* Nature Cell Biology, 2004. **6**: p. 427-435.
27. Carson, J.H., et al., *Translocation of myelin basic protein mRNA in oligodendrocytes requires microtubules and kinesin.* Cell Motil Cytoskeleton, 1997. **38**(4): p. 318-28.
28. Messitt, T.J., et al., *Multiple kinesin motors coordinate cytoplasmic RNA transport on a subpopulation of microtubules in Xenopus oocytes.* Dev Cell, 2008. **15**(3): p. 426-36.
29. Kanai, Y., N. Dohmae, and N. Hirokawa, *Kinesin transports RNA: isolation and characterization of an RNA-transporting granule.* Neuron, 2004. **43**(4): p. 513-25.
30. Elvira, G., et al., *Characterization of an RNA granule from developing brain.* Mol Cell Proteomics, 2006. **5**(4): p. 635-51.
31. Chen, N., Onisko, B., Napoli, J.L., *The nuclear transcription factor RARa associates with neuronal RNA granules and suppresses translation.* Journal of Biological Chemistry, 2008. **283**: p. 20841-20847.
32. Lange, S., Katayama, Y., Schmid, M., Burkacky, O., Bräuchle, C., Lamb, D.C., Jansen, R.P., *Simultaneous transport of different localized mRNA species revealed by live-cell imaging.* Traffic, 2008. **8**: p. 1256-1267.
33. Gao, Y., Tatvarty, V., Korza, G., Levin, M.K., Carson, J.H.,, *Multiplexed dendritic targeting of αCaMKII, NG and ARC RNAs by the A2 pathway* Molecular Biology of the Cell, 2008. **19**(5): p. 2311-2327.
34. Mikl , M., Vendra, G., Kiebler, M.A., *Independent localization of MAP2, CaMKIIα and β-actin RNAs in low copy numbers.* Embo J, 2011. **12**: p. 1077-1084.
35. Kosturko, L.D., Maggipinto, M.J., Korza, G., Lee, J.W., Carson, J.H., Barbarese, E., *Heterogeneous nuclear ribonucleoprotein (hnRNP) E1 binds to hnRNP A2 and inhibits translation of A2 response element mRNAs.* Mol Biol Cell, 2006. **17**: p. 3521-3533.
36. Ostareck, D.H., Ostareck-Lederer, A.,Shatsky, I.N., Hentze, M.W., *Lipoxygenase mRNA silencing in erythroid differentiation: The'ØTR regulatory complex controls 60S ribosomal subunit joining.* Cell, 2001(104): p. 281-290.
37. White, R., Gonsior, C., Kramer-Albers, E.M., Stohr, N., Huttelmaier, S., Trotter, J., *Activation of oligodendroglial Fyn kinase enhances translation of mRNAs transporterd in hnRNPA2-depedent RNA granules.* Journal of Cell Biology, 2008. **181**(4): p. 579-586.
38. Wu, L., et al., *CPEB-mediated cytoplasmic polyadenylation and the regulation of experience-dependent translation of alpha-CaMKII mRNA at synapses.* Neuron, 1998. **21**(5): p. 1129-39.
39. Wells, D.G., et al., *A role for the cytoplasmic polyadenylation element in NMDA receptor-regulated mRNA translation in neurons.* J Neurosci, 2001. **21**(24): p. 9541-8.
40. Huang, Y.S., Jung, M.Y., Sarkissian, M., Richter, J.D., *N-methyl-d-aspartate receptor signaling results in Aurora kinase-catalyzed CPEB phosphorylation and alpha CaMKII mRNA polyadenylation at synapses.* Embo J, 2002. **22**: p. 2139-2148.
41. Alarcon, J.M., Hodgman, R.,Theis, M., Huang, Y.S., Kandel, E.R., Richter, J.D., *Selective modulation of some forms of schaffer collateral-CA1 synaptic plasticity in mice with a disruption of the CPEB-1 gene.* Learn Mem, 2004. **11**: p. 318-327.

42. Atkins, C.M., et al., *Cytoplasmic polyadenylation element binding protein-dependent protein synthesis is regulated by calcium/calmodulin-dependent protein kinase II.* J Neurosci, 2004. **24**(22): p. 5193-201.
43. Zearfoss, N.R., Alarcon, J.M.,Trifilieff, P., Kandel, E., Richter, J.D., *A molecular circuit composed of CPEB-1 and c-Jun controls growth hormone-mediated synaptic plasticity in the mouse hippocampus.* Journal of NEuroscience, 2008. **28**: p. 8502-8509.
44. Si, K., Giustetto, M.,Etkin, A.,Hsu, R.,Janisiewicz, A.M.,Miniaci, M.C.,Kim, J.H., *A neuronal isoform of CPEB regulates local protein synthesis and stabilizes synapse-specific long-term facilitation in aplysia.* Cell, 2003. **115**: p. 893-904.
45. Giuditta, A., Cuppelo, A., Lazzarini, G., *Ribosomal RNA in the axoplasm of the squid giant axon.* Journal of Neurochemistry, 1980. **34**: p. 1757-1760.
46. Giuditta, A., Hunt, T., Santella, L., *Messenger RNA in squid axoplasm.* Neurochemistry International, 1986. **8**: p. 435-442.
47. Giuditta, A., Dettbarn, W.D., Brzin, M., *Protein synthesis in the isolated giant axon of the squid.* Proc Natl Acad Sci U S A, 1968. **59**: p. 1284-1287.
48. Koenig, E.a.A., P., *Local protein synthesizing activity in axonal fields regenerating in vitro.* Journal of Neurochemistry, 1982. **39**: p. 386-400.
49. Koenig, E., *Synthetic mechanisms in the axon; in vitro incoproration of ^{3}H precursors into axonal protein and RNA.* Journal of Neurochemistry, 1967. **14**: p. 437-446.
50. Tobias, G.S., and Koenig, E., *Axonal protein synthesizing activity during the early outgrowth period following neurotomy.* Experimental Neurology, 1975. **49**: p. 221-234.
51. Tobias, G.S., and Koenig, E., *Influence of nerve cell body and neurolemma cell on local axonal protein synthesis following neurotomy.* Experimental Neurology, 1975. **49**: p. 235-245.
52. Koenig, E., *Evaluation of local synthesis of axonal proteins in the goldfish Mauthner of cell axon and axons of dorsal and ventral roots of the rat in vitro.* Molecular and Cellular Neuroscience, 1991. **2**: p. 384-394.
53. Merianda, T.T., et al., *A functional equivalent of endoplasmic reticulum and Golgi in axons for secretion of locally synthesized proteins.* Mol Cell Neurosci, 2009. **40**(2): p. 128-42.
54. Ming, G.L., Wong, S.T., Henley, J., Yuan, X.B., Song, H.J., Spitzer, N.C., Poo, M.M., *Adaptation in the chemotactic guidance of nerve growth cones.* Nature, 2002. **417**: p. 411-418.
55. Harris, W.A., Holt, C.E., Bonhoeffer, F., *Retinal axons with and without their somata, growing to and arborizing in the tectum of Xenopus embryos: a time lapse video study of single fibers in vivo.* Development, 1987. **101**: p. 123-133.
56. Campbell, D.S., and Holt, C.E., *Chemotropic responses of retinal growth cones mediated by rapid local protein synthesis and degradation.* Neuron, 2001. **32**: p. 1013-1026.
57. Leung, K.M., et al., *Asymmetrical beta-actin mRNA translation in growth cones mediates attractive turning to netrin-1.* Nat Neurosci, 2006. **9**(10): p. 1247-56.
58. Gumy, L.F., Yeo, G.S., Tung, Y.C., Zivraj, K.H., Willis, D., Coppola, G., Lam, B.Y., Twiss, J.L., Holt, C.E., Fawcett, J.W., *Transcriptome analysis of embryonic and adult sensory axons reveals changes in mRNA repertoire localization.* RNA, 2011. **17**: p. 85-98.
59. Willis, D.E., et al., *Extracellular stimuli specifically regulate localized levels of individual neuronal mRNAs.* J Cell Biol, 2007. **178**(6): p. 965-80.
60. Taylor, A.M., Berchtold, N.C., Perreau, V.M., Tu, C.H., Li Jeon, N., Cotman, C.W., *Axonal mRNA in uninjured and regenerating cortical mammalian axons.* JOurnal of Neuroscience, 2009. **29**: p. 4697-4707.
61. Zivraj, K.H., Tung, Y.C., Piper, M., Gumy, L., Fawcett, J.W., Yeo, G.S., Holt, C.E., *Subcellular profiling reveals distinct and developmentally regulated repertoire of growth cone mRNAs.* Journal of Neuroscience, 2010. **30**(46): p. 15464-15478.
62. Willis, D., et al., *Differential transport and local translation of cytoskeletal, injury-response, and neurodegeneration protein mRNAs in axons.* J Neurosci, 2005. **25**(4): p. 778-91.

63. Taylor, A.M., et al., *Axonal mRNA in uninjured and regenerating cortical mammalian axons.* J Neurosci, 2009. **29**(15): p. 4697-707.
64. Cox, L.J., et al., *Intra-axonal translation and retrograde trafficking of CREB promotes neuronal survival.* Nat Cell Biol, 2008. **10**(2): p. 149-59.
65. Ben-Yaakov K., D.S.Y., Segal-Ruder Y., Shalem O., Vuppalanchi, D., Willis D.E., Yudin D., Rishal I., Rother F., Bader M., Blesch A., Pilpel Y., Twiss J.L., Fainzilber M., *Axonal transcription factors signal retrogradely in lesioned peripheral nerve.* Embo J, 2012. **31**: p. 1350-1363.
66. Yan, D., Wu, Z., Chisholm, S.D. Jin, Y., *The DLK-1 kinase promotes mRNA stability and local translation in C. elegans synapses and axon regeneration.* Cell, 2009. **138**: p. 1005-1018.
67. Garner, C.C., Tucker, R.P., Matus, A., *Selective localization of messenger RNA for cytoskeletal protein MAP2 in dendrites.* Nature, 1988. **36**: p. 674–677.
68. Miyashiro, K., Dichter, M., Eberwine, J., *On the nature and differential distribution of mRNAs in hippocampal neurites: implications for neuronal functioning.* Proc Natl Acad Sci U S A, 1994. **91**: p. 10800–10804.
69. Lyford, G.L., Yamagata, K., Kaufmann, W.E., Barnes, C.A., Sanders, L.K., Copeland, N.G., Gilbert, D.J., Jenkins, N.A., Lanahan, A.A., Worley, P.F., *1995.* Neuron, Arc, a growth factor and activity-regulated gene, encodes a novel cytoskeleton-associated protein that is enriched in neuronal dendrites. **14**: p. 433–445.
70. Poon, M.M., et al., *Identification of process-localized mRNAs from cultured rodent hippocampal neurons.* J Neurosci, 2006. **26**(51): p. 13390-9.
71. Lein, E.S., et al., *Genome-wide atlas of gene expression in the adult mouse brain.* Nature, 2007. **445**(7124): p. 168-76.
72. Cajigas, I.J., Tushev, G., Will, T.J., tom Dieck, S., Fuerst, N., Schuman, E.M., *The local transcriptome in the synaptic neuropil revealed by deep sequencing and high-resolution imaging.* Neuron, 2012. **74**: p. 453-466.
73. Crino, P.a.E., J, *Molecular Characterization of the Dendritic Growth Cone: Regulated mRNA Transport and Local Protein Synthesis.* Neuron 1996. **17**: p. 1173–1187.
74. Rook, M.S., M. Lu, and K.S. Kosik, *CaMKIIalpha 3' untranslated region-directed mRNA translocation in living neurons: visualization by GFP linkage.* J Neurosci, 2000. **20**(17): p. 6385-93.
75. Tiruchinapalli, D.M., et al., *Activity-dependent trafficking and dynamic localization of zipcode binding protein 1 and beta-actin mRNA in dendrites and spines of hippocampal neurons.* J Neurosci, 2003. **23**(8): p. 3251-61.
76. Steward, O. and P.F. Worley, *A cellular mechanism for targeting newly synthesized mRNAs to synaptic sites on dendrites.* Proc Natl Acad Sci U S A, 2001. **98**(13): p. 7062-8.
77. Grooms, S.Y., et al., *Activity bidirectionally regulates AMPA receptor mRNA abundance in dendrites of hippocampal neurons.* J Neurosci, 2006. **26**(32): p. 8339-51.
78. Broadus, J., Fuerstenberg, S., Doe, C.Q., *Staufen-dependent localization of prospero mRNA contributes to neuroblast daughter-cell fate.* Nature, 1998. **391**: p. 792-795.
79. Vessey, J.P., Amadei, G., Burns, S.E., Kiebler, M.A., Kaplan, D.R., Miller, F.D., *An asymmetrically localized Staufen2-dependent RNA complex regulates maintenance of mammalian neural stem cells.* Cell Stem Cell, 2012. **11**: p. 517-528.
80. Kusek, G., Campbell, M., Doyle, F., Tenenbaum, S.A., Kiebler, M., Temple, S., *Asymmetric segregation of the double-stranded RNA binding protein Staufen2 during mammalian neural stem cell divisions promotes lineage progression.* Cell Stem Cell, 2012(11): p. 505-516.
81. Kislauskis, E.H., X. Zhu, and R.H. Singer, *Sequences responsible for intracellular localization of beta-actin messenger RNA also affect cell phenotype.* J Cell Biol, 1994. **127**(2): p. 441-51.
82. Zhang, H.L., et al., *Neurotrophin-induced transport of a beta-actin mRNP complex increases beta-actin levels and stimulates growth cone motility.* Neuron, 2001. **31**(2): p. 261-75.

83. Yao, J., et al., *An essential role for beta-actin mRNA localization and translation in Ca2+-dependent growth cone guidance.* Nat Neurosci, 2006. **9**(10): p. 1265-73.
84. Eom, T., et al., *Localization of a beta-actin messenger ribonucleoprotein complex with zipcode-binding protein modulates the density of dendritic filopodia and filopodial synapses.* J Neurosci, 2003. **23**(32): p. 10433-44.
85. Donnelly, C.J., Willis, D.E., Xu, M., Tep, C., Jiang, C., Yoo, S., Schanen, N.C., Kirn-Safran, C.B., van Minnen, J., English, A., Yoon, S.O., Bassell, G.J., Twiss, J.L., *Limited availability of ZBP1 restricts axonal mRNA localization and nerve regeneration capacity.* Embo J, 2011(22): p. 4665-4677.
86. Willis, D.E., Xu, M., Donnelly, C.J., Tep, C., Kendall, M., Erenstheyn, M., English, A.W., Schanen, N.C., Kirn-Safran, C.B., Yoon, S.O., Bassell, G.J., Twiss, J.L., *Axonal Localization of transgene mRNA in mature PNS and CNS neurons.* Journal of Neuroscience, 2011. **31**: p. 14481-14487.
87. Donnelly, C.J., Park, M., Spillane, M., Yoo, S., Pacheco, A., Gomes, C., Vuppalanchi, D., McDonald, M., Kim, H.H., Merianda, T.T., Gallo, G., Twiss, J.L., *Axonally synthesized β-actin and GAP-43 proteins support distinct modes of axonal growth.* Journal of Neuroscience, 2013. **33**: p. 3311-3322.
88. Lionnet, T., Czaplinski, K., Darzacq, X., Shav-Tal, Y., Wells, A.L., Chao, J.A., Park, H.Y., de Turris, V., Lopez-Jones, M., Singer, R.H., *A transgenic mouse for in vivo detection of endogenous labeled mRNA.* Nature Methods, 2011. **8**(2): p. 165-170.
89. Ross, A.F., et al., *Characterization of a beta-actin mRNA zipcode-binding protein.* Mol Cell Biol, 1997. **17**(4): p. 2158-65.
90. Farina, K.L., et al., *Two ZBP1 KH domains facilitate beta-actin mRNA localization, granule formation, and cytoskeletal attachment.* J Cell Biol, 2003. **160**(1): p. 77-87.
91. Gu, W., et al., *A predominantly nuclear protein affecting cytoplasmic localization of beta-actin mRNA in fibroblasts and neurons.* J Cell Biol, 2002. **156**(1): p. 41-51.
92. Huttelmaier, S., et al., *Spatial regulation of beta-actin translation by Src-dependent phosphorylation of ZBP1.* Nature, 2005. **438**(7067): p. 512-5.
93. Hansen, T.V., Hammer, N.A., Nielsen, J., Madsen, M., Dalbaeck, C., Wewer, U.M., Christiansen, J., Nielsen, F.C., *Dwarfism and impaired gut development in insulin-like growth factor II mRNA-binding protein 1-deficient mice.* Molecular and Cellular Biology, 2004. **24**(10): p. 4448-4464.
94. Glinka M., H.T., Funk N., Havlicek S., Rossoll W., Winkler C., Sendtner M., *The heterogeneous nuclear ribonucleoprotein-R is necessary for axonal beta-actin mRNA translocation in spinal motor neurons.* Human Molecular Genetics, 2010(10): p. 1951-1966.
95. Rossoll, W., Jablonka, S., Andreassi, C., Kröning, A.K., Karle, K., Monani, U.R., Sendtner, M., *Smn, the spinal muscular atrophy-determining gene product, modulates axon growth and localization of beta-actin mRNA in growth cones of motoneurons.* Journal of Cell Biology, 2003. **4**: p. 801-812.
96. Chen, H.H., Yu, H.I., Chiang, W.C., Lin, Y.D., Shia, B.C., Tarn, W.Y., *hnRNP Q regulates Cdc42-mediated neuronal morphogenesis.* Molecular and Cellular Biology, 2012. **12**: p. 2224-2238.
97. Itoh, M., Haga, I., Li, Q.H., Fujisawa, J., *Identification of cellular mRNA targets for RNA-binding protein Sam68.* Nucleic Acids Res, 2002. **30**(24): p. 5452-5464.
98. Lin, Q., Taylor, S.J., Shalloway, D., *Specificity and determinants of Sam68 RNA binding. Implications for the biological function of K homology domains.* Journal of Biological Chemistry, 1997. **272**: p. 27274-27280.
99. Klein, M.E., Younts, T.J., Castillo, P.E., Jordan, B.A., *RNA-binding protein Sam68 controls synapse number and local β-actin mRNA metabolism in dendrites.* Proc Natl Acad Sci U S A, 2013. **110**(8): p. 3125-3130.

100. Ma, S., et al., *Relocalization of the polypyrimidine tract-binding protein during PKA-induced neurite growth.* Biochim Biophys Acta, 2007. **1773**(6): p. 912-23.
101. Xie, J., et al., *Protein kinase A phosphorylation modulates transport of the polypyrimidine tract-binding protein.* Proc Natl Acad Sci U S A, 2003. **100**(15): p. 8776-81.
102. Boutz, P.L., Stoilov, P., Li, Q., Lin, C.H., Chawla, G., Ostrow, K., Shiue, L., Ares, M. Jr, Black, D.L., *A post-transcriptional regulatory switch in polypyrimidine tract-binding proteins reprograms alternative splicing in developing neurons.* Genes Dev, 2007. **21**(13): p. 1636-1652.
103. Czaplinski, K., et al., *Identification of 40LoVe, a Xenopus hnRNP D Family Protein Involved in Localizing a TGF-beta-Related mRNA during Oogenesis.* Dev Cell, 2005. **8**(4): p. 505-15.
104. Raju, C.S., et al., *In Cultured Oligodendrocytes the A/B-type hnRNP CBF-a Accompanies MBP mRNA Bound to mRNA Trafficking Sequences.* Mol Biol Cell, 2008.
105. Delanoue, R., et al., *Drosophila Squid/hnRNP helps Dynein switch from a gurken mRNA transport motor to an ultrastructural static anchor in sponge bodies.* Dev Cell, 2007. **13**(4): p. 523-38.
106. Jaramillo, A.M., et al., *The dynamics of fluorescently labeled endogenous gurken mRNA in Drosophila.* J Cell Sci, 2008. **121**(Pt 6): p. 887-94.
107. Norvell, A., et al., *Squid is required for efficient posterior localization of oskar mRNA during Drosophila oogenesis.* Dev Genes Evol, 2005. **215**(7): p. 340-9.
108. Sinnamon, J.R., et al., *Hnrpab regulates neural development and neuron cell survival after glutamate stimulation.* RNA, 2012. **18**(4): p. 704-719.
109. Hill, M.A. and P. Gunning, *Beta and gamma actin mRNAs are differentially located within myoblasts.* J Cell Biol, 1993. **122**(4): p. 825-32.
110. Bassell, G.J., et al., *Sorting of beta-actin mRNA and protein to neurites and growth cones in culture.* J Neurosci, 1998. **18**(1): p. 251-65.
111. Sinnamon, J.R.C., K., *RNA detection in situ with FISH-STICs*, in *RNA*. 2013. p. .
112. Dormoy-Raclet, V., et al., *The RNA-binding protein HuR promotes cell migration and cell invasion by stabilizing the beta-actin mRNA in a U-rich-element-dependent manner.* Mol Cell Biol, 2007. **27**(15): p. 5365-80.
113. Myer, V. and J.A. Steitz, *Isolation and characterization of a novel, low abundance hnRNP protein: A0.* RNA, 1995. **1**: p. 171-182.
114. Rousseau, S., et al., *Inhibition of SAPK2a/p38 prevents hnRNP A0 phosphorylation by MAPKAP-K2 and its interaction with cytokine mRNAs.* The Embo Journal, 2002. **21**(23): p. 6505-6514.
115. Reinhard, H.C., et al., *DNA Damage Activates a Spatially Distinct Late Cytoplasmic Cell-Cycle Checkpoint Network Controlled by MK2-Mediated RNA Stabilization.* Molecular Cell, 2010. **40**: p. 34-49.
116. Yao, K.M., Samson, M.L., Reeves, R., White, K., *Gene elav of Drosophila melanogaster: a prottype for neuronal specific RNA binding protein gene family that is conserved in flies and humans.* Journal of Neurobiology, 1993. **24**: p. 723-739.
117. Szabo, A., Dalmau, J., Manley, G., Rosenfeld, M., Wong, E., Henson, J., Posner, J.B., Furneaux, H.M., *HuD, a paraneoplastic encephalomyelitis antigen, contains RNA-binding domains and is homologous to ELAV and Sex-lethal.* Cell, 1991. **67**(2): p. 325–333.
118. Dalmau, J., Furneaux, H.M., Cordon-Cardo, C., Posner, J.B. , *The expression of the Hu (paraneoplastic encephalomyelitis/sensory neuronopathy) antigen in human normal and tumor tissues.* American Journal of Pathology, 1992. **141**(4): p. 881-888.
119. Hinman, M.N.a.L., H., *Diverse molecular functions of Hu proteins.* Cell Molecular Life Sciences, 2008. **65**(20): p. 3168-3181.
120. Katsanou, V., Papadaki, O., Milatos, S., Blackshear, P.J., Anderson, P., Kollias, G., Kontoyiannis, D.L., *HuR as a negative posttranscriptional modulator in inflamation.* Molecular Cell, 2005. **19**: p. 777-789.

121. Yoo, S., Kim, H.H., Kim, P., Donnelly, C.J., Kalinski, A.L., Vuppalanchi, D., Park, M., Lee, S.J., Merianda, T.T., Perrone-Bizzozero, N.I., Twiss, J.L., *A HuD-ZBP1 ribonucleoprotein complex localizes GAP-43 mRNA into axons through its 3' untranslated region AU-rich regulatory element.* Journal of Neurochemistry, 2013. **126**: p. 792-804.
122. Zhang, W., et al., *Purification, characterization, and cDNA cloning of an AU-rich element RNA-binding protein, AUF1.* Mol Cell Biol, 1993. **13**(12): p. 7652-65.
123. Wagner, B.J., et al., *Structure and genomic organization of the human AUF1 gene: alternative pre-mRNA splicing generates four protein isoforms.* Genomics, 1998. **48**(2): p. 195-202.
124. DeMaria, C.T., et al., *Structural determinants in AUF1 required for high affinity binding to A + U-rich elements.* J Biol Chem, 1997. **272**(44): p. 27635-43.
125. Zucconi, B.E., Ballin, J.D., Brewer, B.Y., Ross, C.R., Huang, J., Toth, E.A., Wilson, G.M., *Alternatively expressed domains of AU-rich element RNA binding protein 1 (AUF1) regualte RNA-binding affinity, RNA-induced protein oligomerization and the local conformation of bound RNA ligands.* Journal of Biological Chemistry, 2010. **285**: p. 39127-39139.
126. Mazan-Mamczarz, K., et al., *Identification of a signature motif in target mRNAs of RNA-binding protein AUF1.* Nucleic Acids Res, 2009. **37**(1): p. 204-14.
127. Sarkar, B., J.Y. Lu, and R.J. Schneider, *Nuclear import and export functions in the different isoforms of the AUF1/heterogeneous nuclear ribonucleoprotein protein family.* J Biol Chem, 2003. **278**(23): p. 20700-7.
128. Okuwaki, M., *The structure and function of NPM1/Nucleophosmin/B23, a multifucntional nucleolar acidic protein.* Journal of Biological Chemistry, 2008. **143**: p. 441-448.
129. Sagawa, F., Ibrahim, H., Morrison, A.L., Wilusz, C.J., Wilusz, J., *Nucleophosmin deposition during mRNA 3' end processing influences poly(A) tail length.* Embo J, 2011. **30**(19): p. 3994-4005.
130. Mukudai, Y., Kubota, S., Kawaki, H., Kondo, S., Eguchi, T., Sumiyoshi, K., Ohgawara, T., Shimo, T., Takigawa, M., *Posttranscriptional regulation of chicken ccn2 gene expression by nucleophosmin/B23 during chondrocyte differentiation.* Mol Cell Biol, 2008. **28**(19): p. 6134-6147.
131. Shav-Tal, Y.a.Z., D., *PSF and P54nrb/NonO - multi-functional nuclear proteins.* FEBS Lett, 2002. **531**: p. 109-114.
132. Peng, R., et al., *PSF and p54nrb bind a conserved stem in U5 snRNA.* RNA, 2002. **8**: p. 1334–1347.
133. Kameokaab, S., Duqea, P., Konarska, M.M., *p54nrb associates with the 5' splice site within large transcription/splicing complexes.* Embo J, 2004. **23**: p. 1782 - 1791.
134. Bladen, C.L., et al., *Identification of the Polypyrimidine Tract Binding Protein-associated Splicing Factor□p54(nrb) Complex as a Candidate DNA Double-strand Break Rejoining Factor.* Journal of Biological Chemistry, 2002. **280**(7): p. 5205-5210.
135. Kaneko, S., et al., *The multifunctional protein P54nrb/PSF recruits the exonnuclease XRN2 to facilitate pre-mRNA 3' processing and transcriptional termination.* Genes and Development, 2007. **21**: p. 1779-1789.
136. Andersen, J.S., Lyon, C.E., Fox, A.H., Leung, A.K., Lam, Y.W., Steen, H., Mann, M., Lamond, AI., *Directed proteomic analysis of the human nucleolus.* Current Biology, 2002. **12**: p. 1-11.
137. Fox, A.H., Lam, Y.H., Leung, A.K., Lyon, C.E., Andersen, J., Mann, M., Lamond, A.I., *Paraspeckles: a novel nuclear domain.* Current Biology, 2002. **12**: p. 13-25.
138. Fox, A.H., C.S. Bond, and A.I. Lamond, *P54nrb Forms a Heterodimer with PSP1 That Localizes to Paraspeckles in an RNA-dependent Manner.* Mol Biol Cell, 2005. **16** p. 5304–5315.
139. Fox, A.H.a.L., A.I., *Paraspeckles.* Cold Spring Harbor Perspectives in Biology, 2010. **2**: p. 1-14.
140. von Lindern, M., van Baal, S., Wiegant, J., Raap, A., Hagemeijer, A. and Grosveld, G. , *Can, a putative oncogene associated with myeloid leukemogenesis, may be activated by fusion of its 3' half to different genes: characterization of the set gene.* Mol. Cell Biol., 1992. **12**: p. 3346–3355.

141. Canela, N., Rodriguez-Vilarrupla, A., Estanyol, J. M., Diaz, C., Pujol, M. J.,Agell, N,. and Bachs, O., *The SET protein regulates G2/M transition by modulating cyclin B-cyclin-ependent kinase 1activity.* Journal of Biological Chemistry, 2003. **278**: p. 1158-1164.
142. Adler, H.T., Nallaseth, F. S., Walter, G., and Tkachuk D. C., *HRX leukemic fusion proteins form a heterocomplex with the leukemiaassociated protein SET and protein phosphatase 2A.* Journal of Biological Chemistry, 1997. **272**: p. 28407-28414.
143. Estanyol, J.M., Jaumot, M., Casanovas, O., Rodriguez-Vilarrupla, A.,Agell, N. and Bachs O, *The protein SET regulates the inhibitory effect of p21(Cip1) on cyclin E-cyclin-dependent kinase 2 activity.* Journal of Biological Chemistry, 1999. **274**: p. 33161-33165.
144. Seo, S.B., McNamara, P., Heo, S., Turner, A., Lane, W. S,. and Chakravarti, D., *Regulation of histone acetylation and transcription by INHAT, a human cellular complex containing the set oncoprotein.* Cell, 2001. **104**: p. 119-130.
145. Madeira, A., Pommet, J.M., Prochiantz, A., Allinquant, B., *SET protein (TAF1beta, I2PP2A) is involved in neuronal apoptosis induced by an amyloid precursor protein cytoplasmic subdomain.* Faseb J, 2005(19): p. 1905-1907.
146. Tanimukai, H., Grundke-Iqbal, I., and Iqbal, K., *Up-regulation of inhibitors of protein phosphatase-2A in Alzheimer's disease.* American Journal of Pathology, 2005. **166**: p. 1761-1771.
147. ten Klooster, J.P., Leeuwen, I.v., Scheres, N., Anthony, E.C., Hordijk, P.L., *Rac1-induced cell migration requires membrane recruitment of the nuclear oncogene SET.* Embo J, 2007. **26**: p. 336-345.
148. Brennan, C.M., Gallouzi, I.E., Steitz, J.A., *Protein ligands to HuR modulate its interaction with target mRNAs in vivo.* Journal of Cell Biology, 2000. **151**: p. 1-14.
149. Vera, J., Jaumot, M., Estanyol, J.M., Brun, S., Agell, N., Bachs, O., *Heterogeneous nuclear ribonucleoprotein A2 is a SET-binding protein and a PP2A inhibitor.* Oncogene, 2006. **25**: p. 260-270.
150. Czaplinski, K. and I.W. Mattaj, *40LoVe interacts with Vg1RBP/Vera and hnRNP I in binding the Vg1-localization element.* Rna, 2006. **12**(2): p. 213-22.
151. Qian, X. and R.V. Lloyd, *Recent developments in signal amplification methods for in situ hybridization.* Diagn Mol Pathol, 2003. **12**(1): p. 1-13.
152. Itzkovitz, S. and A. van Oudenaarden, *Validating transcripts with probes and imaging technology.* Nat Methods, 2011. **8**(4 Suppl): p. S12-9.
153. Grunwald, D., R.H. Singer, and K. Czaplinski, *Cell biology of mRNA decay.* Methods Enzymol, 2008. **448**: p. 553-77.
154. Femino, A.M., et al., *Visualization of single molecules of mRNA in situ.* Methods Enzymol, 2003. **361**: p. 245-304.
155. Raj, A., et al., *Imaging individual mRNA molecules using multiple singly labeled probes.* Nat Methods, 2008. **5**(10): p. 877-9.
156. Player, A.N., et al., *Single-copy gene detection using branched DNA (bDNA) in situ hybridization.* J Histochem Cytochem, 2001. **49**(5): p. 603-12.
157. Collins, M.L., et al., *A branched DNA signal amplification assay for quantification of nucleic acid targets below 100 molecules/ml.* Nucleic Acids Res, 1997. **25**(15): p. 2979-84.
158. Latham, V.M., Jr., et al., *Beta-actin mRNA localization is regulated by signal transduction mechanisms.* Journal of Cell Biology, 1994(126): p. 1211-1219.
159. Lawrence, J.B. and R.H. Singer, *Intracellular localization of messenger RNAs for cytoskeletal proteins.* Cell, 1986(45): p. 407-415.
160. Jourdren, L., et al., *CORSEN, a new software dedicated to microscope-based 3D distance measurements: mRNA-mitochondria distance, from single-cell to population analyses.* RNA, 2010(16): p. 1301-1307.

161. Park, H.Y., et al., *An unbiased analysis method to quantify mRNA localization reveals its correlation with cell motility.* Cell Reports, 2012. **1**(2): p. 179-184.
162. Mei, L. and W.C. Xiong, *Neuregulin 1 in neural development, synaptic plasticity and schizophrenia.* Nat Rev Neurosci, 2008. **9**(6): p. 437-52.
163. Femino, A.M., et al., *Visualization of single RNA transcripts in situ.* Science, 1998. **280**(5363): p. 585-90.
164. Katz, Z.B., et al., *β-Actin mRNA compartmentalization enhances focal adhesion stability and directs cell migration.* Genes Dev, 2012. **26**(17): p. 1885-1890.
165. Lau, A. and M. Tymianski, *Glutamate receptors, neurotoxicity and neurodegeneration.* Pflugers Arch, 2010. **460**(2): p. 525-42.
166. Rushlow, W.J., et al., *Characterization of CArG-binding protein A initially identified by differential display.* Neuroscience, 1999. **94**(2): p. 637-49.
167. Yan, C.Y., et al., *Samba, a Xenopus hnRNP expressed in neural and neural crest tissues.* Dev Dyn, 2009. **238**(1): p. 204-9.
168. Zhivotovsky, B. and S. Orrenius, *Calcium and cell death mechanisms: A perspective from the cell death community.* Cell Calcium, 2011.
169. Wang, Y. and Z.H. Qin, *Molecular and cellular mechanisms of excitotoxic neuronal death.* Apoptosis, 2010. **15**(11): p. 1382-402.
170. Hilton, G.D., et al., *Glutamate-mediated excitotoxicity in neonatal hippocampal neurons is mediated by mGluR-induced release of Ca++ from intracellular stores and is prevented by estradiol.* Eur J Neurosci, 2006. **24**(11): p. 3008-16.
171. Nagel, S., Papadakis, M., Pfleger, K., Grond-Ginsbach, C., Buchan, A.M., Wagner, S., *Microarray analysis of the global gene expression profile following hypothermia and transient focal cerebral ischemia.* Neuroscience, 2012. **208**: p. 109-122.
172. Murgatroyd, C., et al., *Impaired repression at a vasopressin promoter polymorphism underlies overexpression of vasopressin in a rat model of trait anxiety.* J Neurosci, 2004. **24**(35): p. 7762-70.
173. Yabuki, T., et al., *A novel growth-related nuclear protein binds and inhibits rat aldolase B gene promoter.* Gene, 2001. **264**(1): p. 123-9.
174. Gao, C., et al., *S-nitrosylation of heterogeneous nuclear ribonucleoprotein A/B regulates osteopontin transcription in endotoxin-stimulated murine macrophages.* J Biol Chem, 2004. **279**(12): p. 11236-43.
175. Mikheev, A.M., et al., *CArG binding factor A (CBF-A) is involved in transcriptional regulation of the rat Ha-ras promoter.* Nucleic Acids Res, 2000. **28**(19): p. 3762-70.
176. Bemark, M., et al., *Purification and characterization of a protein binding to the SP 6 kappa promoter. A potential role for CArG-box binding factor-A in kappa transcription.* J Biol Chem, 1998. **273**(30): p. 18881-90.
177. Smidt, M.P., et al., *Cloning and characterisation of a nuclear, site specific ssDNA binding protein.* Nucleic Acids Res, 1995. **23**(13): p. 2389-95.
178. Giorgi, C. and M.J. Moore, *The nuclear nurture and cytoplasmic nature of localized mRNPs.* Semin Cell Dev Biol, 2007. **18**(2): p. 186-93.
179. Norvell, A., et al., *Specific isoforms of squid, a Drosophila hnRNP, perform distinct roles in Gurken localization during oogenesis.* Genes Dev, 1999. **13**(7): p. 864-76.
180. Clouse, K.N., S.B. Ferguson, and T. Schupbach, *Squid, Cup, and PABP55B function together to regulate gurken translation in Drosophila.* Dev Biol, 2008. **313**(2): p. 713-24.
181. Raju, C.S., et al., *In neurons, activity-dependent association of dendritically transported mRNA transcripts with the transacting factor CBF-A is mediated by A2RE/RTS elements.* Mol Biol Cell, 2011. **22**(11): p. 1864-77.
182. Raju, C.S., et al., *In cultured oligodendrocytes the A/B-type hnRNP CBF-A accompanies MBP mRNA bound to mRNA trafficking sequences.* Mol Biol Cell, 2008. **19**(7): p. 3008-19.

183. Zeituni, A.E., et al., *The native 67-kilodalton minor fimbria of Porphyromonas gingivalis is a novel glycoprotein with DC-SIGN-targeting motifs.* J Bacteriol, 2010. **192**(16): p. 4103-10.
184. Tanner, S., et al., *InsPecT: identification of posttranslationally modified peptides from tandem mass spectra.* Anal Chem, 2005. **77**(14): p. 4626-39.
185. Mostoslavsky, G., et al., *Complete correction of murine Artemis immunodeficiency by lentiviral vector-mediated gene transfer.* Proc Natl Acad Sci U S A, 2006. **103**(44): p. 16406-11.
186. Nielsen, J., et al., *Sequential dimerization of human zipcode-binding protein IMP1 on RNA: a cooperative mechanism providing RNP stability.* Nucleic Acids Res, 2004. **32**(14): p. 4368-76.
187. Sinnamon, J.R., et al., *Hnrpab regulates neural development and neuron cell survival after glutamate stimulation.* Rna, 2012. **18**(4): p. 704-19.
188. Meberg, P.J. and M.W. Miller, *Culturing hippocampal and cortical neurons.* Methods Cell Biol, 2003. **71**: p. 111-27.
189. Goslin, K. and G. Banker, *Rat Hippocampal Neurons in LowDensity Culture*, in *Culturing nerve cells*, G. Banker and K. Goslin, Editors. 1998, MIT press: Cambridge. p. 339-370.
190. Kersey, P.J., et al., *The International Protein Index: an integrated database for proteomics experiments.* Proteomics, 2004. **4**(7): p. 1985-8.
191. Elias, J.E. and S.P. Gygi, *Target-decoy search strategy for increased confidence in large-scale protein identifications by mass spectrometry.* Nat Methods, 2007. **4**(3): p. 207-14.
192. Eng, J.K., A.L. McCormack, and r. J.R. Yates, *An Approach to Correlate Tandem Mass Spectral Data of Peptides with Amino Acid Sequences in a Protein Database.* J Am Soc Mass Spectrom, 1994. **5**: p. 976-989.
193. Yates, J.R., 3rd, et al., *Method to correlate tandem mass spectra of modified peptides to amino acid sequences in the protein database.* Anal Chem, 1995. **67**(8): p. 1426-36.
194. Tabb, D.L., W.H. McDonald, and r. J.R. Yates, *DTASelect and Contrast: Tools for Assembling and Comparing Protein Identification from Shotgun Proteomics.* J. Proteome Res., 2002. **1**: p. 21-26.
195. Park, S.K., et al., *A quantitative analysis software tool for mass spectrometry-based proteomics.* Nat Methods, 2008. **5**(4): p. 319-22.